

Resilient Modulus Properties of New Jersey Subgrade Soils

FINAL REPORT
September 2000

Submitted by

Dr. Ali Maher*
Professor and Chairman

Thomas Bennert*
Senior Research Engineer

Dr. Nenad Gucunski*, Professor
Walter J. Papp, Jr.,** Engineer

* Dept. of Civil & Environmental Engineering
Center for Advanced Infrastructure &
Transportation (CAIT)
Rutgers, The State University
Piscataway, NJ 08854-8014

** Mueser-Rutledge Consulting Engineers
708 Third Avenue
New York, NY 10017



NJDOT Research Project Manager
Mr. Anthony Chmiel

In cooperation with

New Jersey
Department of Transportation
Division of Research and Technology
and
U.S. Department of Transportation
Federal Highway Administration

Disclaimer Statement

"The contents of this report reflect the views of the author(s) who is (are) responsible for the facts and the accuracy of the data presented herein. The contents do not necessarily reflect the official views or policies of the New Jersey Department of Transportation or the Federal Highway Administration. This report does not constitute a standard, specification, or regulation."

The contents of this report reflect the views of the authors, who are responsible for the facts and the accuracy of the information presented herein. This document is disseminated under the sponsorship of the Department of Transportation, University Transportation Centers Program, in the interest of information exchange. The U.S. Government assumes no liability for the contents or use thereof.

1. Report No. FHWA 2000-01	2. Government Accession No.	3. Recipient's Catalog No.	
4. Title and Subtitle Resilient Modulus Properties of New Jersey Subgrade Soils		5. Report Date September 2000	
		6. Performing Organization Code CAIT/Rutgers	
7. Author(s) Dr. Ali Maher, Mr. Thomas Bennert, Dr. Nenad Gucunski, and Mr. Walter J. Papp, Jr.		8. Performing Organization Report No. FHWA 2000-01	
9. Performing Organization Name and Address New Jersey Department of Transportation CN 600 Trenton, NJ 08625		10. Work Unit No.	
		11. Contract or Grant No.	
12. Sponsoring Agency Name and Address Federal Highway Administration U.S. Department of Transportation Washington. D.C.		13. Type of Report and Period Covered Final Report 9/1997 - 9/2000	
		14. Sponsoring Agency Code	
15. Supplementary Notes			
16. Abstract <p>To effectively and economically design pavement systems, subgrade response must be evaluated. Understanding the importance of subgrade soil response to various loading conditions, the American Association of State Highway and Transportation Officials (AASHTO) and the Strategic Highway Research Program (SHRP) established and refined a Standard Test Method for Determining the Resilient Modulus of Soils and Aggregate Materials. Mechanistic design methods for flexible pavements require the specification of subgrade resilient modulus. The resilient modulus is measured under laboratory conditions that should reflect the conditions the subgrades are prepared and subjected to in the field.</p> <p>In this study, a laboratory-testing program was developed to determine the resilient modulus of typical New Jersey subgrade soils. A total of eight soils were tested at different molded water contents to determine their sensitivity to moisture content and cyclic stress ratio. Repeated loading or pumping of the pavement system may induce excess pore water pressure within the subgrade layer whereby reducing the resilient modulus, leading to the premature failure of the pavement system.</p> <p>A sensitivity analysis was conducted using an elastic layer computer program to demonstrate the effect of subgrade stiffness on the design thickness of the asphalt layer. As expected, the subgrade stiffness has a dramatic effect on the eventual thickness of the asphalt layer.</p> <p>Laboratory results were used to calibrate a statistical model for effectively predicting the resilient modulus of subgrade soils at various moisture contents and stress ratios. This model will prove to be a valuable tool for pavement engineers to effectively and economically design a pavement system.</p>			
17. Key Words Resilient Modulus, Subgrade Soils, Sensitivity Analysis, Universal Model		18. Distribution Statement	
19. Security Classif (of this report) Unclassified	20. Security Classif. (of this page) Unclassified	21. No of Pages 136 pp.	22. Price

I. INTRODUCTION

1.1 Statement of the Problem

The characteristics and behavior of subgrade soils have a major influence in the design and performance of flexible pavement systems. Previous methods have been used to help evaluate the properties and behavior of subgrades to design pavement systems based on empirical methods. Specifically, the California Bearing Ratio test (CBR) has been used to help determine the minimum pavement thickness based on the potential strength of the subgrade. The empirical "soil support value" obtained from static tests did not effectively model the types of stresses experienced by the subgrade. Concerns about this empirical approach forced highway engineers develop new techniques to perform dynamic tests on subgrade soils to reflect the dynamic response of soil to vehicular traffic loads.

In 1982, the American Association of State Highway and Transportation Officials (AASHTO) establish the Standard Method of Test for Resilient Modulus of Subgrade soil AASHTO Designation T 274-82 (AASHTO Specifications 1986). Since then, several workshops have been held to further revise testing method to improve it's repeatability and loading sequence to represent actual loading conditions experienced by subgrade soil. To date, AASHTO has adopted a procedure for determining the resilient modulus of subgrade soil from the Strategic Highway Research Program (SHRP). The Standard Test Method for Determining the Resilient Modulus of Soils and Aggregate Materials, AASHTO Designation TP46-94 has been adopted as the universal laboratory testing procedure to determine resilient modulus of subgrade soils. Although the use of resilient modulus in mechanistic design procedures offers many advantages over the earlier

empirical design methods, a resilient modulus value for different subgrade soils must be specified. To effectively utilize the new mechanistic design procedure, subgrade resilient modulus should be evaluated under simulated construction and seasonal conditions.

Resilient modulus is defined as shown in figure 1.1; where $(\sigma_1 - \sigma_3) = \sigma_d =$ deviatoric stress (applied stress due to the vertical load).

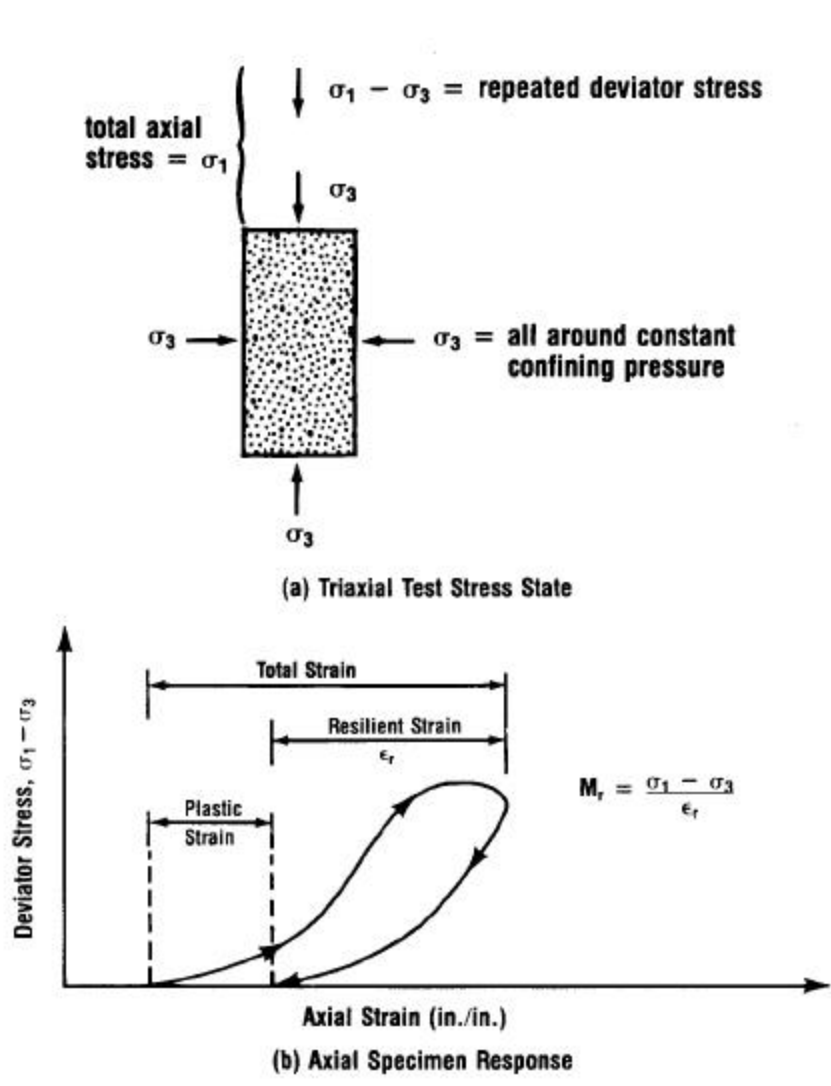


Figure 1.1 Definition of Resilient Modulus (Barksdale, 1993)

1.2 Objectives of the Study

The overall objectives were to:

1. Determine resilient properties of subgrade soils specific to combined residual/transported soils of New Jersey and determination of proper predictive procedures for determination of their value.
2. Evaluate the effect of varying moisture content on the resilient modulus properties of New Jersey subgrade soils.
3. Provide a statistical model to predict the resilient modulus of different New Jersey soil types under varying confining pressure and deviatoric stress schemes, as well as moisture contents.

Resilient modulus testing is a difficult and time consuming testing procedure designed to predict the response of subgrade soils under various stress levels to simulate vehicular traffic loading. Several different soils have been tested to:

1. Determine the effect of moisture content on the compaction of granular and cohesive subgrade soils.
2. Adopt a statistical model and develop soil parameters for each material tested.
3. Verify statistical model by predicting the resilient modulus with similar properties as determined by peers.
4. Provide a database of resilient modulus values for use in New Jersey mechanistic pavement design.

1.3 Scope and Outline of the Report

In this report, many parameters affecting resilient modulus have been addressed, for cohesive fine-grained material and granular non-cohesive materials. Chapter 2 of this report presents a comprehensive review of the history of resilient modulus testing methodologies and loading sequences, which have evolved into the current resilient modulus test TP46-94. Chapter 3 describes the experimental program, materials and equipment used for this research and presents specific material properties for each of the six soils tested. Chapter 4 presents the results of the resilient modulus tests compacted at various moisture contents and confining pressures. Chapter 5 presents the results of post-saturated samples to evaluate the effect of pore pressure generation during the resilient modulus test. Chapter 6 describes statistical models typically used for predicting resilient modulus. The model used for this study predicts the resilient modulus for a given soil under any stress level. Chapter 7 involves a sensitivity analysis to show the effect the change in subgrade resilient modulus will have on the design thickness of the asphalt layer. Two separate pavement conditions were evaluated; a full-depth pavement and a conventional pavement that included a base/subbase layer. Chapter 8 describes a design procedure for the pavement engineer. The procedure shows step-by-step calculations, along with helpful figures and tables, on how to design a pavement system. A summary of the report, conclusions from the experimental program and future research recommendations are presented in Chapter 9.

II. LITERATURE REVIEW

2.1 Introduction

Pavement life depends on the performance and condition of the pavement system, which consists of a bituminous overlay, base, subbase and subgrade. During the life of the system, the subgrade is subjected to variations in moisture content, and depending on the soil type of the subgrade, could result in variations of the moduli. In optimum conditions, the subgrade would be compacted to 99% of dry unit weight and at optimum moisture content. During seasonal changes, storm and groundwater may infiltrate the subgrade, changing the moisture content and, therefore, changing the resilient modulus. Temperature fluctuations (freezing and thawing) in the subgrade, depending on the depth, may also affect the performance of the subgrade resilient modulus. The 1993 AASHTO Guide for the Design of Pavement Structures uses an effective resilient modulus that has been implemented for evaluating the relative damage to flexible pavement systems due to seasonal changes. The effective roadbed soil resilient modulus is an equivalent modulus that would result in the same reduction as if the resilient modulus were actually calculated during these seasonal conditions (Huang, 1993). Figure 2.1 shows a worksheet that may be used to estimate the effective roadbed soil resilient modulus for seasonal conditions. The sum of the relative damage divided by the number of months would be the average relative damage. From the vertical scale the effective roadbed resilient modulus can be obtained for the average effective damage. Therefore it is necessary to have a large database of resilient modulus values for different soil types, at different seasons of the year, subjected to these typical seasonal moisture changes.

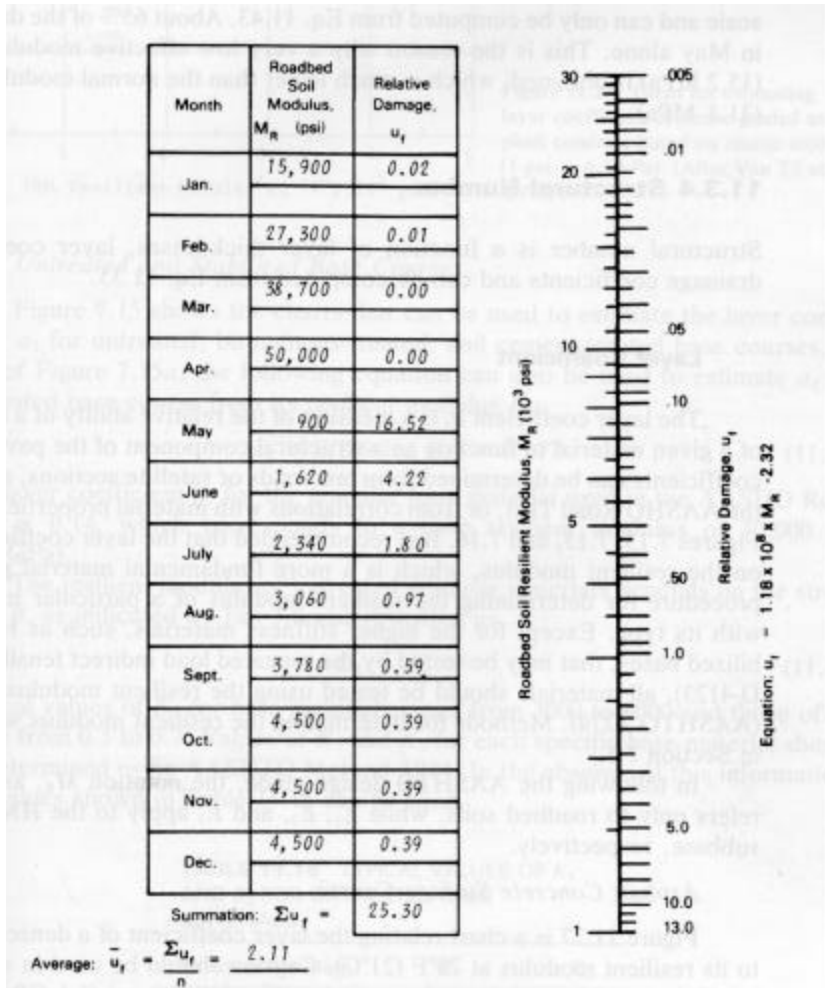


Figure 2.1 Estimating Effective Roadbed Resilient Modulus (Huang, 1993)

2.2 Historical Background

Resilient modulus is an index that describes the nonlinear stress-strain behavior of soils under cyclic loads. Mechanistic design procedures of pavements and overlays require the specification of subgrade resilient modulus to determine layer thickness and the overall system response to traffic type loads. In AASHTO specification T-274 adopted in 1986 based on mechanistic methods, resilient modulus is considered as an important design input parameter.

In general, the laboratory procedures for determination of resilient modulus are essentially based on existing cyclic triaxial methods used for determination of soil properties under repeated loads. Following the AASHTO T274 requirements in 1986, a workshop was held at the University of Oregon to review the state of practice in resilient modulus testing. Since then a number of important improvements have been made leading to the Strategic Highway Research Program's (SHRP) revised testing procedure TP-46-94. The revisions are included in the new AASHTO procedure TP46-94.

Some of the most recognized changes from AASHTO T274 to the most recent AASHTO TP46-94 are:

1. The loading sequences, and the number of loading cycles per sequence, have been reduced from AASHTO specification T-274, which include 27 loading sequences each with 200 loading cycles as compared to AASHTO specification TP46-94 which has 15 loading sequences with 100 loading cycles per sequence. The decrease in testing sequences led to a reduction sample deformation and testing time from approximately 5 hours to 2 hours.

2. The maximum axial stress range was also changed from 1.0 – 20.0 psi to 3.0 – 40.0 psi for base and subbase materials, and from 1.0 – 10.0 psi to 2.0 – 10.0 psi for subgrade materials.
3. Methodology of classifying the soil types and compaction methods.
4. Different testing sequences for base and subgrade soils independent of soil type.
5. Change of confining stress in subbase testing sequence from an unrealistic confining stress of 0 psi to 2.0 psi.
6. Implementing a contact stress of 10% of the deviatoric stress applied to the sample. The contact stress provides a small axial stress on the sample during the rest period of the cyclic loading sequence to ensure full contact of the specimen and sample.
7. Type I soils, of non-plastic, granular nature, are tested at a sample size of 6.0 inches in diameter, with a height of 12.0 inches. Type II soils, fine-grained cohesive soils, are tested at a sample size of 2.8 inches in diameter, with a height of 5.6 inches.

These changes are shown in tables 2.1 - 2.4.

Table 2.1 Testing Sequence for Fine Grained Materials Under AASHTO T274-82

Sequence Number	Confining Pressure, σ_3 (psi)	Maximum Axial Stress, σ_d (psi)	Number of Load Applications
Conditioning	6.0	1.0	200
Conditioning	6.0	2.0	200
Conditioning	6.0	3.0	200
Conditioning	6.0	8.0	200
Conditioning	6.0	10.0	200
1	6.0	1.0	200
2	3.0	1.0	200
3	0	1.0	200
4	6.0	2.0	200
5	3.0	2.0	200
6	0	2.0	200
7	6.0	4.0	200
8	3.0	4.0	200
9	0	4.0	200
10	6.0	8.0	200
11	3.0	8.0	200
12	0	8.0	200
13	6.0	10.0	200
14	3.0	10.0	200
15	0	10.0	200

Table 2.2 Testing Sequence for Subgrade Materials Under AASHTO T-274-82

Sequence Number	Confining Pressure, σ_3 (psi)	Maximum Axial Stress, σ_d (psi)	Number of Load Applications
Conditioning	5.0	6.0	200
Conditioning	5.0	10.0	200
Conditioning	10.0	10.0	200
Conditioning	10.0	15.0	200
Conditioning	15.0	15.0	200
Conditioning	15.0	20.0	200
1	20.0	1.0	200
2	20.0	2.0	200
3	20.0	5.0	200
4	20.0	10.0	200
5	20.0	15.0	200
6	20.0	20.0	200
7	15.0	1.0	200
8	15.0	2.0	200
9	15.0	5.0	200
10	15.0	10.0	200
11	15.0	15.0	200
12	15.0	20.0	200
13	10.0	1.0	200
14	10.0	2.0	200
15	10.0	5.0	200
16	10.0	10.0	200
17	10.0	15.0	200
18	5.0	1.0	200
19	5.0	2.0	200
20	5.0	5.0	200
21	5.0	10.0	200
22	5.0	15.0	200
23	1.0	1.0	200
24	1.0	2.0	200
25	1.0	5.0	200
26	1.0	7.5	200
27	1.0	10.0	200

Table 2.3 Testing Sequence for Subgrade Materials Under AASHTO TP46-94

Sequence Number	Confining Pressure, σ_3 (psi)	Maximum Axial Stress, σ_d (psi)	Cyclic Stress, σ_{cd} (psi)	Contact Stress, σ_d (psi)	Number of Load Applications
Conditioning	6.0	4.0	3.6	0.4	500-1000
1	6.0	2.0	1.8	0.2	100
2	6.0	4.0	3.6	0.4	100
3	6.0	6.0	5.4	0.6	100
4	6.0	8.0	7.2	0.8	100
5	6.0	10.0	9.0	1.0	100
6	4.0	2.0	1.8	0.2	100
7	4.0	4.0	3.6	0.4	100
8	4.0	6.0	5.4	0.6	100
9	4.0	8.0	7.2	0.8	100
10	4.0	10.0	9.0	1.0	100
11	2.0	2.0	1.8	0.2	100
12	2.0	4.0	3.6	0.4	100
13	2.0	6.0	5.4	0.6	100
14	2.0	8.0	7.2	0.8	100
15	2.0	10.0	9.0	1.0	100

Table 2.4 Testing Sequence Base/Subbase Materials Under AASHTO TP46-94

Sequence Number	Confining Pressure, σ_3 (psi)	Maximum Axial Stress, σ_d (psi)	Cyclic Stress, σ_{cd} (psi)	Contact Stress, σ_d (psi)	Number of Load Applications
Conditioning	15.0	15.0	13.5	1.5	500-1000
1	3.0	3.0	2.7	0.3	100
2	3.0	6.0	5.4	0.6	100
3	3.0	9.0	8.1	0.9	100
4	5.0	5.0	4.5	0.5	100
5	5.0	10.0	9.0	1.0	100
6	5.0	15.0	13.5	1.5	100
7	10.0	10.0	9.0	1.0	100
8	10.0	15.0	13.5	1.5	100
9	10.0	30.0	27.0	3.0	100
10	15.0	10.0	9.0	1.0	100
11	15.0	15.0	13.5	1.5	100
12	15.0	30.0	27.0	3.0	100
13	20.0	15.0	13.5	1.5	100
14	20.0	20.0	18.0	2.0	100
15	20.0	40.0	36.0	4.0	100

The revised AASHTO TP46-94 procedure is more accurate in laboratory simulation of loading due to vehicular traffic and is more accurate in representing actual stresses, which may be experienced in the field. Moreover, in a number of recent studies including Maher et al. (1996), Pezo et al. (1991), and Nazarian and Feliberti (1993) have addressed several of issues that require further research. These include the effect of preconditioning on sample integrity, contact of sample and end platens, grouting of the end platens to the specimen, the viability of existing loading sequences, and placement of LVDT's on the specimen inside the chamber or outside the chamber on the loading piston.

2.3 Factors Affecting Resilient Modulus

2.3.1 Effect of Confining Stress

Resilient modulus is derived from elastic, stress-strain relationships. Subgrade material derive their resistance to stress-caused deformation from interparticle friction, therefore, their stiffness depends very substantially on the intergranular (effective) confining stress existing at the location being considered as well as on the applied deviatoric stress (Hardcastle, 1992). The effect of confining stress is more pronounced on granular non-cohesive soils than on cohesive fine-grained soils. Granular soils develop interparticle friction from effective confining stress. Cohesive soils generate resistance from cohesion as well as confining stress. An example of resilient modulus as a function of confining stress is presented on figure 2.2. The degree to which the confining stress effects resilient modulus depends on the material properties for a given soil. Resilient modulus of fine-grained cohesive soils increase slightly with increasing

confining stress. This behavior is typical for fine-grained soils as noted by (Seed et al. 1962, Thomson and Robnett 1976, Pezo and Hudson 1994). In coarse grained materials, the increase of confining pressure (Rada and Witzack 1981) can significantly influence dynamic response of aggregate based materials. From this understanding (AASHTO T 274-82) the resilient modulus of coarse-grained materials is usually described as a function of the bulk stress θ (where $\theta = \sigma_1 + \sigma_2 + \sigma_3$), with a major influence placed on the confining stress or the first stress tensor.

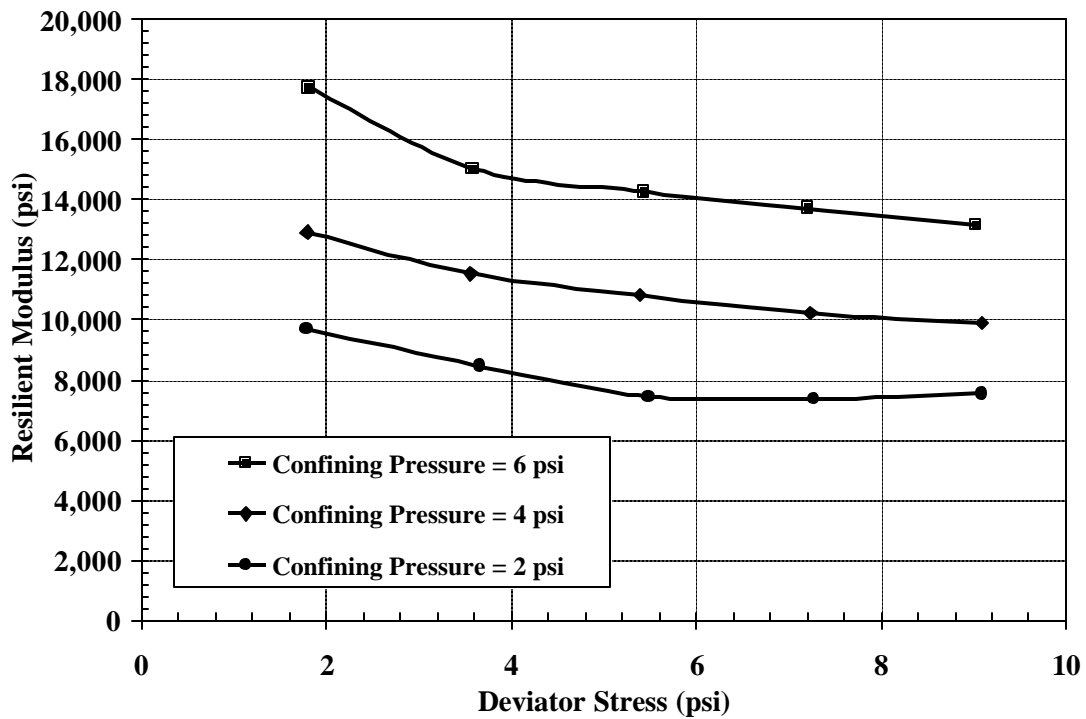


Figure 2.2 Effect of Resilient Modulus as a Function of Confining Stress

2.3.2 Effect of Deviatoric Stress

The resilient modulus of fine-grained, cohesive soils generally decreases with increasing deviatoric stress, referred to as stress softening behavior (Boateng-Poku and Drumm, 1989). As the deviator stress increases, the resilient modulus rapidly decreases,

as shown in figure 2.3 and referred to as strain softening. For coarse grained soils, the resilient modulus increases with increasing deviatoric stress as shown in figure 2.4 which indicates a strain hardening effect due to the reorientation of the grains into a denser state.

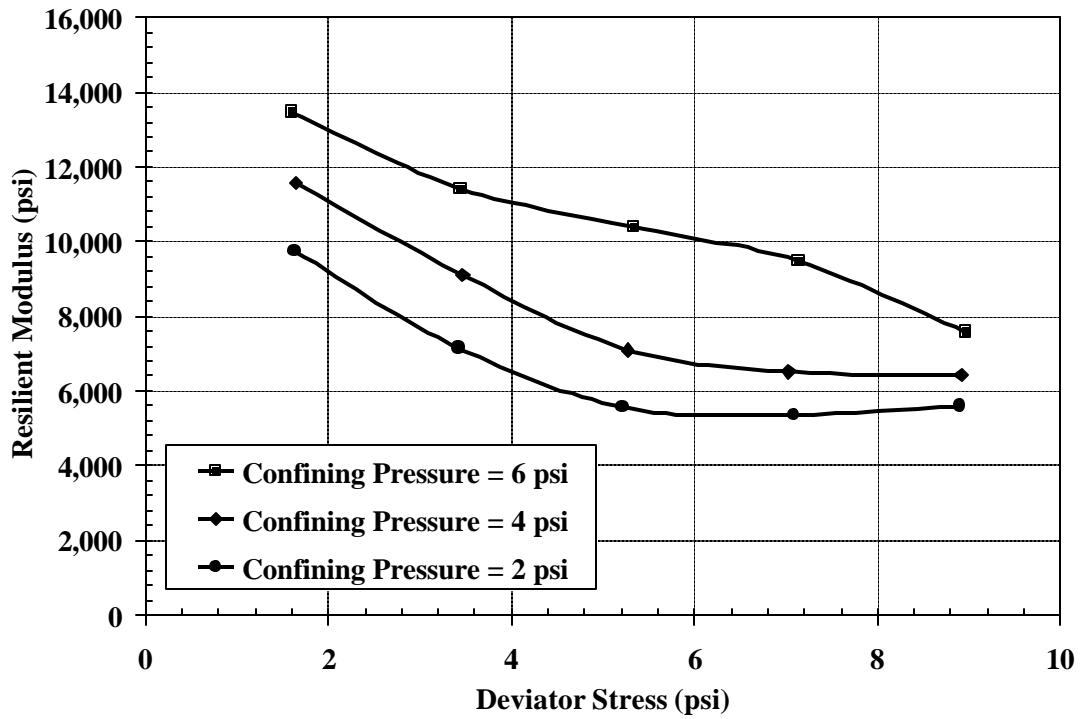


Figure 2.3 Effect of Deviatoric Stress on Fine-Grained Cohesive Material.

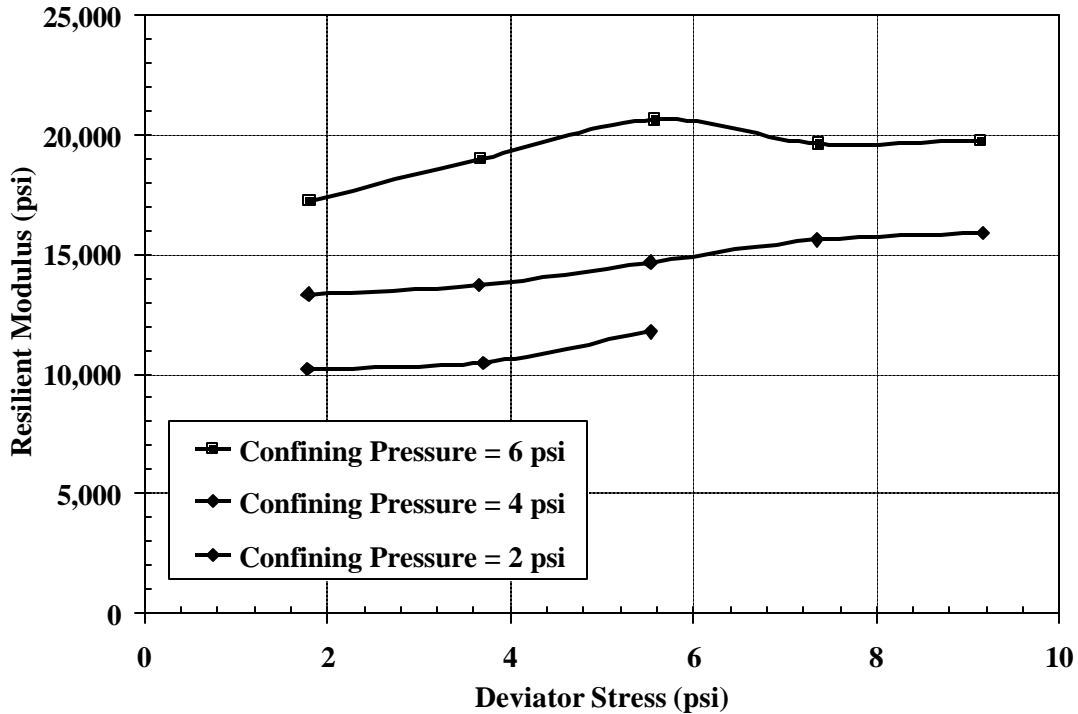


Figure 2.4 Effect of Deviatoric Stress on Coarse-Grained Non-Cohesive Material.

2.3.3 Moisture Effects on Resilient Modulus

For cohesive soils, a linear relationship between resilient modulus and soil moisture suction has been shown by (Dehlen 1969 and Finn et al. 1972). It has been proposed by Fredlund et al. (1975,1977) the resilient modulus is a function of three stress variables: net confining stress, the axial stress, and the matrix suction. The change in water content on fine-grained soils changes the effective (inter-granular) stresses take place as a result of the changes in soil suction (negative porewater pressures) which must accompany changes in soil water content in unsaturated soils. When the water content decreases in these materials, the suction along with effective stress and soil stiffness generally increase until very low water contents are reached. (Hardcastle 1992) Fine-

grained subgrade soils are especially problematic due to the generation of pore pressure during cyclic loading and their inability to rapidly to dissipate the excess pore pressure due to low hydraulic conductivity. As a result the effective stress will decrease resulting in excess permanent deformation of the pavement system, and a reduction of resilient modulus.

Previous studies have found the degree of saturation for granular non-cohesive soil depends on the amount of fines present in the soil matrix. Clean gravels and sands are less sensitive to moisture content due to the absence of small voids necessary to develop suction between soil particles.

In general, the increase of moisture content decreases the resilient modulus of soils as shown on figure 2.5. The rate of degradation is dependent on the soil type and gradation.

2.3.4 Temperature Effects

Temperature effects may have a great influence on the resilient modulus of the pavement system. In general, the significant effect of the system can be classified in three different categories: frozen, unfrozen or recently thawed condition. Freezing of fine and coarse-grained soils (Figure 2.6) has been shown to significantly increase the resilient modulus compared to the unfrozen conditions as shown by Chamberlain et. al. 1989, Smith et al. 1978, Vinson 1978, and Cole et al. 1981. The resilient modulus of frozen soil is practically independent confining stress, however it varies slightly with higher deviator stress levels and temperatures (Cole et al. 1981).

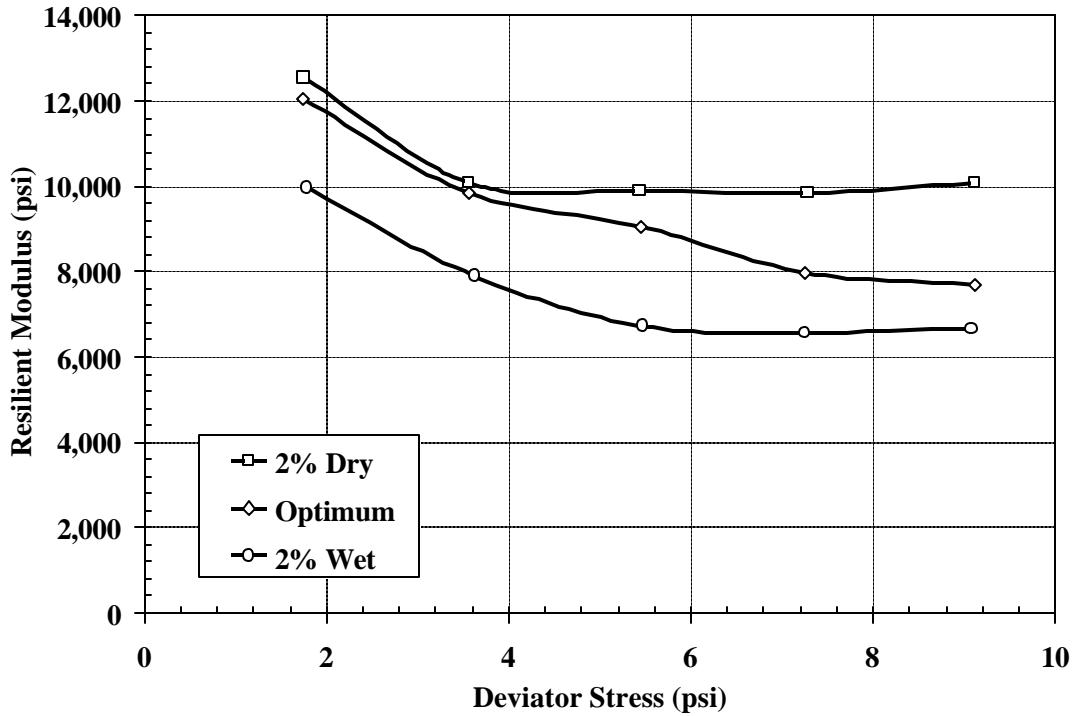


Figure 2.5 Effect of Moisture Content on Resilient Modulus (2 psi Confining Pressure).

Resilient modulus of recently thawed soils have found to exhibit a significant decrease in resilient modulus as compared to the unfrozen or frozen conditions as shown by Cole et al. 1981, Bergen et al. 1973,). Chamberlain concluded that the decrease in resilient modulus accompanying freezing and thawing were caused by the increase in water content and decrease in unit weight that occurred when soils are frozen with free access to water (open system freezing).

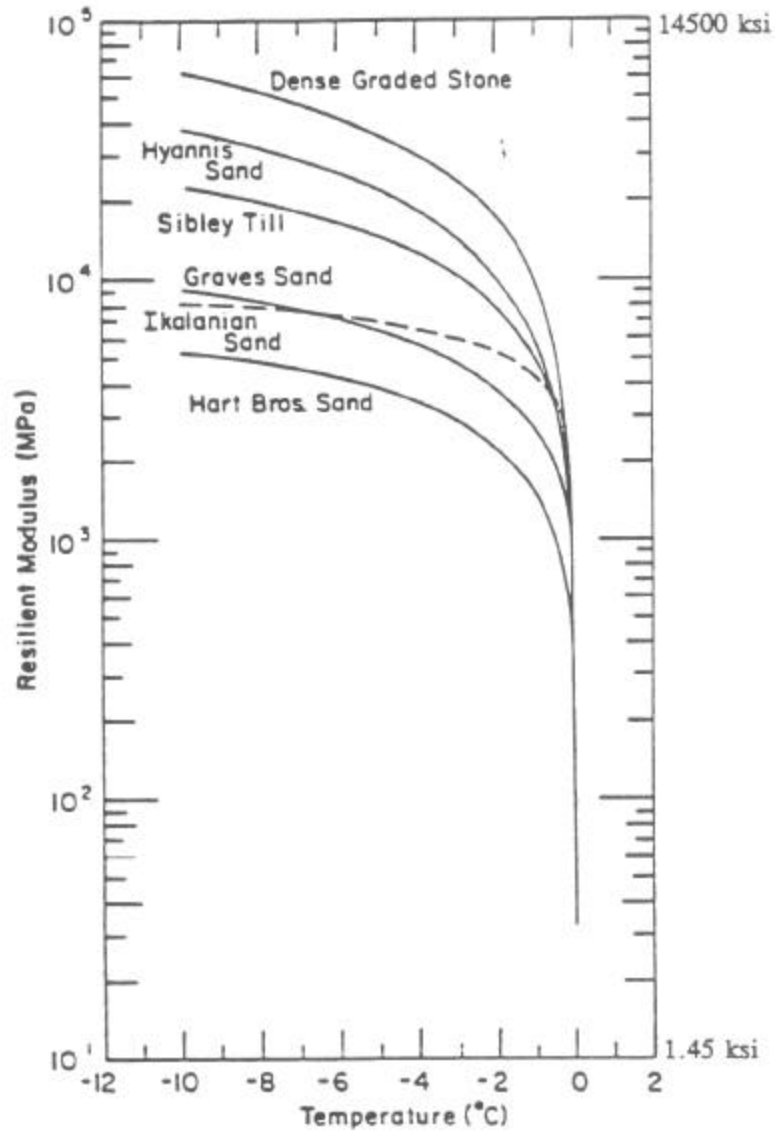


Figure 2.6 Effect of Temperature on Resilient Modulus of Frozen Coarse-grained Soils (Chamberlain et.al. 1989)

2.3.5 Effects of End Conditions

Before conducting a resilient modulus test, AASHTO requires the specimen to undergo 500-1000 conditioning cycles to provide a uniform contact between the top and bottom platens and the soil specimen. The main purpose of conditioning sequence is to

minimize an uneven contact between the specimen and platens. Pezo et al. (1992) concluded that the conditioning sequence is an unnecessary step if the ends of the specimen are grouted to the platens. They felt that specimen conditioning did not provide an intimate contact between the specimen and platens. In their opinion, specimen conditioning affected the resilient modulus of the material by subjecting it to high stresses before running the resilient modulus test. Nazarian and Feliberti (1993) corroborated with Pezo et al. (1992) and indicated stress history plays an important role in the modulus of soils. Therefore they concluded grouting the specimen to the top and bottom platens should be implemented and the conditioning sequence eliminated.

Grouting the specimen to the top and bottom platens imposes additional problems. To accurately measure the resilient modulus of specimen, the axial deformations must be measured. In the case of the grouted specimen, the axial deformations could not be measured using the full length of the specimen due to large shear stress generated in the grout zone. Therefore if the specimens were grouted to the top and bottom loading platens, deformations must be made on the middle third of the specimen. Taken the deformation measurements within the middle third of the sample proved to be a better method (Maher et.al. 1996). An additional problem with grouting the specimen ends is the effect of pore pressure generation. If a sample is tested under saturated conditions, pore pressures might develop since the grout would not allow the excess pore pressure to dissipate. These methods were implemented for research purposes, and do not comply with the current AASHTO TP46-94 specification for determining the resilient modulus of soils.

2.3.6 Specimen Size and Preparation

Specimen size and preparation has been changing throughout the inception of the AASHTO resilient modulus test. Specimen sizes have varied from 2.8 in. (71.1 mm) and 4.0 in. (101.6 mm) diameter for fine-grained soils and 4.0 in. (101.6 mm) and 6.0 in. (152.4 mm) diameter for coarse-grained soils.

Compaction methods have also varied depending on the soil type and gradation of the soil. Methods of compaction implemented for resilient modulus tests have varied from vibrating tables and probes for granular materials and static and dynamic compaction techniques for cohesive fine grains. The current methods used for conduction a resilient modulus test in accordance to AASHTO specifications are reported in Chapter 3.

III. EXPERIMENTAL PROGRAM

3.1 Introduction

Resilient modulus of base, subbase and subgrade materials is determined by repeated load triaxial tests on unbound material specimens. Resilient modulus is the ratio of axial cyclic stress to the recoverable strain. In order to determine the resilient modulus of unbound materials, a cyclic stress of fixed magnitude for a duration of 0.1 sec must be applied to the specimen followed by a 0.9 sec rest period. During the test the specimen is subjected to a confining stress provided by means of a triaxial pressure chamber.

The resilient modulus test provides a means of characterizing base, subbase and subgrade material for the design of pavement systems. These materials can be tested under a variety of conditions, some of which include stress state, moisture content, temperature, gradation and density. In order to accurately measure the resilient modulus of these materials, a sophisticated testing system must be utilized.

3.2 Experimental Equipment

3.2.1 Resilient Modulus Testing Device

The loading system used was a MTS “soil machine”, which consists of an eight foot loading frame and servo controlled hydraulic actuator as shown in figure 3.1. The loading frame has a movable crosshead to allow for easy placement and removal of the triaxial chamber. A 22,500 lbf (100 kN) servo controlled actuator is mounted on the movable crosshead, and is capable of providing displacements of ± 5.0 in. (± 125 mm). For the resilient modulus test, the actuator was equipped with a 5,600 lbf (25 kN) load cell for increased accuracy of the measured load. When testing the 6.0 in. diameter

specimen, full scale of the 5,600 lbf load cell was used, however when testing the 2.8 in. diameter sample, 20% of full scale was used to achieve a higher resolution.

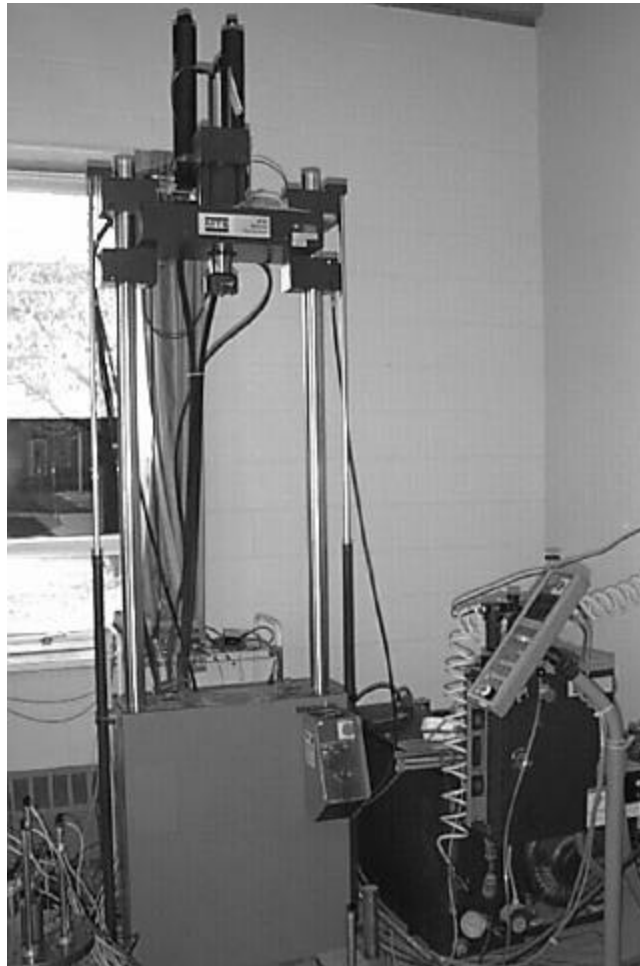


Figure 3.1 Load Frame with 5,600 lbf Load Cell and Hydraulic Pump

3.2.2 Triaxial Cell

A triaxial cell capable of testing specimens with a diameter of 2.8 in. to 6.0 in. and a height of 5.6 in. to 12.0 in. as shown in Figures 3.2 and 3.3 respectively. The top

plate of the chamber was modified to hold a pressure transducer, two pore water pressure transducers, six proximity sensors, and four linear variable differential transformers (LVDT's). The pressure transducer was used to measure the cell pressure that provided confining stress to the specimen. Pore pressure transducers were connected to the top and bottom platens to measure the pore pressure in the sample. The three pressure transducers have a full-scale capacity of 100 psi and an accuracy of 0.1 psi. The proximity sensors were not used in this research project.

The LVDT's used had a measuring range of ± 0.25 in. and an accuracy of 0.0005 in., for measuring the deformations in the 6.0 in. diameter sample and the ± 0.05 in. with an accuracy of 0.00001 in., for measuring deformations in the 2.8 in. specimen. Specimens were measured using two LVDT's mounted externally on the triaxial chamber with gage ratio of one for all the tests in this study.

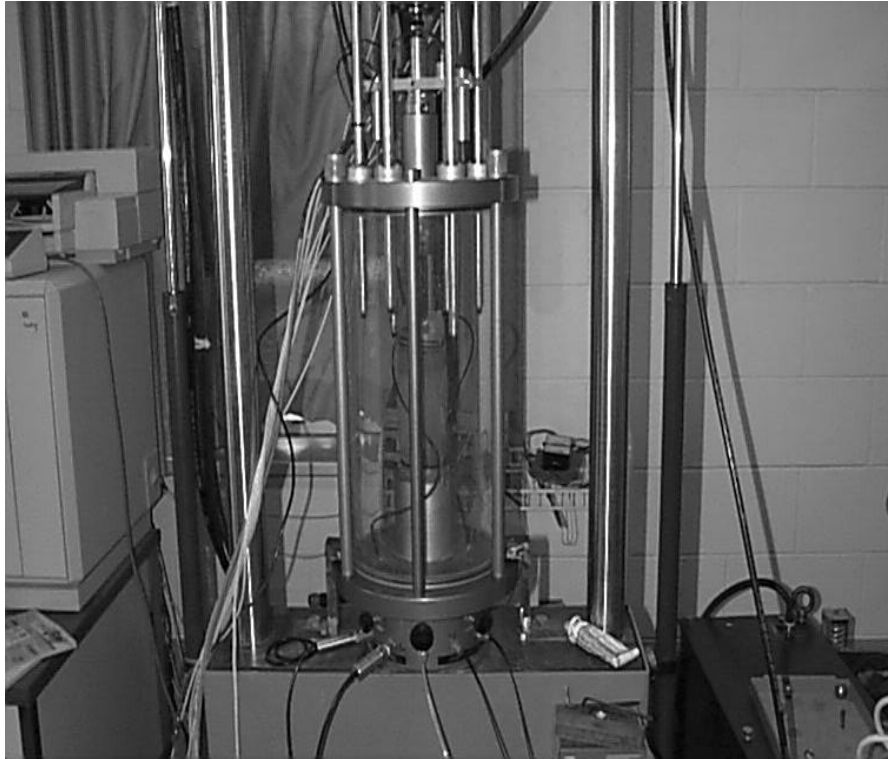


Figure 3.2 2.8 in. Diameter Specimen in Triaxial Pressure Chamber



Figure 3.3 6.0 in. Diameter Specimen in Triaxial Pressure Chamber

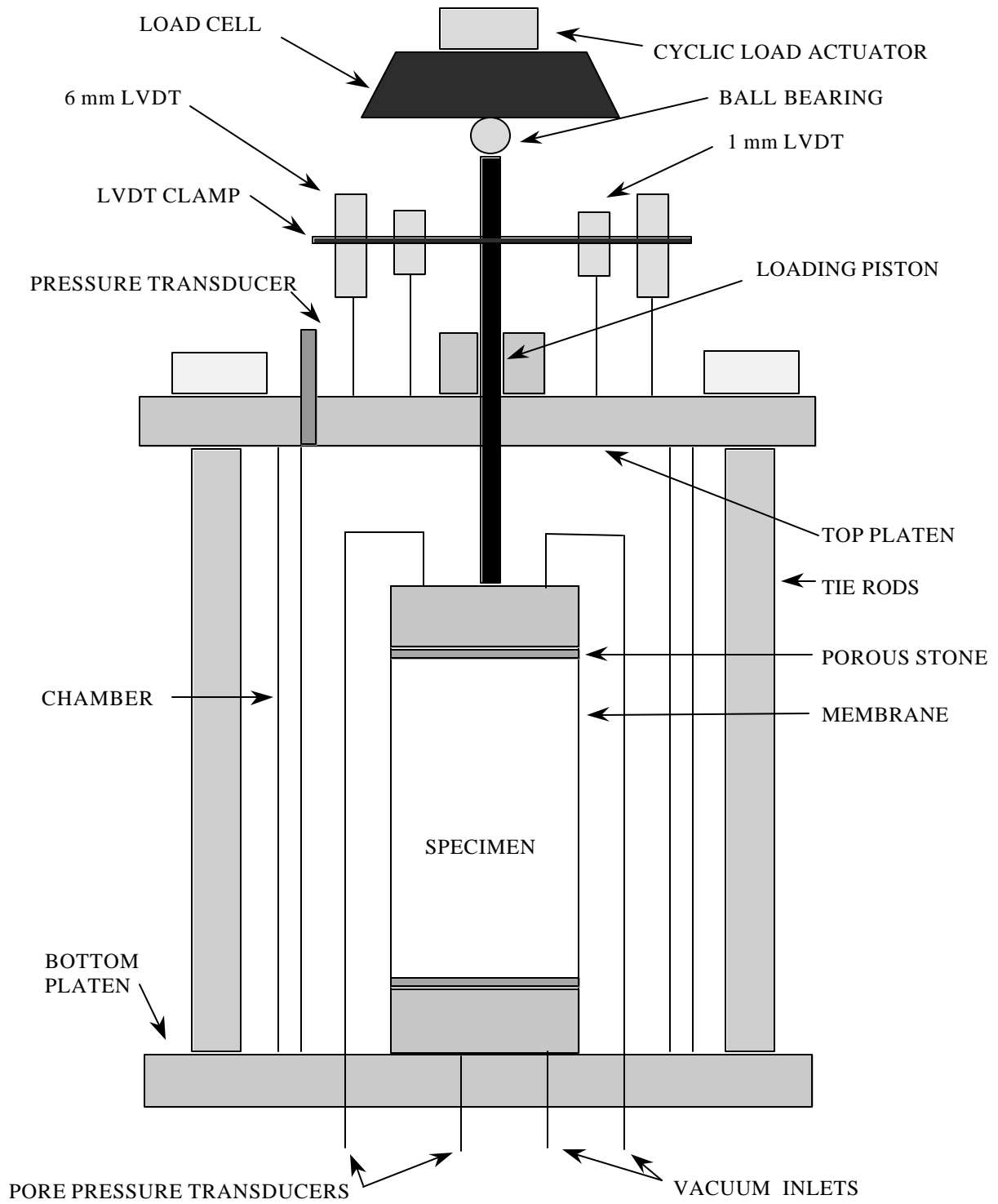


Figure 3.4 Schematic of Triaxial Chamber and Test Specimen

3.2.2 Calibration of System

Prior to testing soil specimens, the testing system was evaluated using three synthetic samples. The three synthetic samples were classified as soft, medium, and hard with known moduli of 8700 psi, 18,700 psi, and 76,600 psi, respectively. (Nazarian et al., 1996). The actual resilient modulus of these samples is compared to experimental resilient modulus as shown in Table 3.1.

Table 3.1 Calibration of Resilient Modulus Setup

Specimen Type	Actual Resilient Modulus (psi)	Experimental Resilient Modulus (psi)	Difference (%)
SOFT	8700	7250	16.67
MEDIUM	18,700	18,400	1.55
HARD	76,600	89,840	17.23

The measured resilient modulus of the soft specimen yielded a M_r value of 7250 psi with an underestimation of approximately 16 %, while the hard specimen yielded a M_r value of 89,840 psi, with an overestimation of the actual M_r by approximately 17 %. The medium specimen yielded a resilient modulus value of 18,400 psi, which underestimated the actual specimen by approximately 1 %. The specimens were tested without the use of grout between the specimen and platens, which may explain the scattered results on soft and hard samples, due to imperfections of the ends. Without precision machining of the ends, practically any modulus value could be obtained depending on the setup (Nazarian and Feliberti, 1993). The medium specimen had

parallel ends, therefore the use of grout was not considered. Better results have been shown on ungrouted materials when the ends were precisely machined (Nazarian and Feliberti, 1993).

3.2.3 Data Acquisition and Reduction

The data was acquired through the MTS Teststar II system and saved on a 486/66 PC computer with 16 megabytes of ram. A program was written to execute the 15 loading sequences use to determine the resilient modulus at different stress states. The system was programmed using Testware SX to acquire data from four external LVDT's, and two pore water pressure transducers, and a chamber pressure transducer, every time a peak and valley transpired from the load cell during the resilient modulus test. The data was saved in a spreadsheet format where the analysis was performed. A reduction and data analysis program was written to calculate the mean resilient modulus for the last five cycles of each loading sequence.

3.3 Specimen Preparation

Specimen preparation is accomplished in accordance with AASHTO TP46-94 Standard Test Method for Determining the Resilient Modulus of Soils and Aggregate Materials. This test method classifies subgrade soils in two categories. Type 1 soil is classified as all materials which meet the criteria of less than 70% passing the number 0.0787 in. (2.00 mm) sieve and less than 20% passing the No. 200 sieve (75- μ m), and which have a plasticity index of 10 or less. These soils are compacted in a 6.0 in.

diameter mold. Type 2 soils include all material that does not meet the criteria for type 1. These soils are compacted in 2.8 in. diameter mold.

3.3.1 Preparation and Compaction of Type 1 Soils

1. Approximately 26.5 lb (12 kg) of soil was mixed with the appropriate amount of water to achieve desired moisture content for the test specimen.
2. For the 6.0 in. diameter sample, the specimen height is 12.0 in. The sample was compacted in 6 equal layers (N) of 2.0 in. The mass of each layer (W_1) of wet soil was determined to produce the appropriate density (W_t).

$$W_1 = W_t / N \quad (3.1)$$

3. A rubber membrane was placed over the bottom platen and lower porous stone, with an O-ring securing the membrane to the lower platen to obtain an air tight seal.
4. A compaction split mold was placed around the bottom platen and tightened firmly in place.
5. The membrane was then stretched over the upper rim of the mold, while applying a vacuum to draw the membrane to the inside of the mold (Figure 3.5)
6. The amount of wet soil was placed into the mold equal to the weight of one layer.
7. The vibrating compaction head was inserted into the mold and the soil was vibrated until the height of the compacted layer was 2.0 in. Steps 6 through 7 were repeated until a final of height of 6.0 in. was achieved.

8. The top platen was placed onto the compacted sample and the membrane was rolled off the mold and over the platens. An O-ring was placed over the membrane to ensure an air tight seal between the membrane and platens.
9. A vacuum was applied to the sample through a bubble chamber to check for leaks in the membrane that may have occurred during compaction (Figure 3.6).
10. The triaxial chamber was assembled and a confining pressure of 15.0 psi was applied.
11. The triaxial chamber was placed into the loading frame to conduct the resilient modulus test.



Figure 3.5 Compaction Mold and Vibrating Compaction Hammer

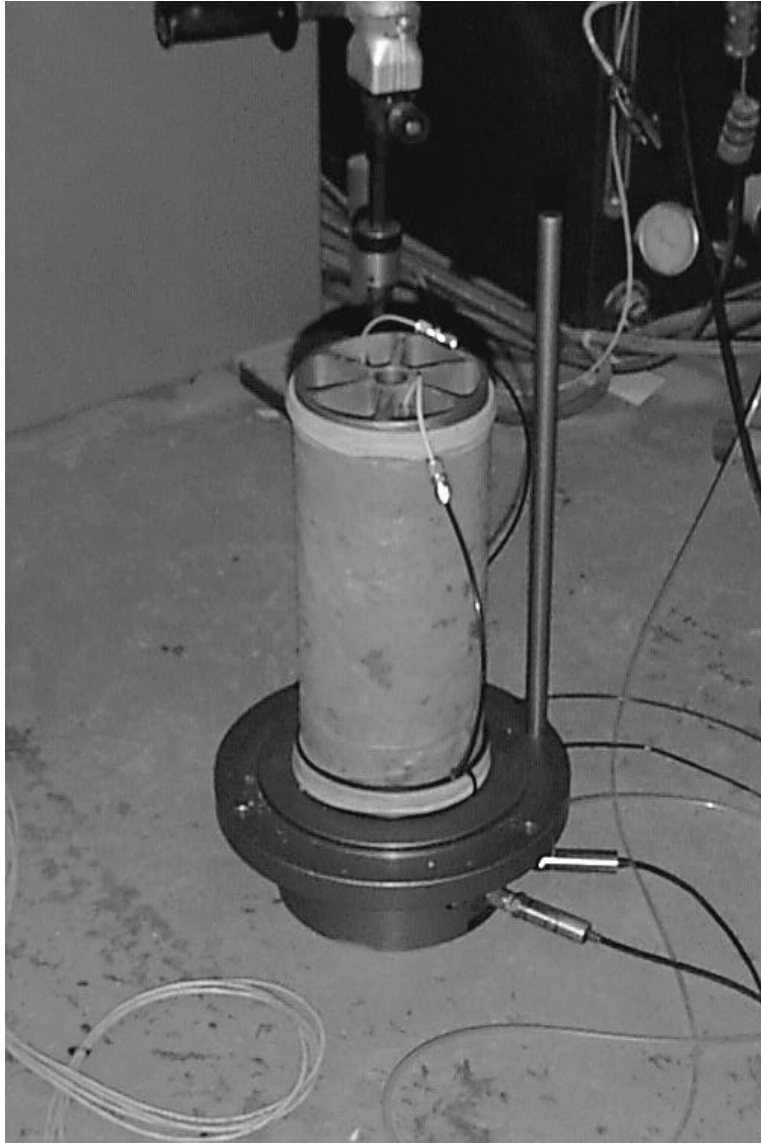


Figure 3.6 Compacted Specimen Confined with Applied Vacuum.

3.3.2 Preparation and Compaction of Type 2 Soils

1. Approximately 3.3 lb (1500 g) of soil was mixed with the appropriate amount of water to achieve desired moisture content for the test specimen.
2. For Type 2 soils, the sample was compacted in 5 equal layers of 1.12 in. with a diameter of 2.8 in. and a final height of 5.6 in. The weight of each layer was determined to produce the appropriate density (Equation 3.1).
3. One of the plungers was placed into the specimen mold prior to the addition of the soil mass.
4. After the soil was added, the second plunger was inserted into the compaction mold. The compaction mold and plungers were placed into the loading frame. A load was placed on the plunger to compact the layer until the plungers rested firmly on the compaction mold. The load was then decreased and the compaction mold was removed from the loading frame.
5. One of the plungers was removed and the top of the compacted layer was scarified to ensure integration of the next layer.
6. The next layer of soil was added to the compaction mold. A spacer equal to the height of the prior layer was placed on top of the compaction mold before the insertion of the plunger as shown in figure 3.7.
7. Steps 4 through 6 were repeated until all 5 layers were compacted.
8. Using the extrusion ram, the compacted specimen was pressed out of the compaction mold.

9. The specimen was then placed on the bottom platen of the triaxial chamber. Using a vacuum membrane expander, the membrane was placed over the specimen and rolled over the top and bottom platens. O-rings were used to secure the membrane to the platens to ensure an air tight seal.
10. A vacuum was applied to the sample with a bubble chamber to check for leaks in the membrane.
11. The triaxial chamber was assembled and a confining pressure of 6.0 psi was applied.
12. The triaxial chamber was placed into the loading frame to conduct the resilient modulus test.

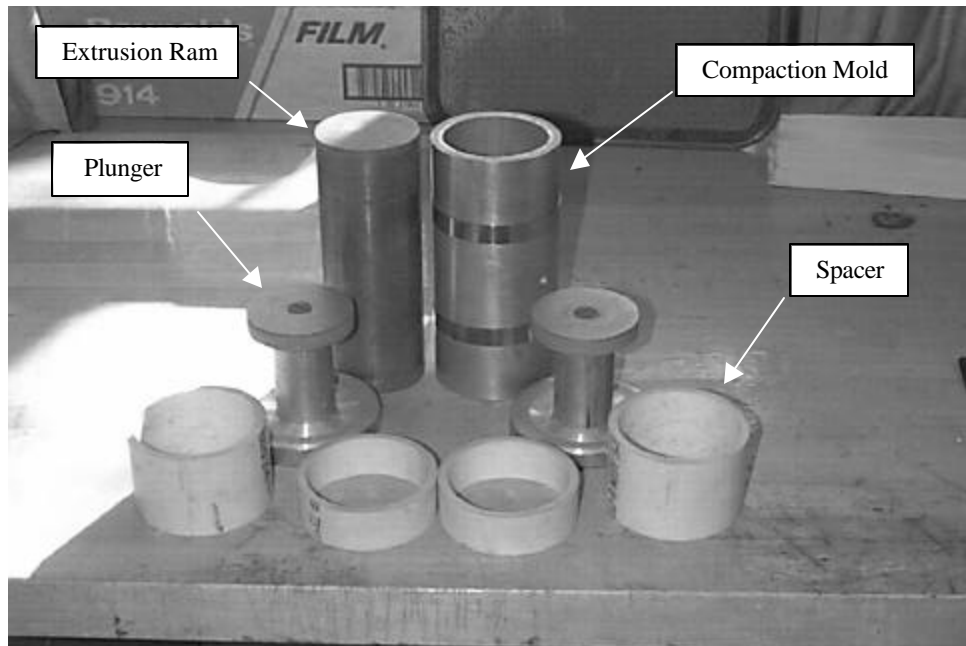


Figure 3.7 Compaction Mold, Plungers, Spacers, and Extrusion Ram

3.3.3 Saturation Procedure

The objective of saturating the specimen is to fill all the voids in the specimen with water without prestressing the specimen or allowing it to bulge.

1. Assemble the triaxial chamber with compacted specimen in place.
2. Apply a small confining pressure (typically 5 psi) to assure rigidity of the sample and open the drainage valves.
3. Allow the top and bottom pore pressure transducers to equalize.
4. Simultaneously increase chamber and back pressure with the drainage valves open to allow deaired water from the burette connected to the bottom flow through the specimen. The differences in back pressure and chamber pressure should not exceed 5 psi.
5. When water appears in the upper burette, close the upper and lower drainage valves and measure the change in pore pressure over a 1 minute interval. If the change in pore pressure is less than 1 %, check for B value.

3.3.4 B-Determination

Upon completion of the saturation procedure, it is necessary to determine if the sample is sufficiently saturated. A sufficiently saturated soil should have a B value of at least 0.95.

The pore pressure parameter B is defined by the following equation;

$$B = \Delta u / \Delta \sigma_3$$

where :

Δu = the change in the specimen pore pressure that occurs as a result of a
change in the chamber pressure when the drainage valves are closed

$\Delta \sigma_3$ = the change in chamber pressure

3.4 Testing Sequence

The testing sequence for this experimental program to evaluate the resilient modulus of subgrade soils is presented in Table 3.2. The cyclic load is applied a haversine shape form of $(1-\cos \Theta)/2$ as shown in figure 3.8. The maximum axial stress is defined as the cyclic stress plus the contact stress, where the contact stress is 10% of the maximum axial stress. A contact stress on the specimen is necessary to insure an intimate contact between the specimen and platens throughout the cyclic process. If an intimate contact between the loading platens and the specimen is not achieved, an inaccurate measurement of resilient modulus may result. The cyclic stress is 90% of the maximum applied axial stress of which the resilient modulus is calculated. The cyclic stress pulse has a duration of 0.1 s with a rest period of 0.9 s. During the rest period of 0.9 s. a contact stress is maintained to ensure contact between the loading platens and the specimen.

Table 3.2. Testing Sequence for Subgrade Materials

Sequence Number	Confining Pressure, σ_3 (psi)	Maximum Axial Stress, σ_d (psi)	Cyclic Stress, σ_{cd} (psi)	Contact Stress, σ_d (psi)	Number of Load Applications
Conditioning	6.0	4.0	3.6	0.4	500-1000
1	6.0	2.0	1.8	0.2	100
2	6.0	4.0	3.6	0.4	100
3	6.0	6.0	5.4	0.6	100
4	6.0	8.0	7.2	0.8	100
5	6.0	10.0	9.0	1.0	100
6	4.0	2.0	1.8	0.2	100
7	4.0	4.0	3.6	0.4	100
8	4.0	6.0	5.4	0.6	100
9	4.0	8.0	7.2	0.8	100
10	4.0	10.0	9.0	1.0	100
11	2.0	2.0	1.8	0.2	100
12	2.0	4.0	3.6	0.4	100
13	2.0	6.0	5.4	0.6	100
14	2.0	8.0	7.2	0.8	100
15	2.0	10.0	9.0	1.0	100

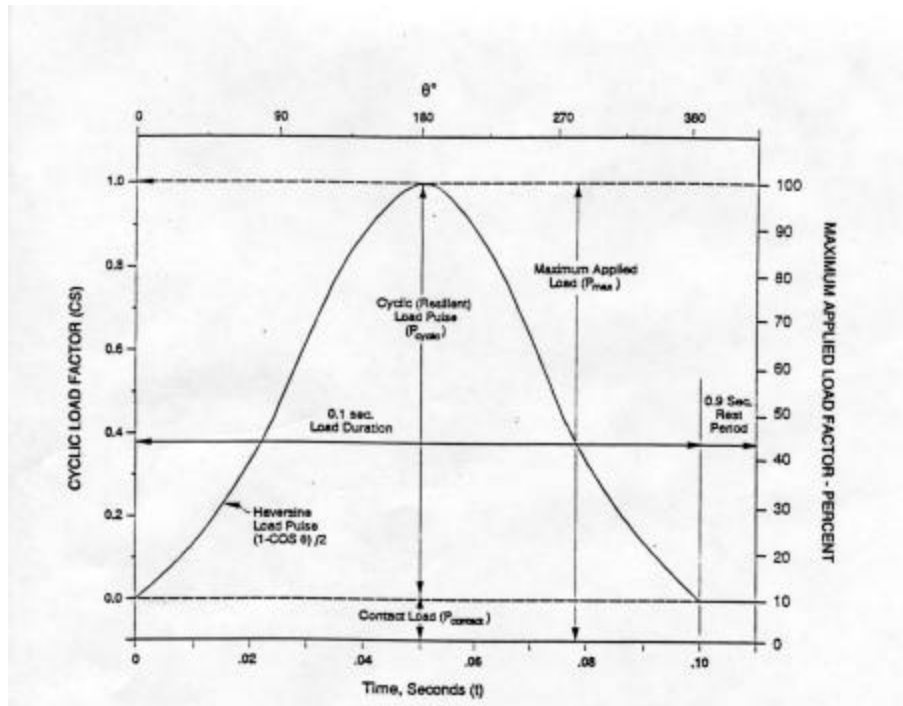


Figure 3.8 Haversine loading Sequence for the Resilient Modulus Test

3.5 Soil Classification

The experimental investigation which provided data for developing empirical relationships between model constants and soil properties included basic soil testing and resilient modulus tests on 6 different subgrade soils which are commonly found in the state of New Jersey. The soils are classified in two main groups as designated by AASHTO TP46-94, and further classified using AASHTO M-145. The soils were classified using sieve analysis (Figure 3.9 & Table 3.3), liquid and plastic limits (Table 3.3).

3.5.1 Type 1 Soils

For the purpose of resilient modulus testing, Type 1 materials include all untreated granular base and subbase material and all untreated subgrade soils which meet the criteria of less than 70 percent passing the 0.0787 in. (2.00 mm) sieve and less than 20 percent passing the No. 200 (75 μ m) sieve, and which have a plasticity index of 10 or less. These soils were molded in 6.0 diameter mold.

3.5.2 Type 2 Soils

For the purpose of resilient modulus testing, Type 2 materials include all granular base/subbase and untreated subgrade soils not meeting the criteria for material type 1 as given above. These soils were compacted in a 2.8 in. diameter mold.

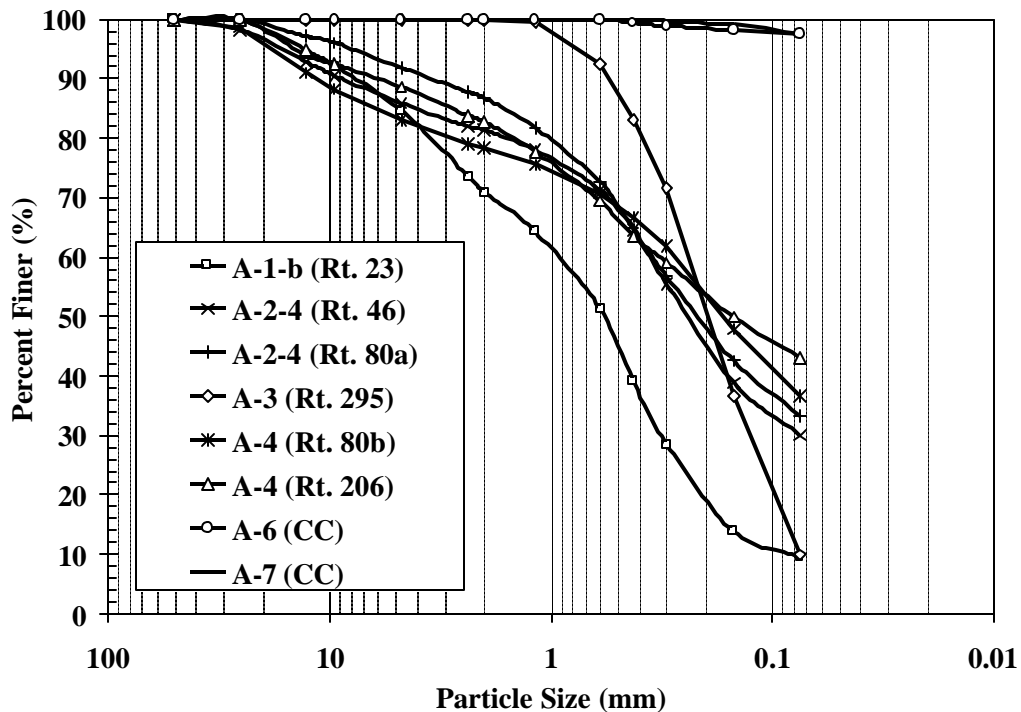


Figure 3.9 Gradation Analysis of Soils Tested

Table 3.3 Type 1 and Type 2 Soil Classifications

Soil Location	Percent Passing 2.00 mm	Percent Passing 75 mm	Liquid Limit (%)	Plastic Limit (%)	Plastic Index (%)	AASHTO TP 46-92 Classification	AASHTO M 145 Classification
Rt. 23	66.6	7.6	0	N.P.	N.P.	Type 1	A-1-b
Rt. 46	81.5	30.1	15	N.P.	N.P.	Type 2	A-2-4
Rt. 80a	86.8	33.3	0	N.P.	N.P.	Type 2	A-2-4
Rt. 295	99.8	9.9	0	N.P.	N.P.	Type 2	A-3
Rt. 80b	78.4	36.6	20.5	19	1.5	Type 2	A-4
Rt. 206	82.8	43	21	17	4	Type 2	A-4
Cumberland County	100	97.5	39.1	20.2	18.9	Type 2	A-6
Cumberland County	100	97.7	52.5	25.1	27.4	Type 2	A-7

3.6 Moisture Density Relationship

A series of compaction tests were conducted to determine the moisture density relationship for each of the soils collected. The optimum moisture content and maximum dry density was determined based on AASHTO T99-94 Moisture-Density Relations of Soils Using a 2.5 kg rammer and a 305 mm drop as presented in Figures 3.10 to 3.17 and table 3.4. However, both the A-6 and the A-7 soils were compacted under AASHTO T180-94 Moisture-Density Relations of Soils Using a 4.5 kg rammer and a 457 mm drop since both soils fall into the category of medium to high plasticity fine-grained soils (FHWA Publication No. FHWA-RD-97-083).

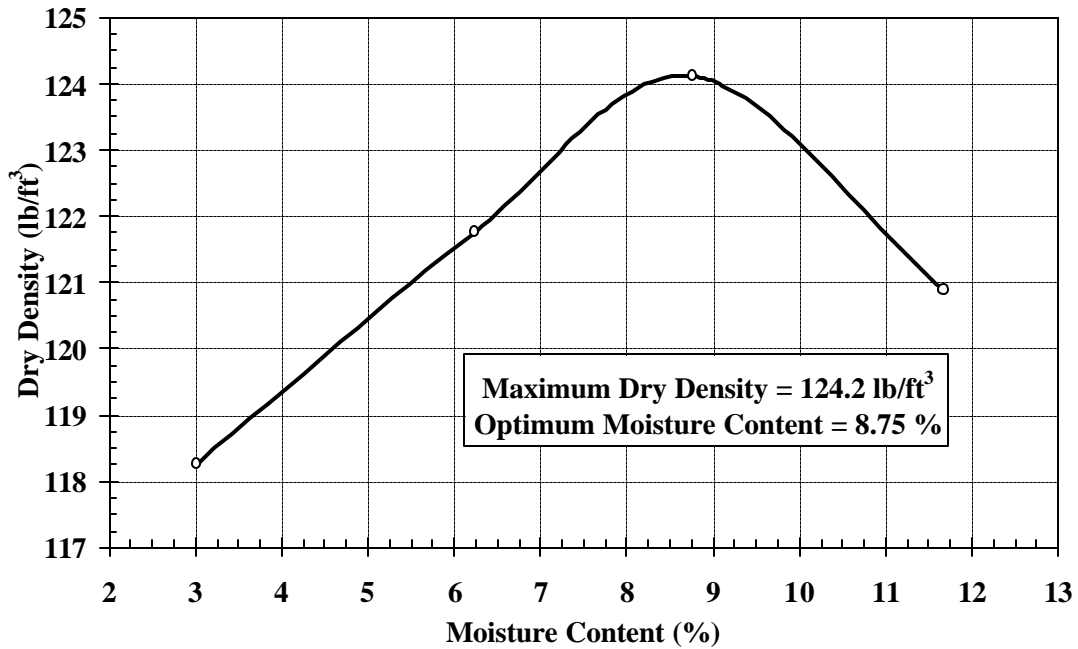


Figure 3.10 Moisture Density Relationship for Rt. 23 soil Soil

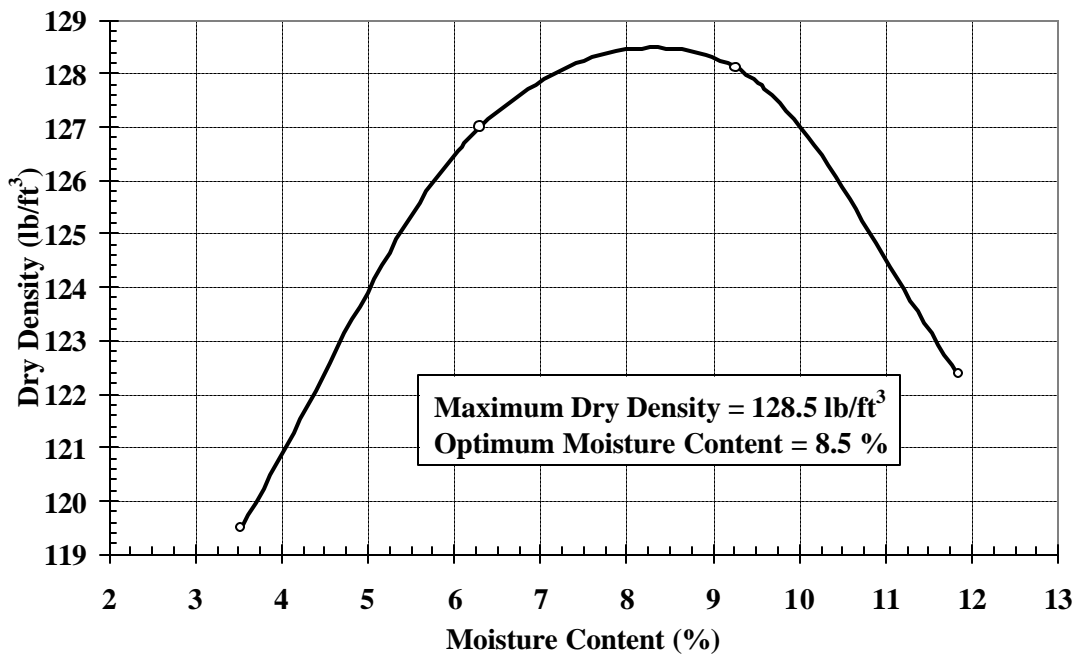


Figure 3.11 Moisture Density Relationship for Rt 46 Soil

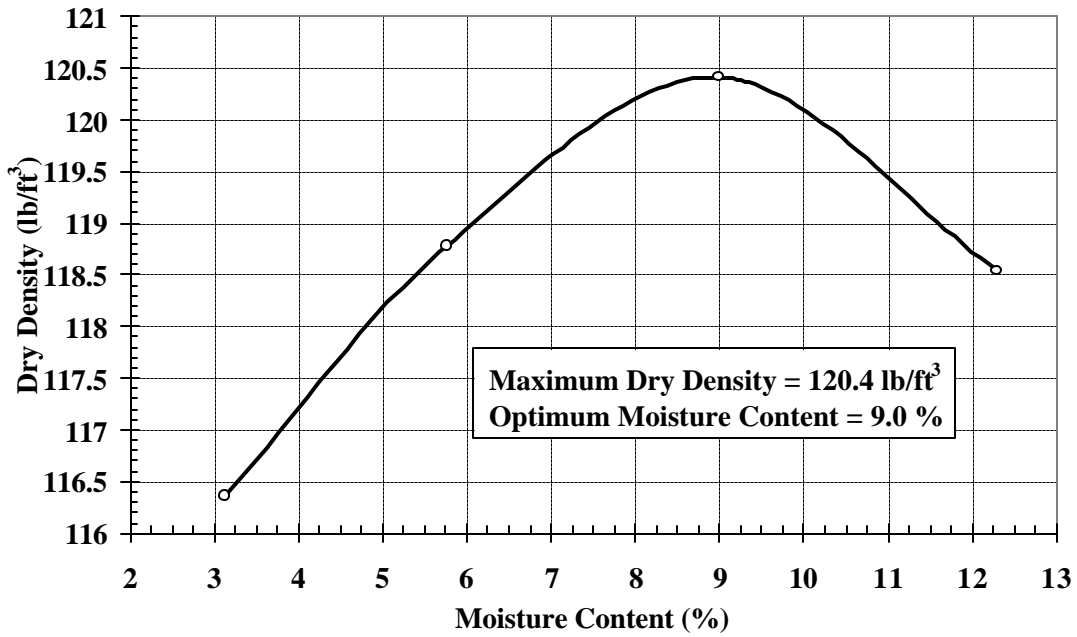


Figure 3.12 Moisture Density Relationship for Rt 80a Soil

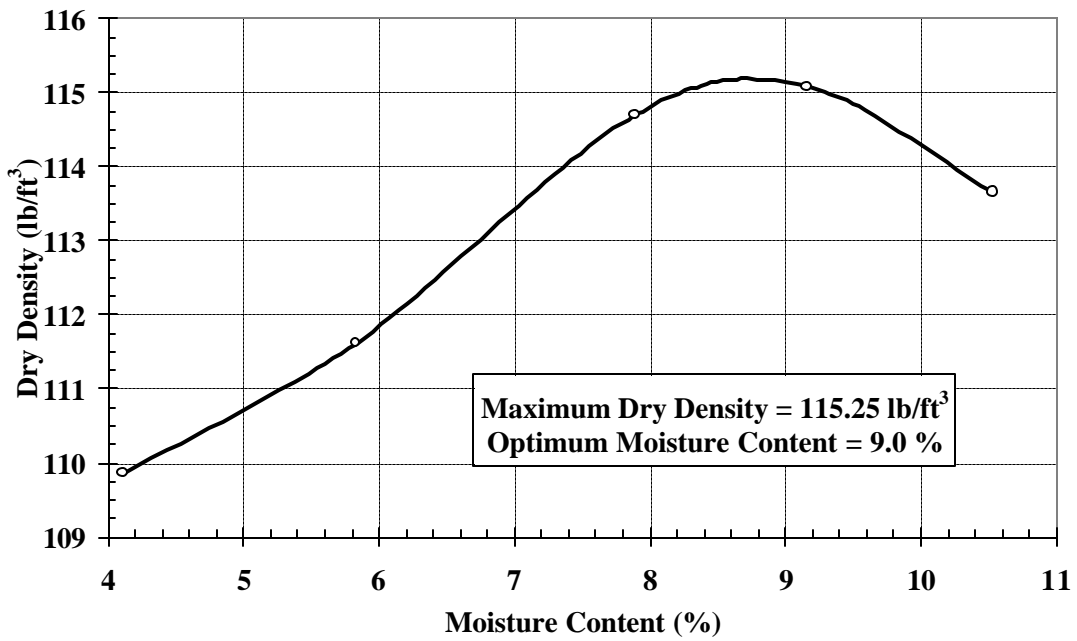


Figure 3.13 Moisture Density Relationship for Rt. 295 Soil

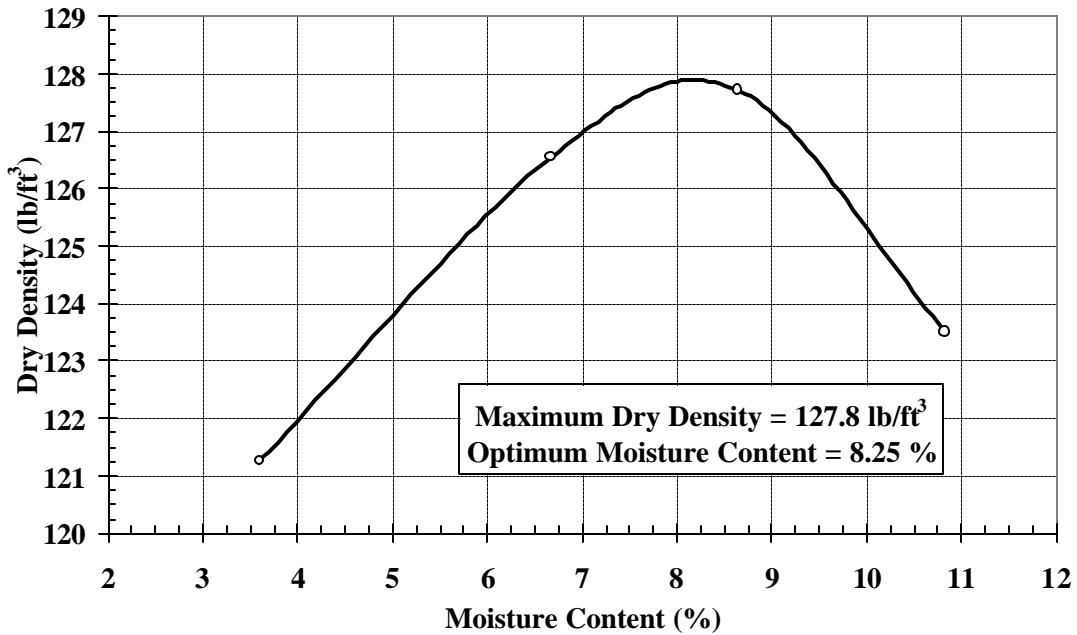


Figure 3.14 Moisture Density Relationship for Rt. 80b Soil

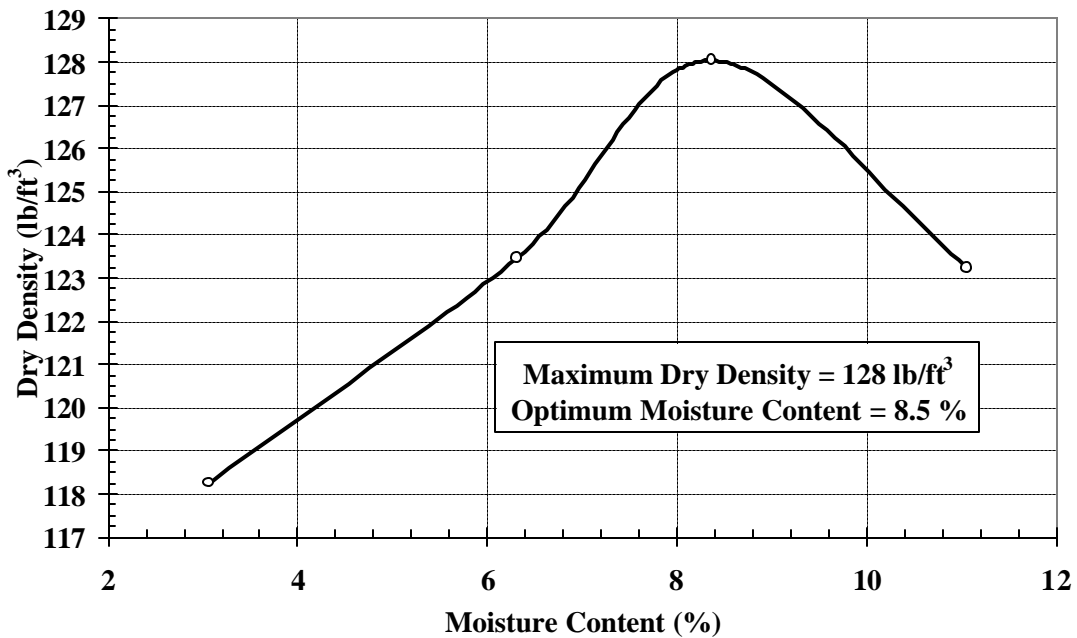


Figure 3.15 Moisture Density Relationship for Rt. 206 Soil

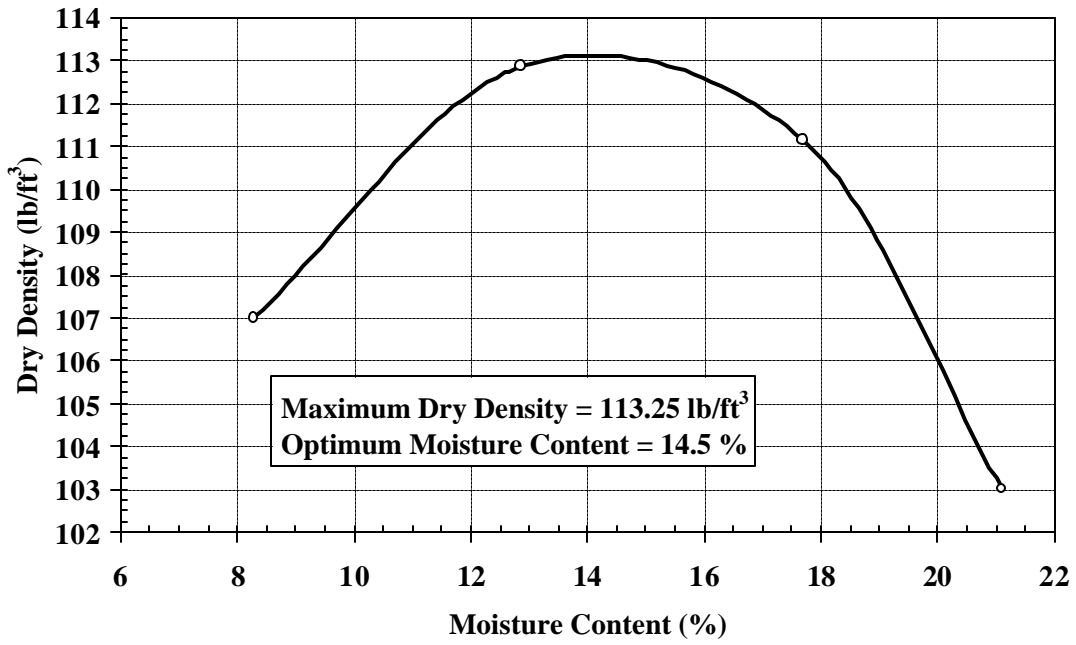


Figure 3.16 Moisture Density for Cumberland County (A-6) Soil

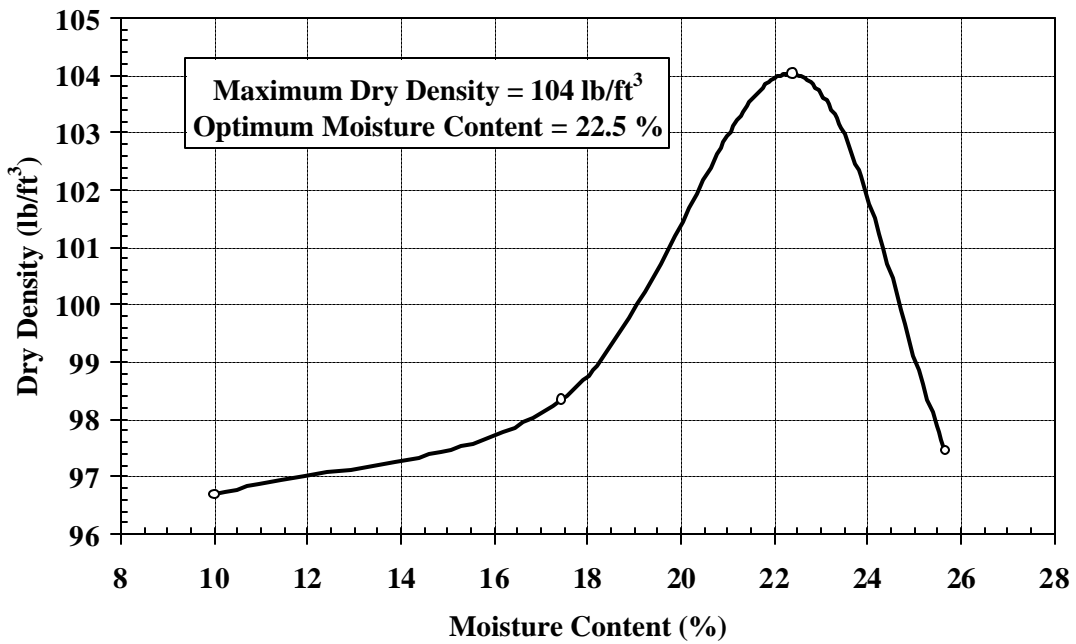


Figure 3.17 Moisture Density for Cumberland County (A-7) Soil

Table 3.4 Maximum Dry Density at Optimum Moisture Content

Soil Location	AASHTO Classification	Maximum Dry Density (lb/ft³)	Optimum Moisture Content (%)
Rt. 23	A-1-b	124.2	8.75
Rt. 46	A-2-4	128.5	8.5
Rt. 80a	A-2-4	120.4	9.0
Rt. 295	A-3	115.25	9.0
Rt. 80b	A-4	127.8	8.25
Rt. 206	A-4	128	8.5
Cumberland County	A-6	113.25	14.5
Cumberland County	A-7	104	22.5

Resilient modulus tests were conducted on specimens compacted at optimum moisture content, 2% wet of optimum, 2% dry of optimum, and saturated for the Rt. 295 soil. The corresponding densities for the different moisture contents were evaluated using the compaction curves for each individual soil.

Table 3.5 Void Ratio and Percent Saturation for Typical Specimens

Soil Location	AASHTO Classification	Moisture Content Type	Moisture Content (%)	Dry Density (lb/ft ³)	Specific Gravity	Void Ratio	% Saturation (%)
Rt. 23	A-1-b	2% Wet	10.5	121.7	2.69	0.37982	74.4
		OMC	8.5	124.2	2.69	0.35205	64.9
		2% Dry	6.5	122.3	2.69	0.37305	46.9
Rt. 46	A-2-4	2% Wet	10.0	126.1	2.67	0.32178	83.0
		OMC	8.0	128.5	2.67	0.29709	71.9
		2% Dry	6.0	127.2	2.67	0.31035	51.6
Rt. 80a	A-2-4	2% Wet	11.0	119.4	2.6	0.35935	79.6
		OMC	9.0	120.4	2.6	0.34806	67.2
		2% Dry	7.0	127.2	2.6	0.27599	65.9
Rt. 295	A-3	2% Wet	11.0	113.2	2.66	0.46689	62.7
		OMC	9.0	115.2	2.66	0.44142	54.2
		2% Dry	7.0	113.2	2.66	0.46719	39.9
Rt. 80b	A-4	2% Wet	10.2	124.8	2.66	0.33054	82.1
		OMC	8.2	127.8	2.66	0.29931	72.9
		2% Dry	6.2	125.8	2.66	0.31997	51.5
Rt. 206	A-4	2% Wet	11.0	124.6	2.69	0.34771	85.1
		OMC	9.0	127.9	2.69	0.31294	77.4
		2% Dry	7.0	123.6	2.69	0.35861	52.5
Cumberland County	A-6	2% Wet	17.0	112	2.73	0.52162	89.0
		OMC	15.0	113.3	2.73	0.50416	81.2
		2% Dry	13.0	112.4	2.73	0.51621	68.8
Cumberland County	A-7	2% Wet	24.5	101.8	2.71	0.66182	100.3
		OMC	22.5	104.0	2.71	0.62666	97.3
		2% Dry	20.5	102.0	2.71	0.65856	84.4

IV. ANALYSIS AND DISCUSSION OF TEST RESULTS

4.1 Introduction

Resilient modulus is affected by several parameters, some of which include: stress history, stress ratio, specimen end effects, temperature, moisture and saturation. A laboratory testing program has been established to study the effects of moisture content and saturation effects in detail. When evaluating the performance of subgrade soils in a pavement system, the major influential factor is water content and drainage. In general, stress history, stress ratio and temperature do not have a significant influence on subgrade soils due to the depth of interest in a pavement system. Furthermore, the end effect was not an issue in this research since all specimens were molded, placed, and tested with the same equipment. (Maher et. al 1996).

Moisture content is known to influence resilient modulus, and subgrade soils are typically subjected to an increase and decrease in water content during the history of the pavement (Drumm et. al. 1997). Therefore, a testing program has been implemented to study the effect of moisture content and more importantly the effect of saturated conditions on resilient modulus. Parameters influencing excess pore water pressure in subgrades are linked to the degradation of asphalt pavements, which may include: reduction of the strength of unbound subgrade soils causing pumping of pavements with subsequent faulting, cracking, and general pavement deterioration. Pumping of fines from the subgrade into the subbase and base course of flexible pavements resulting in loss of support (Huang 1993).

Resilient modulus is the elastic modulus to be used with the elastic theory. The elastic theory holds true if all the permanent deformation is accumulated before measuring resilient modulus. If the magnitude of cyclic loading is small compared to the strength of the material, and is repeated for a large number of times, the deformation under each load cycle is essentially completely recoverable and proportional to the load, the deformation can be considered elastic. Plastic deformations during the resilient modulus test may be excessive, thus resulting to the deterioration in strength of the soil. Excessive plastic deformations and the reduction of resilient modulus may be attributed to the increase in pore pressure within the sample. The increase in pore pressure will not result in soil liquefaction, but a decrease in effective confining stress. This decrease in effective confining stress increases the cyclic stress ratio during the resilient modulus test. Depending on the type of material being tested, the decrease in effective confining stress may decrease the resilient modulus.

4.2 Resilient Modulus Results of Type 1 Material

Only one New Jersey subgrade was classified as an AASHTO Type 1, A-1-b non-cohesive granular subgrade material designated by AASHTO TP46-94.

Resilient modulus of the specimen changes through out the testing sequence depending on the stress ratio. During the resilient modulus test, cyclic stress ratios have been predetermined and range from 0.15 to 1.35 as designated by AASHTO TP46-94 where cyclic stress ratio is defined as:

$$S_r = \frac{\sigma_{cd}}{2\sigma_c} \quad (4.1)$$

Where:

σ_{cd} = Cyclic deviatoric stress

σ_c = Confining stress

Cyclic deviatoric stress ratios of 1.8 and 2.25, corresponding to sequence No. 14 and 15 respectively, are not used for Type 1 soils as shown in table 4.1. Cyclic deviatoric stress ratios over 1.35 may contribute to specimen failure due to excessive permanent strains. In general, cyclic deviatoric stress ratios under 1.35 tend to densify the granular specimen thereby increasing the resilient modulus with increasing deviatoric stress. This densification may be defined as cyclic mobility as defined by Castro (1975). Densification of medium to dense soils occurs when soil particles roll and slide over each other, which may instantaneously increase the volume of the sample until equilibrium is reached and the soil particles are orientated in a new position creating a denser material. If cyclic stress ratios are large enough these dilative soils may not re-orientate into a denser state, thus losing strength that may cause excessive permanent deformation, reduction in resilient modulus, and soil failure.

The variation of resilient modulus with stress ratios at optimum and 2% wet of optimum are shown on figures 4.1 and 4.2, respectively. The resilient modulus increases with increasing deviatoric stress. This may be explained by densification as

describes previously or by capillary effects. Research by Wu (1983) indicated that water in non-saturated soils plays an important role in inter-angular reactions. Thin water films surrounding the soil particles form a meniscus between soil particles, resulting in a pressure deficiency at the interface between water and air. Since the pore water pressure in soil-water-air systems is always negative in non-saturated soil, it adds additional inter-angular forces. These additional forces may be similar to additional effective stress. The water between the soil particles may also be acting as a lubricant and allow the particles to slide and roll over each other, densifying the sample, leading to higher resilient modulus values with increasing deviatoric stress.

Conversely, as the moisture content decreases, the interangular forces also decrease. The decrease in inter-angular forces inhibits any additional effective stress thereby reducing the resilient modulus with increasing deviatoric stress as shown in figure 4.3.

The effect of confining pressure plays a significant role on type 1 granular materials as shown on figures 4.1-4.3. Since this material is granular and non-cohesive in nature, confining pressure plays a significant role in the materials strength. In general type 1 granular material exhibited a 30% increase in resilient modulus with increasing confining pressure, for the range of confining pressure in this experimental program.

All resilient modulus results shown in the figures are shown in the form of the Universal model (Chapter 6, p. 102). Test values are depicted as solid black symbols with a solid black line, while theoretical values are depicted as hollow symbols with dotted lines. The Universal model will be discussed in further detail in Chapter 6.

Table 4.1 Testing Sequence for Subgrade Materials

Sequence Number	Confining Pressure, σ_3 (psi)	Maximum Axial Stress, σ_d (psi)	Cyclic Stress, σ_{cd} (psi)	Contact Stress, σ_c (psi)	Number of Load Applications
Cond.	6.0	4.0	3.6	0.4	500-1000
1	6.0	2.0	1.8	0.2	100
2	6.0	4.0	3.6	0.4	100
3	6.0	6.0	5.4	0.6	100
4	6.0	8.0	7.2	0.8	100
5	6.0	10.0	9.0	1.0	100
6	4.0	2.0	1.8	0.2	100
7	4.0	4.0	3.6	0.4	100
8	4.0	6.0	5.4	0.6	100
9	4.0	8.0	7.2	0.8	100
10	4.0	10.0	9.0	1.0	100
11	2.0	2.0	1.8	0.2	100
12	2.0	4.0	3.6	0.4	100
13	2.0	6.0	5.4	0.6	100
14	2.0	8.0	7.2	0.8	100
15	2.0	10.0	9.0	1.0	100

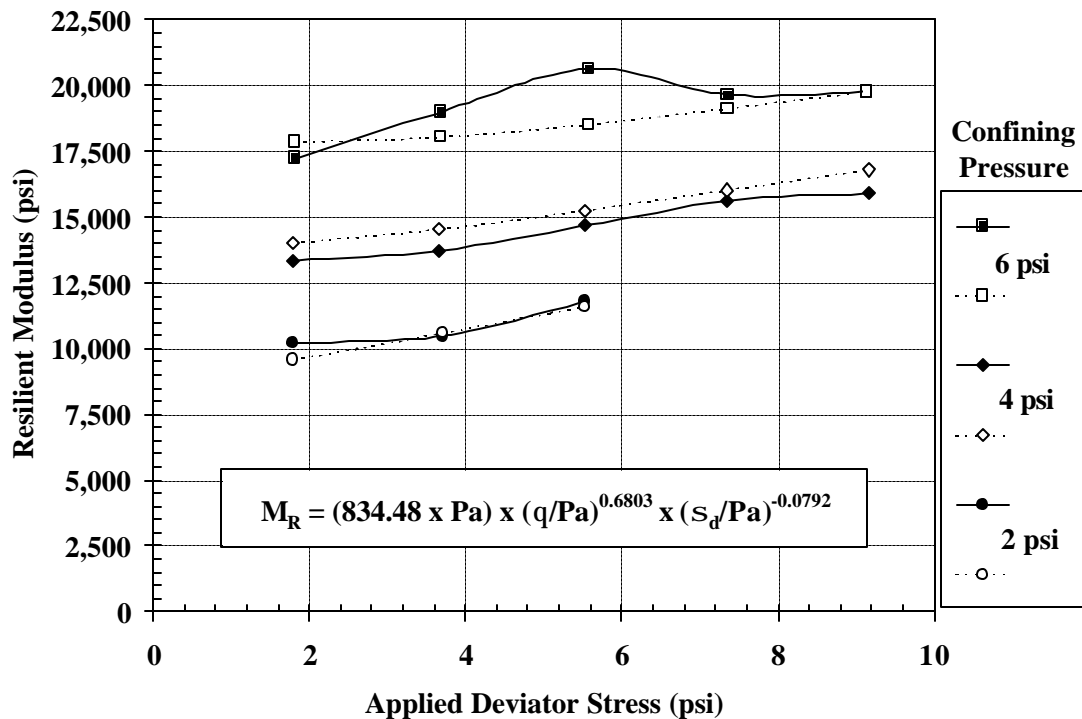


Figure 4.1 AASHTO Type 1 (Rt. 23) Resilient Modulus Test Results at Optimum Moisture Content (Test Results – Solid Line : Model – Dotted Line).

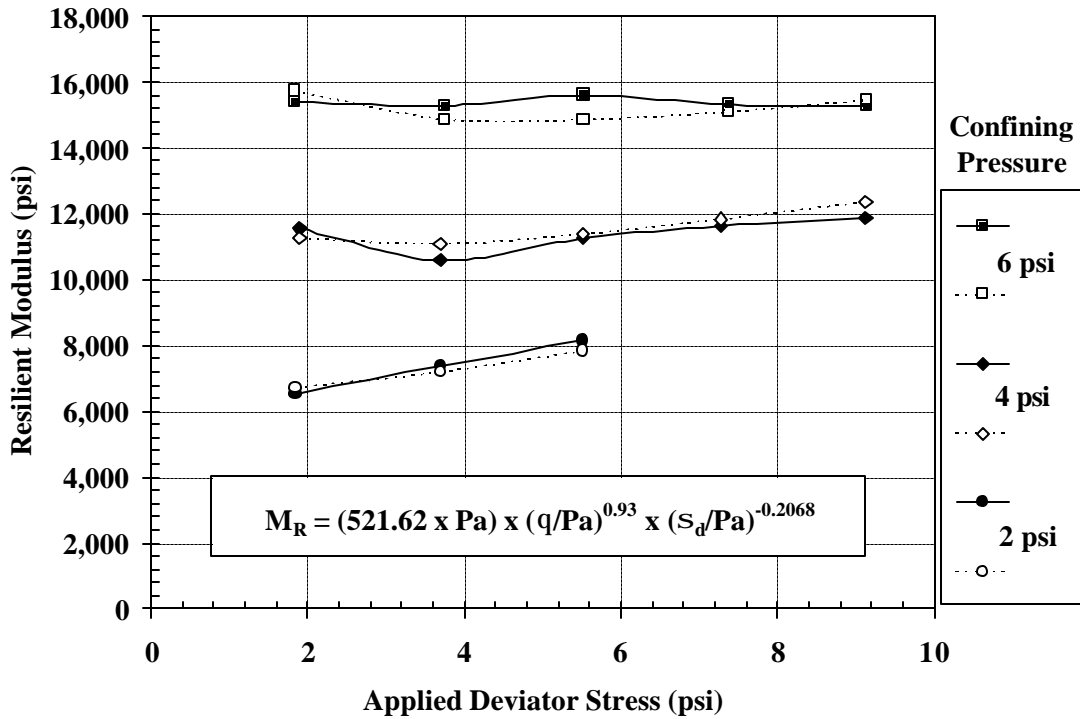


Figure 4.2 AASHTO Type 1 (Rt. 23) Resilient Modulus Test Results at 2 % Wet of Optimum (Test Results – Solid Line: Model – Dotted Line).

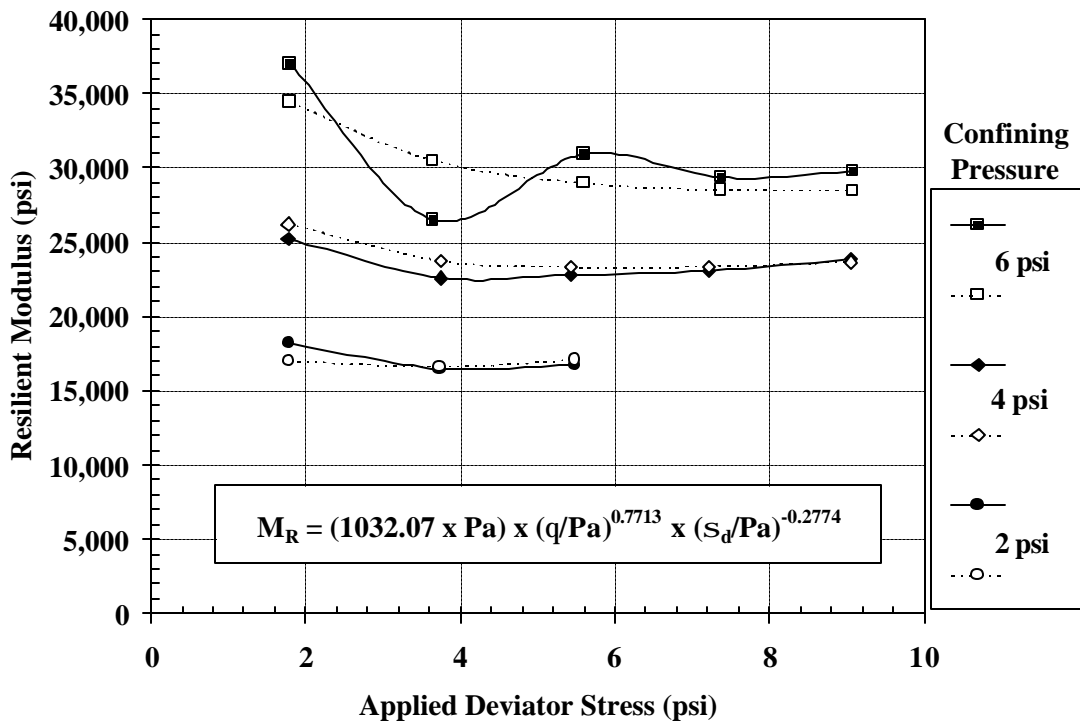


Figure 4.3 AASHTO Type 1 (Rt. 23) Resilient Modulus Test Results at 2 % Dry of Optimum (Test Results – Solid Line: Model – Dotted Line).

4.2.1 Resilient Modulus of Type 1 Materials at Different Moisture Contents

As shown on figure 4.4 the average resilient modulus at 2% dry of optimum is generally 65 % higher than the soil compacted at optimum moisture content, while the resilient modulus of the sample compacted at 2% wet of optimum is generally 25% lower on average. The wide range of resilient modulus values indicates that this particular type 1 granular material is very sensitive to variations in the compacted moisture content.

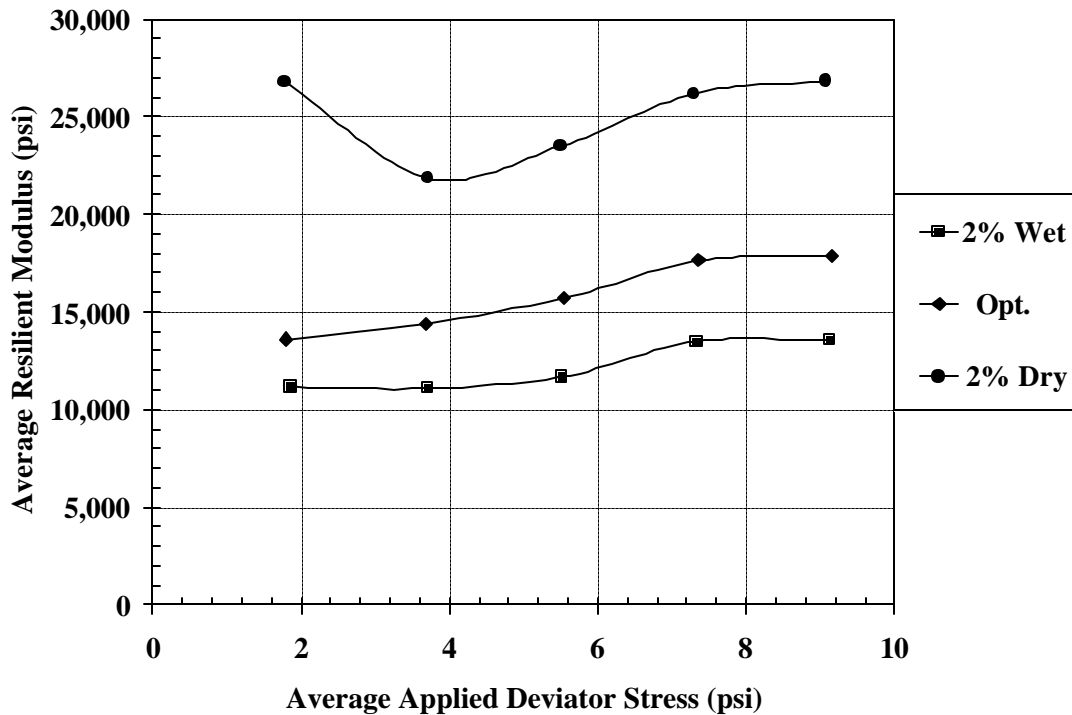


Figure 4.4 Comparison of AASHTO Type 1 (Rt 23) Resilient Modulus Test Results.

4.3 Resilient Modulus Results of Type 2 Material

Seven of the typical New Jersey soils tested were classified as AASHTO type 2 cohesive fine-grained material. Resilient modulus testing of type 2 materials uses the

same testing sequence as type 1 indicated earlier. However, since fine-grained materials are less sensitive to confining pressure, higher cyclic deviatoric stress ratios are required by AASHTO TP46-94 specifications. Cyclic deviatoric stress ratios of 1.8 and 2.25, corresponding to sequence 14 and 15 are used for Type 2 soils as indicated in table 4.2.1.

In general, Type 2 materials are not as sensitive to moisture content and stress ratios as compared to Type 1 material. However, an increase in moisture content and deviatoric stress decreases the resilient modulus and increases the permanent deformation of the fine-grained Type 2 materials.

These seven Type 2 materials were further classified using AASHTO M 145 specifications. Rt. 46 and 80a materials were classified as AASHTO A-2-4 materials, Rt. 80 b and 206 were classified as AASHTO A-4 materials, Rt. 295 was classified as AASHTO A-3 material, and the two Cumberland County soils were classified as A-6 and A-7, respectively.

The variation of resilient modulus for type 2 materials with confining pressure was not as significant as with type 1 material. Unlike the Type 1 material where the resilient modulus increases with increasing deviatoric stress, the resilient modulus decreases with increasing confining pressure as shown on figures 4.5 - 4.25.

By varying the compacted moisture content (i.e. optimum moisture content and \pm 2% of the optimum moisture content), the soils could be properly evaluated for sensitivity due to seasonal moisture changes.

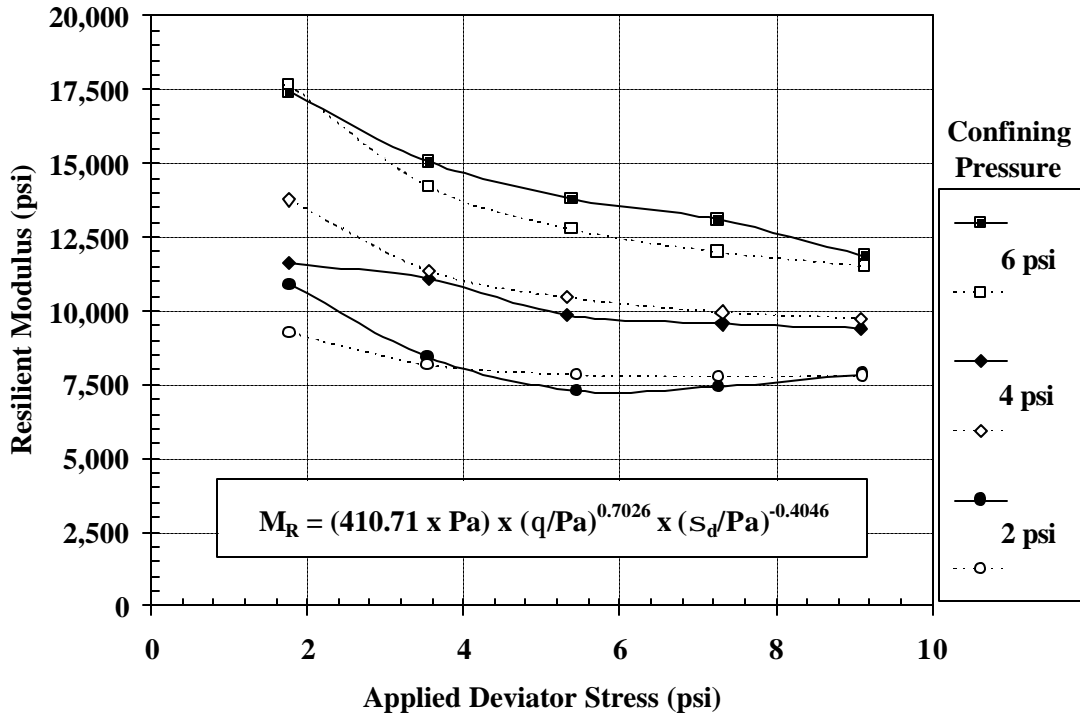


Figure 4.5 AASHTO Type 2 (Rt. 46) Resilient Modulus Test Results at Optimum Moisture Content (Test Results – Solid Line: Model – Dotted Line)

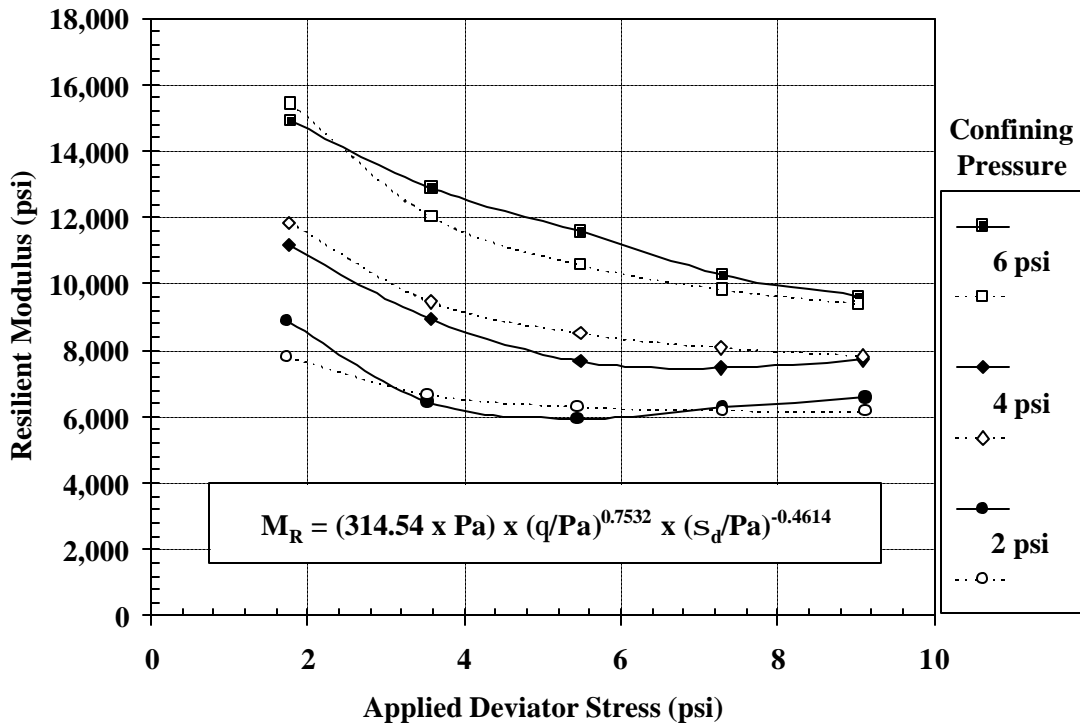


Figure 4.6 AASHTO Type 2 (Rt. 46) Resilient Modulus Test Results at 2% Wet of Optimum Moisture Content (Test Results – Solid Line: Model – Dotted Line)

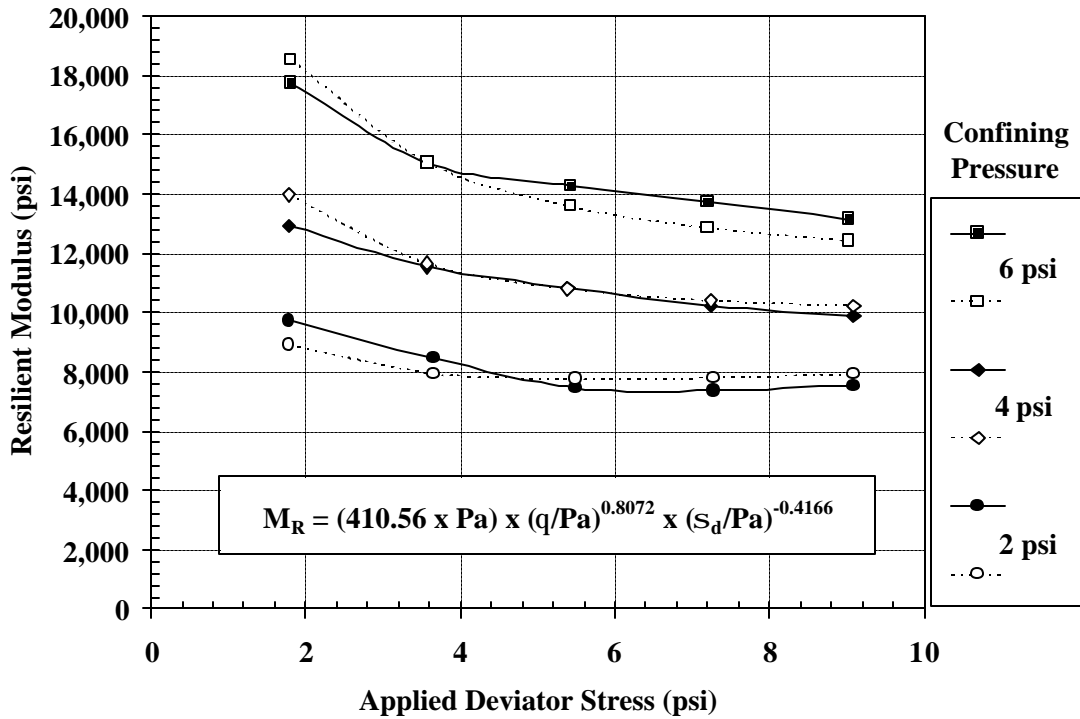


Figure 4.7 AASHTO Type 2 (Rt 46) Resilient Modulus Test Results at 2% Dry of Optimum (Test Results – Solid Line: Model – Dotted Line)

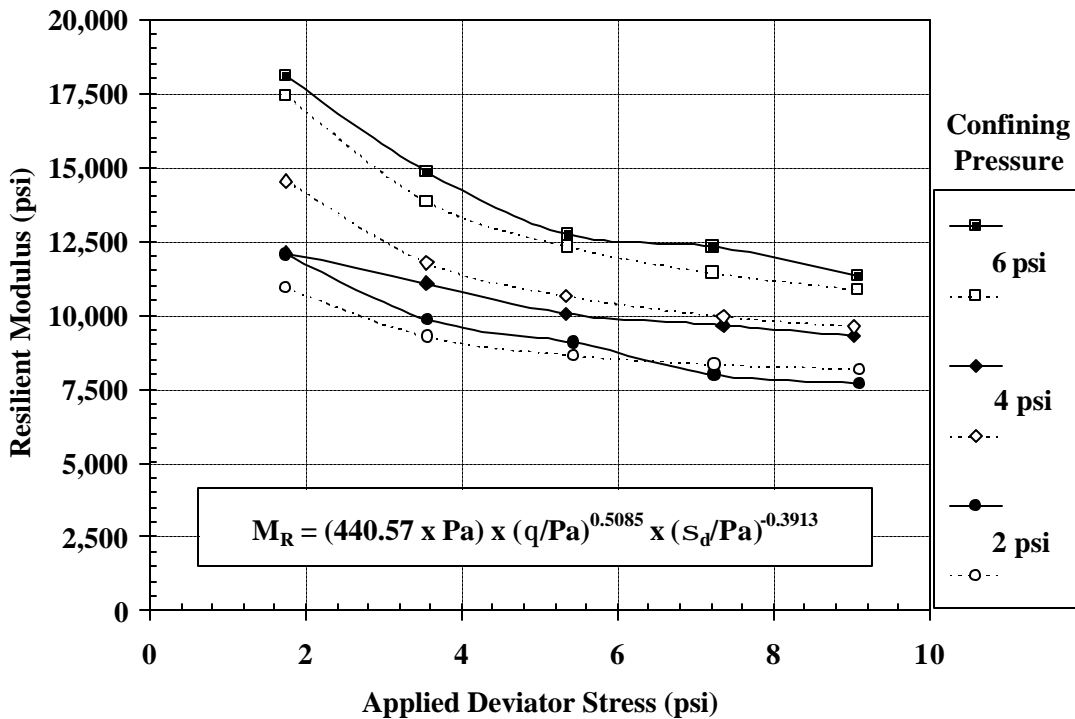


Figure 4.8 AASHTO Type 2 (Rt 80a) Resilient Modulus Test Results at Optimum Moisture Content (Test Results – Solid Line: Model – Dotted Line).

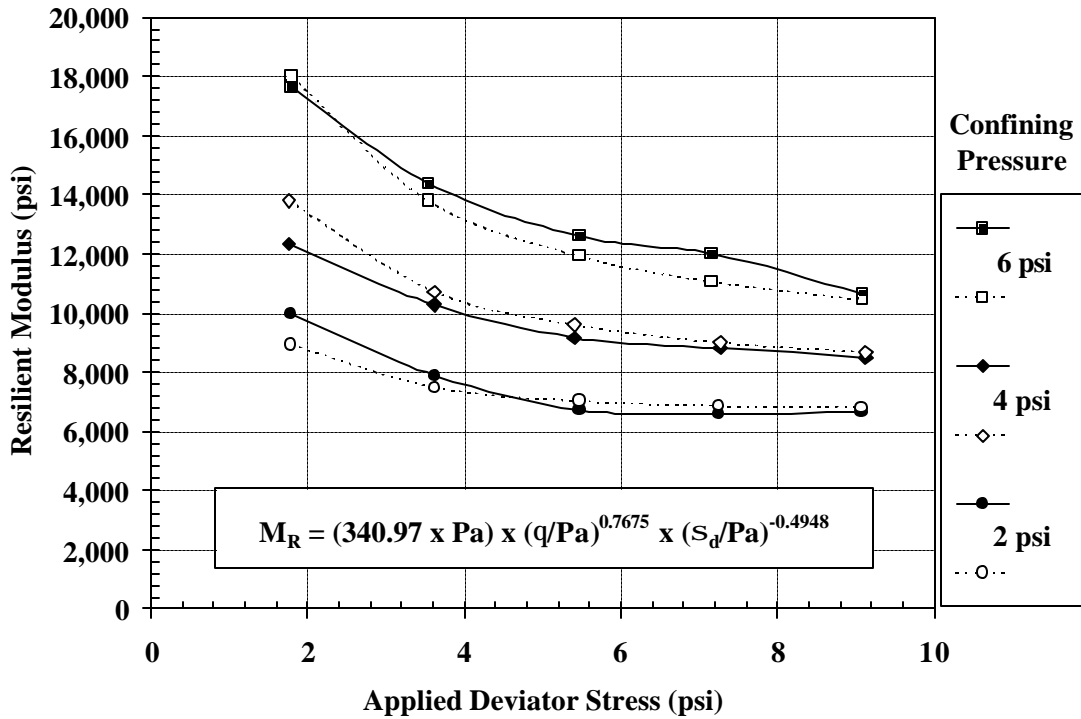


Figure 4.9 AASHTO Type 2 (Rt 80a) Resilient Modulus Test Results at 2% Wet of Optimum (Test Results – Solid Line: Model – Dotted Line)

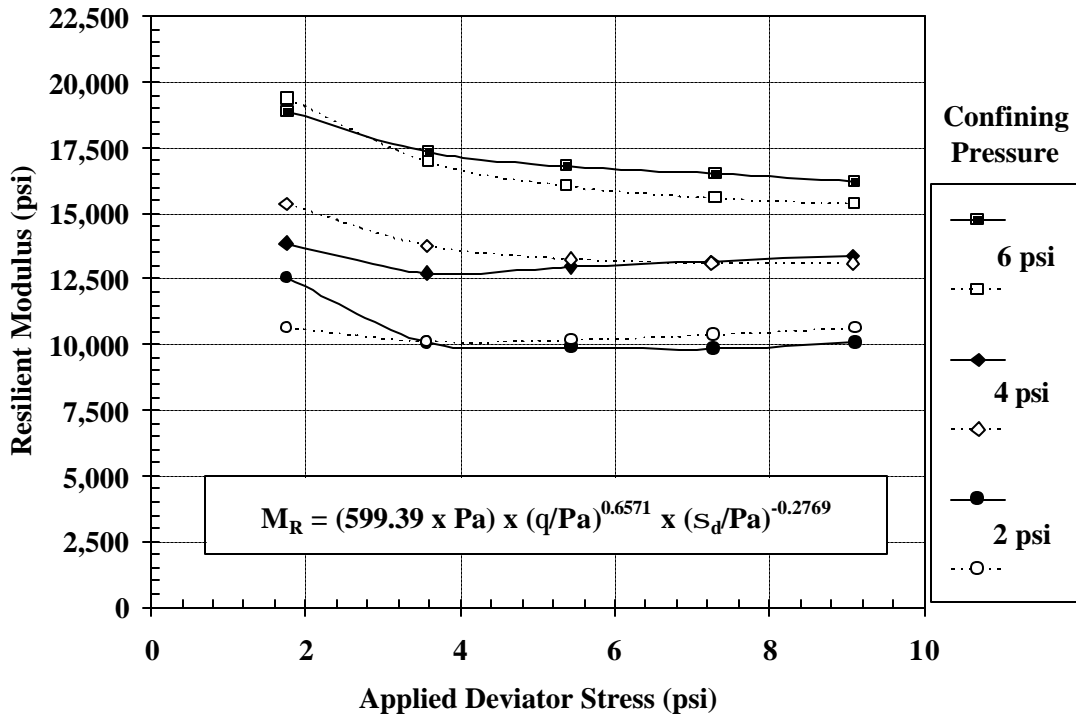


Figure 4.10 AASHTO Type 2 (Rt 80a) Resilient Modulus Test Results at 2% Dry of Optimum (Test Results – Solid Line: Model – Dotted Line)

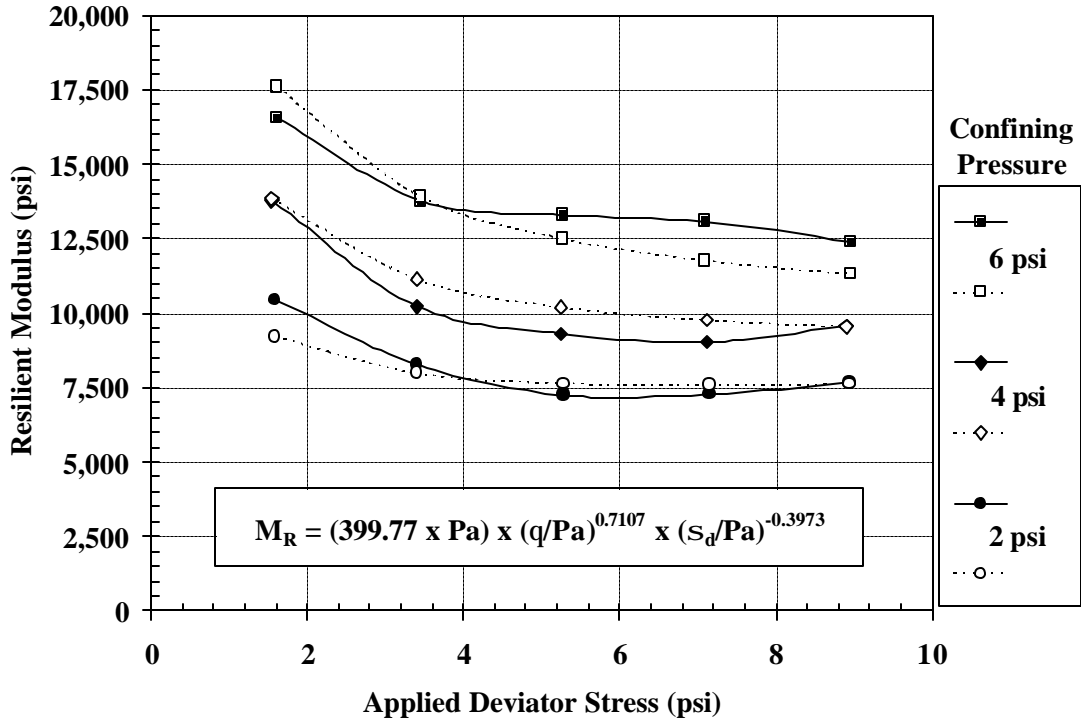


Figure 4.11 AASHTO Type 2 (Rt 295) Resilient Modulus Test Results at Optimum Moisture Content (Test Results – Solid Line: Model – Dotted Line)

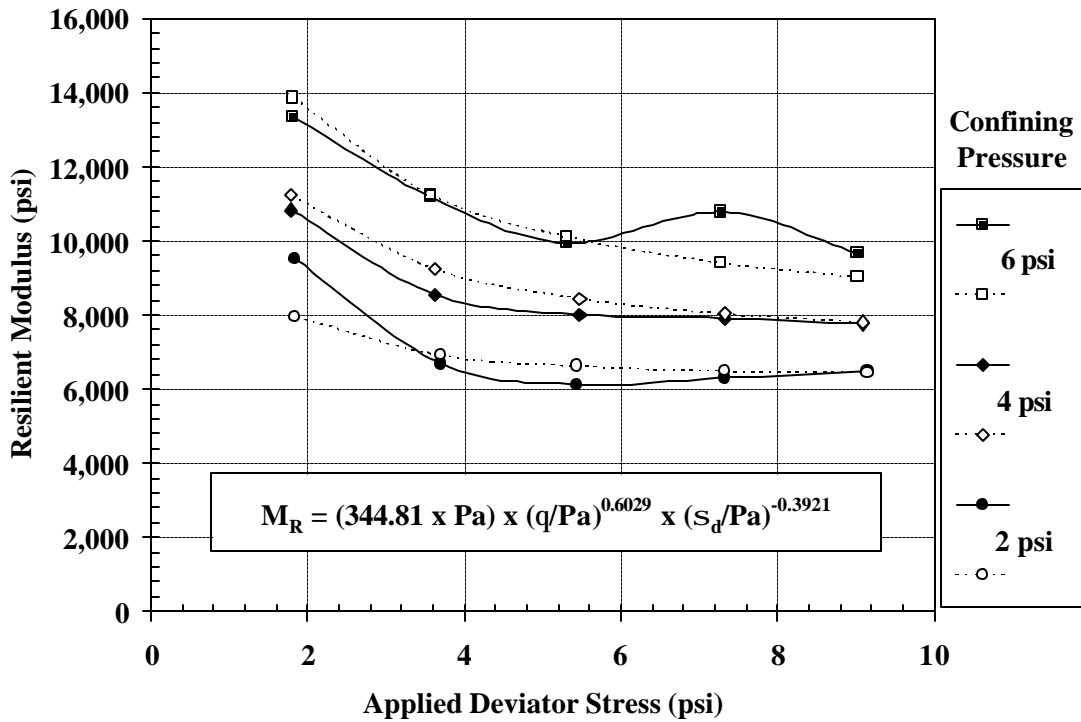


Figure 4.12 AASHTO Type 2 (Rt 295) Resilient Modulus Test Results at 2% Wet of Optimum (Test Results – Solid Line: Model – Dotted Line)

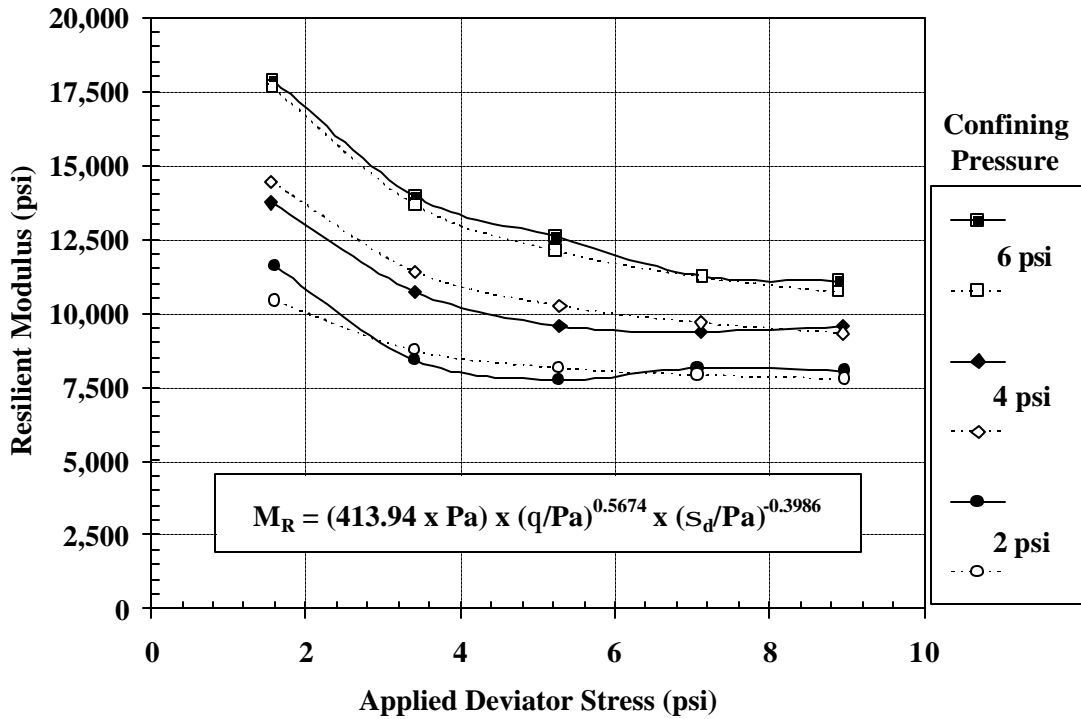


Figure 4.13 AASHTO Type 2 (Rt 295) Resilient Modulus Test Results at 2% Dry of Optimum (Test Results – Solid Line: Model – Dotted Line)

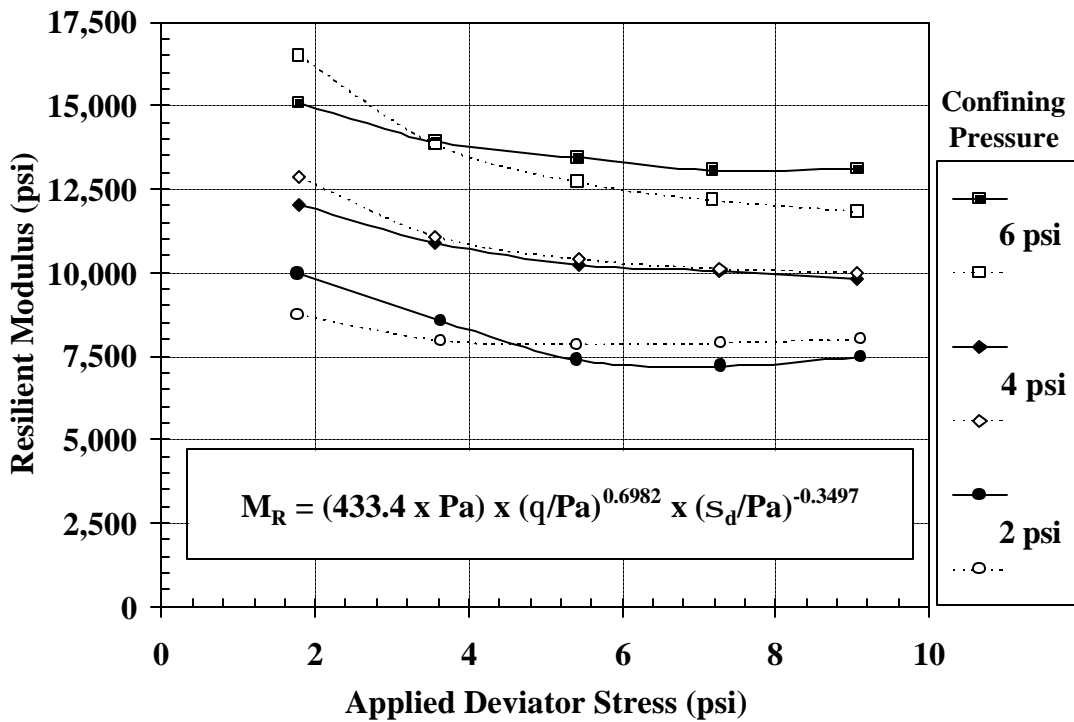


Figure 4.14 AASHTO Type 2 (Rt 80b) Resilient Modulus Test Results at Optimum Moisture Content (Test Results – Solid Line: Model – Dotted Line)

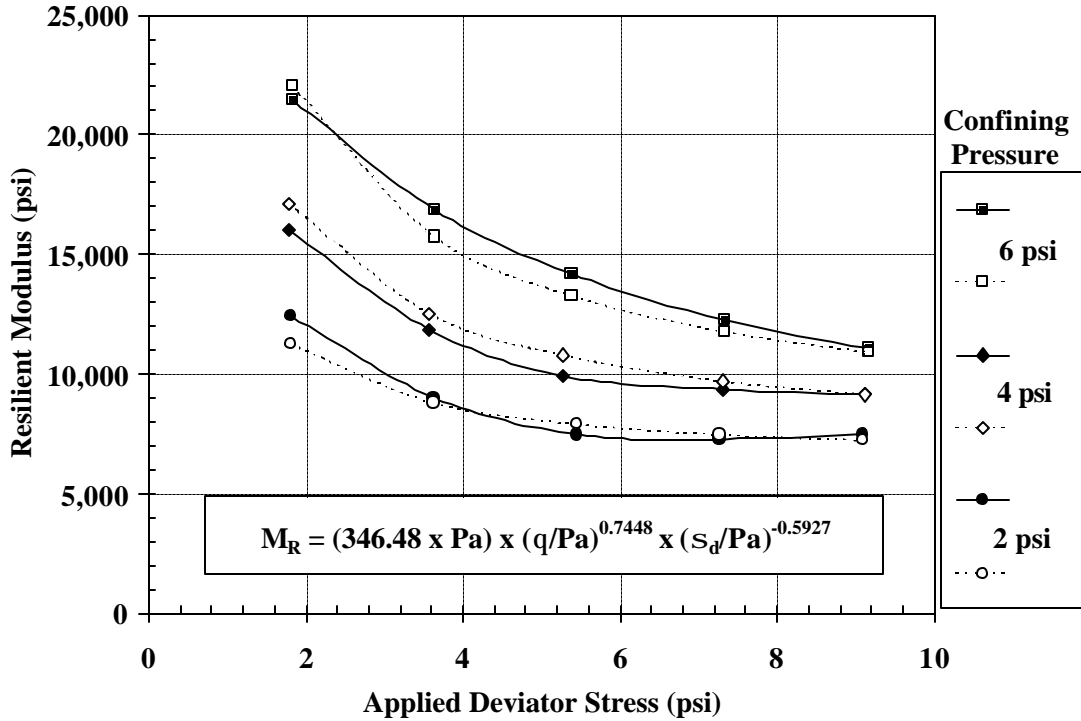


Figure 4.15 AASHTO Type 2 (Rt 80b) Resilient Modulus Test Results at 2% Wet of Optimum (Test Results – Solid Line: Model – Dotted Line)

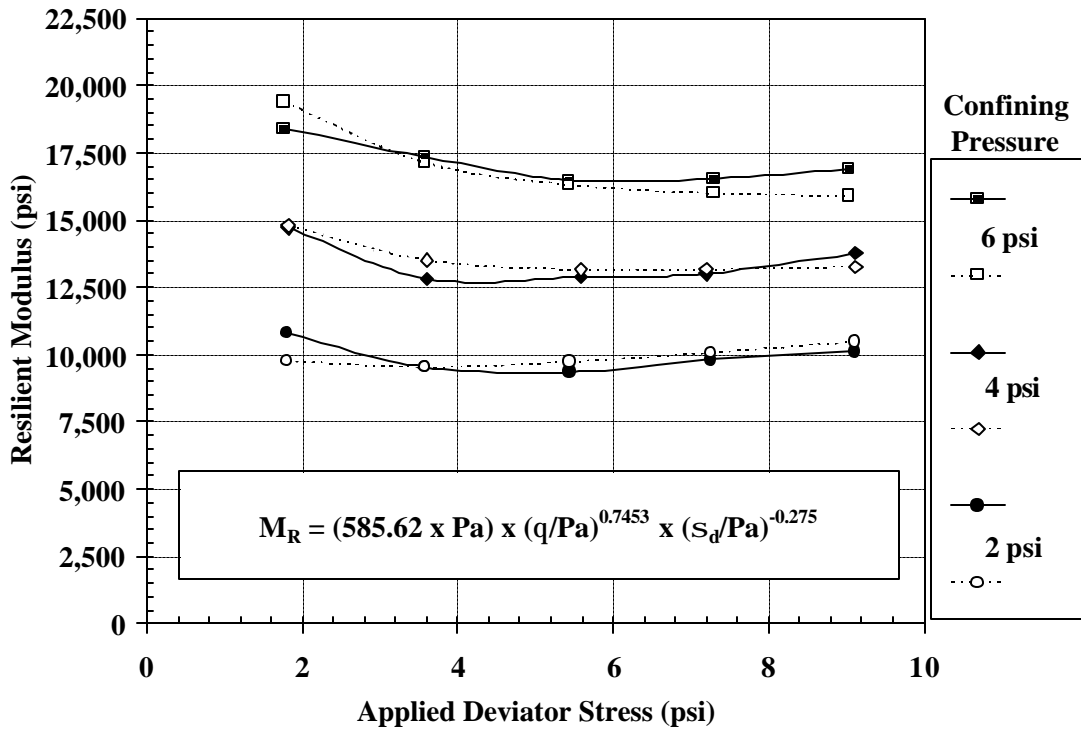


Figure 4.16 AASHTO Type 2 (Rt 80b) Resilient Modulus Test Results at 2% Dry of Optimum (Test Results – Solid Line: Model – Dotted Line)

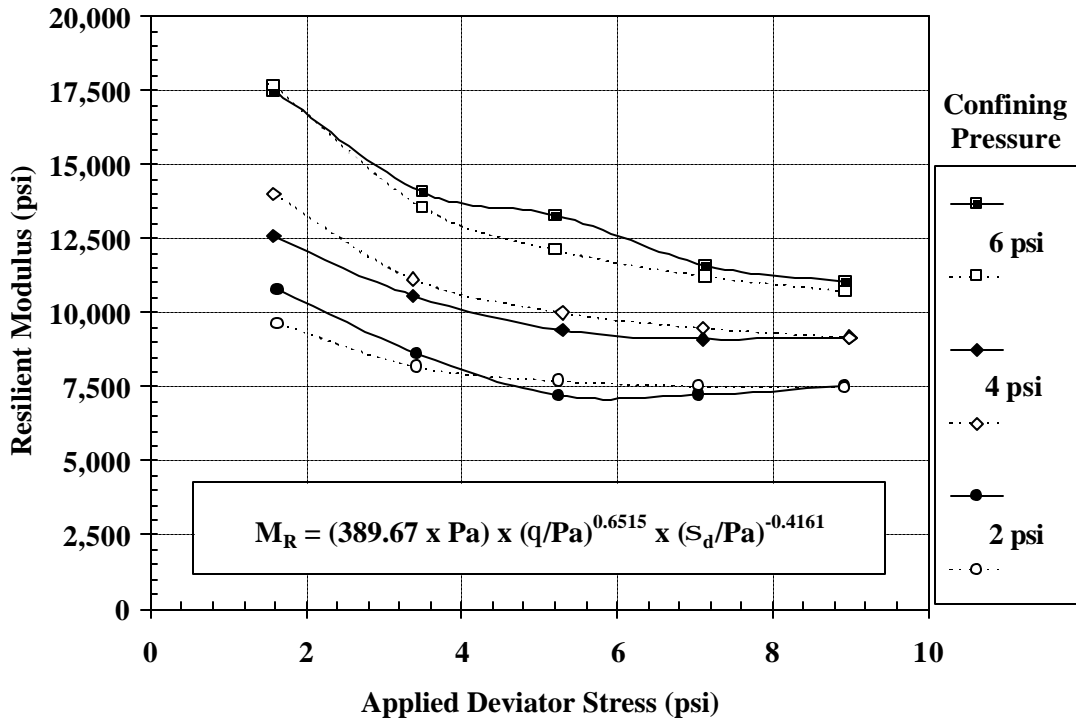


Figure 4.17 AASHTO Type 2 (Rt 206) Resilient Modulus Test Results at Optimum Moisture Content (Test Results – Solid Line: Model – Dotted Line)

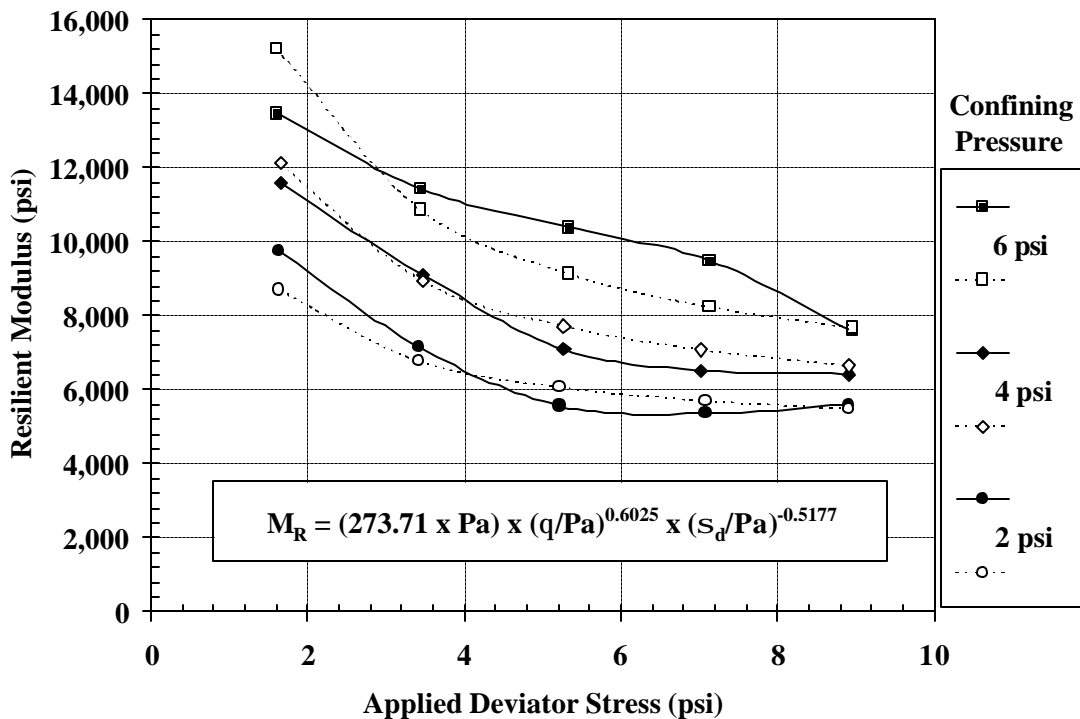


Figure 4.18 AASHTO Type 2 (Rt 206) Resilient Modulus Test Results at 2% Wet of Optimum (Test Results – Solid Line: Model – Dotted Line)

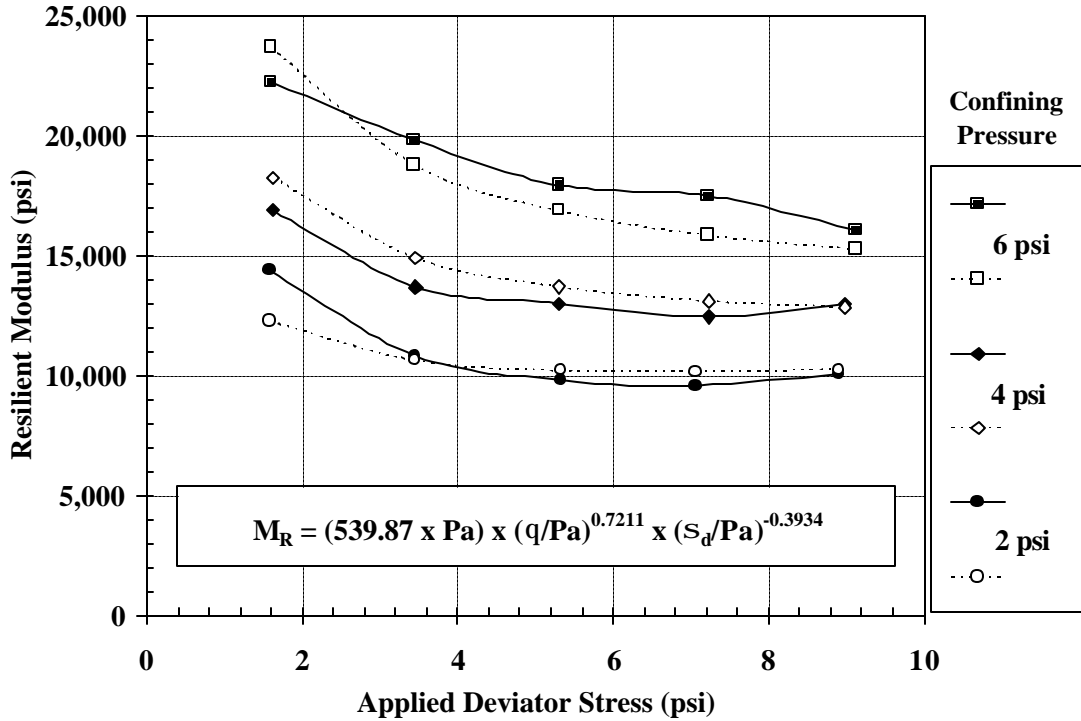


Figure 4.19 AASHTO Type 2 (Rt 206) Resilient Modulus Test Results at 2% Dry of Optimum (Test Results – Solid Line: Model – Dotted Line)

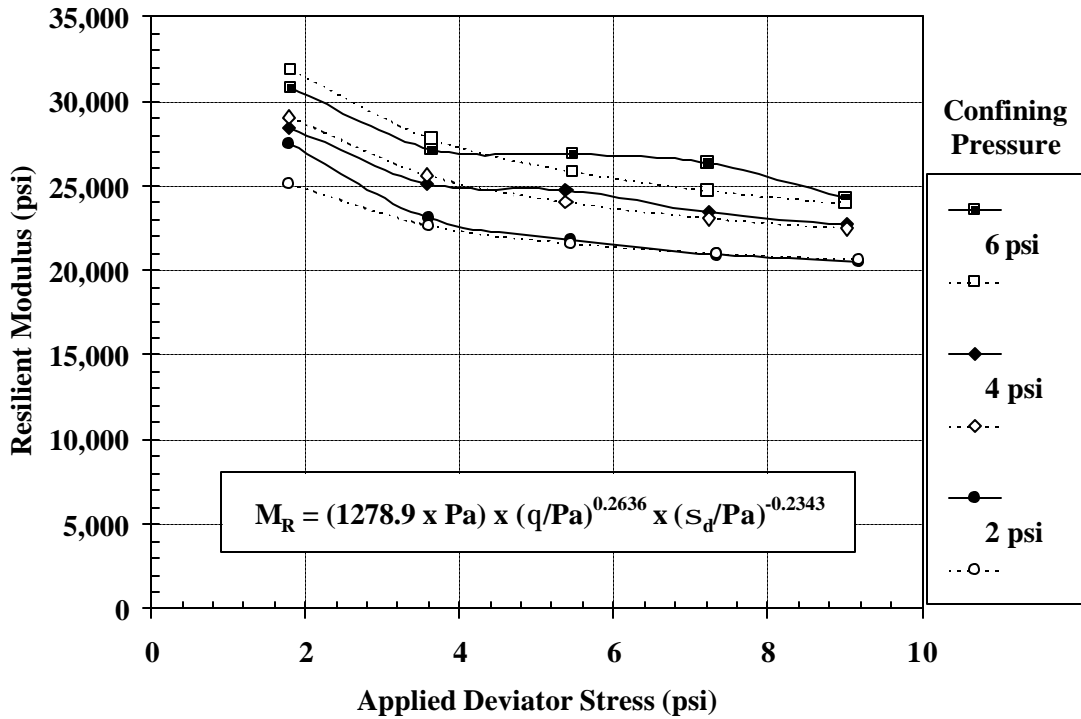


Figure 4.20 AASHTO Type 2 (Cumberland County – A-6) Resilient Modulus Test Results at Optimum Moisture Content (Test Results – Solid: Model – Dotted Line)

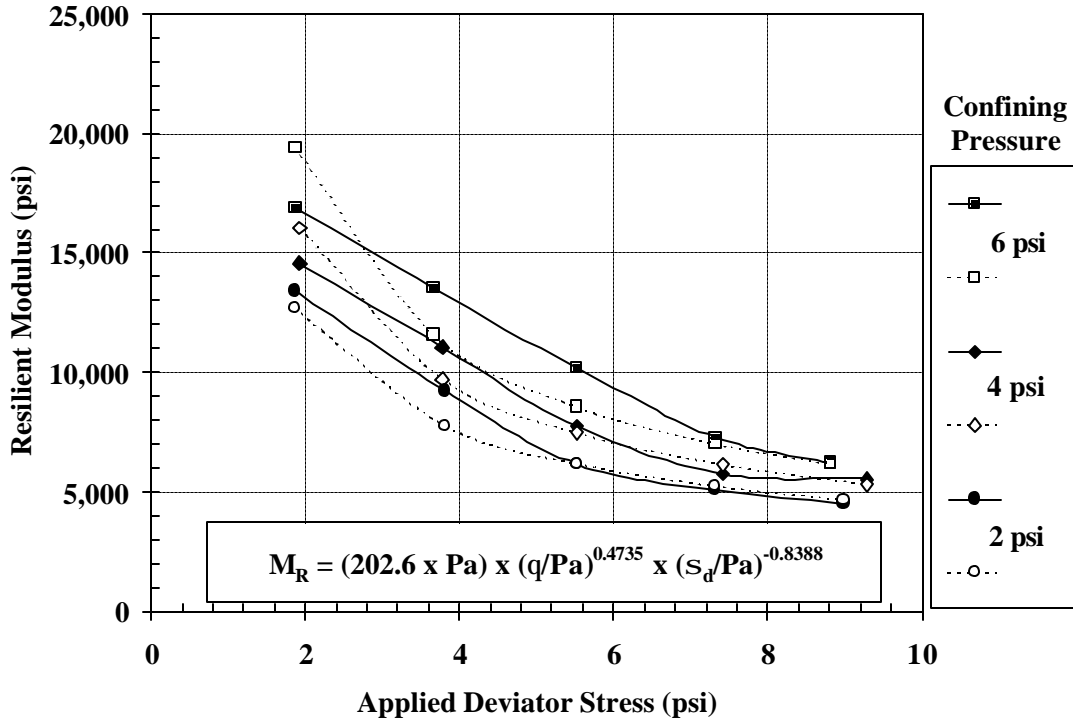


Figure 4.21 AASHTO Type 2 (Cumberland County – A-6) Resilient Modulus Test Results at 2% Wet of Optimum (Test Results – Solid Line: Model – Dotted Line)

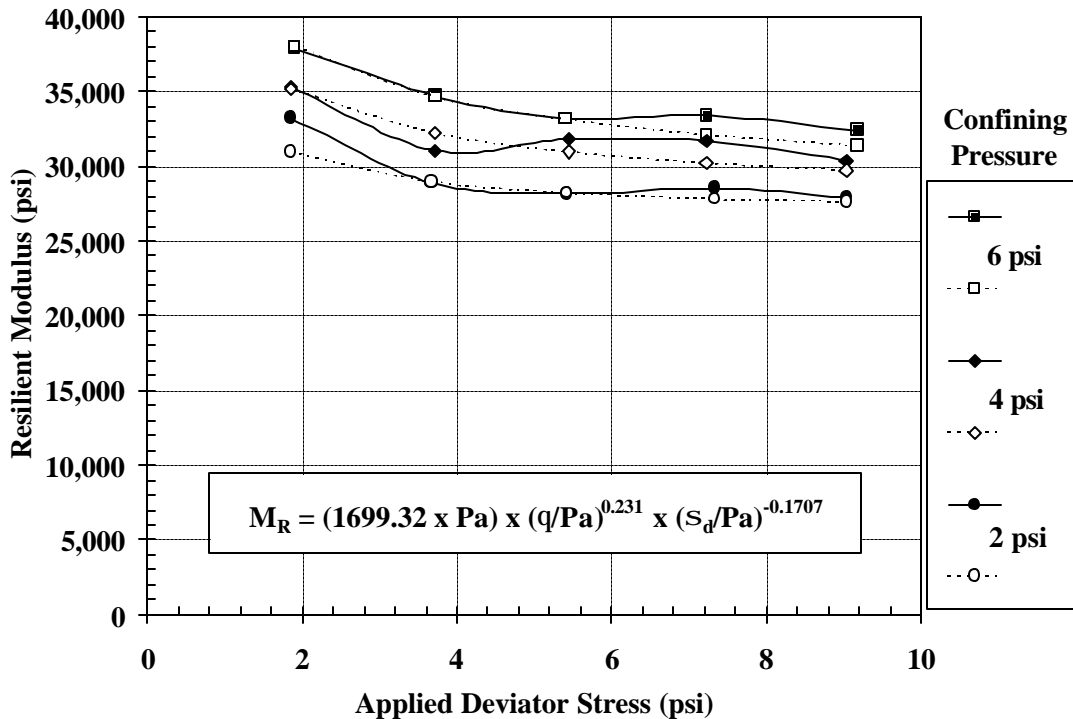


Figure 4.22 AASHTO Type 2 (Cumberland County – A-6) Resilient Modulus Test Results at 2% Dry of Optimum (Test Results – Solid Line: Model – Dotted Line)

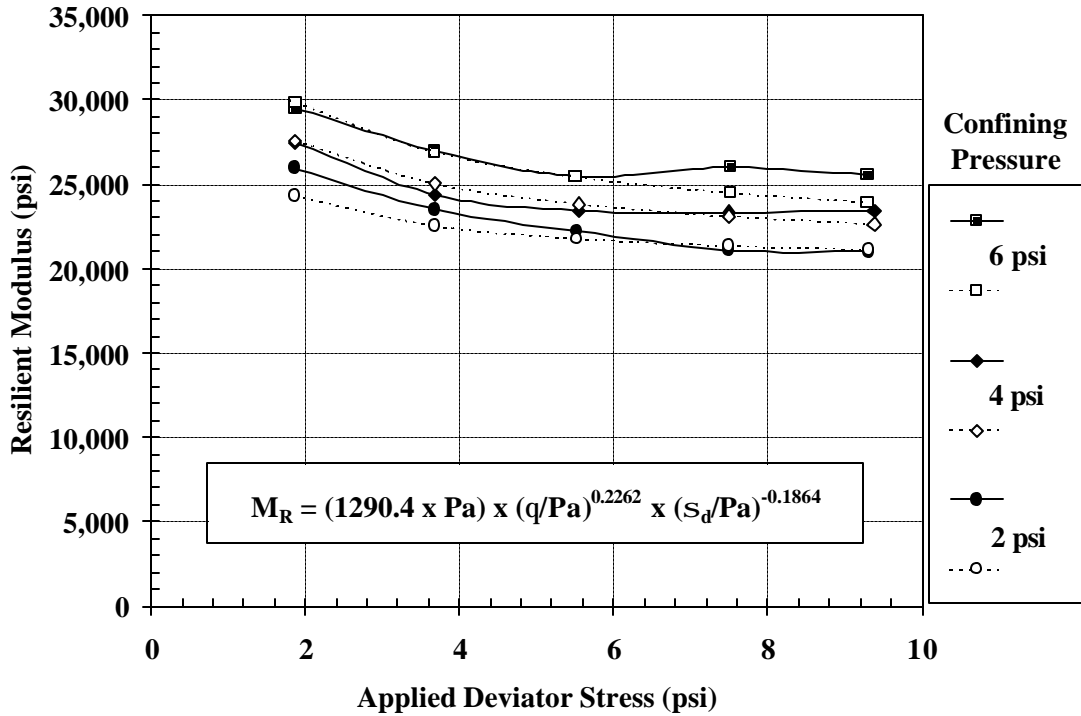


Figure 4.23 AASHTO Type 2 (Cumberland County – A-7) Resilient Modulus Test Results at Optimum Moisture Content (Test Results – Solid: Model – Dotted Line)

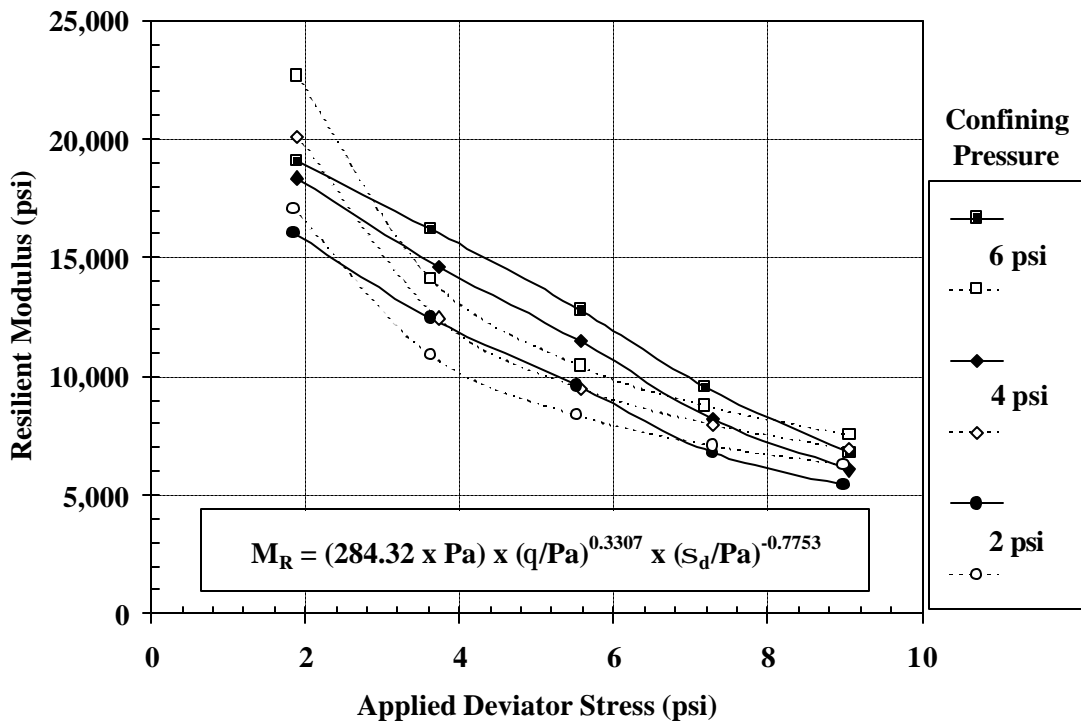


Figure 4.24 AASHTO Type 2 (Cumberland County – A-7) Resilient Modulus Test Results at 2% Wet of Optimum (Test Results – Solid Line: Model – Dotted Line)

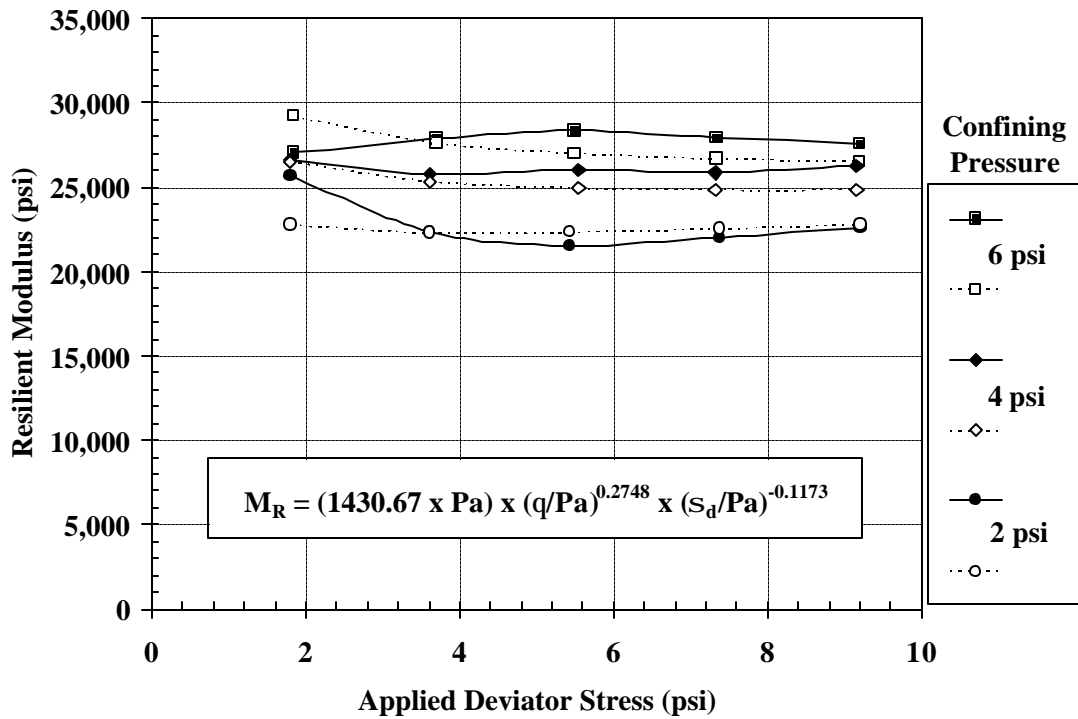


Figure 4.25 AASHTO Type 2 (Cumberland County – A-7) Resilient Modulus Test Results at 2% Dry of Optimum (Test Results – Solid Line: Model – Dotted Line)

Figures 4.26 – 4.34 shows the comparison of all eight soils at different confining pressures (2 psi, 4 psi, and 6 psi), as well as at their respective compacted moisture content designations (optimum, 2 % wet of optimum, and 2 % dry of optimum).

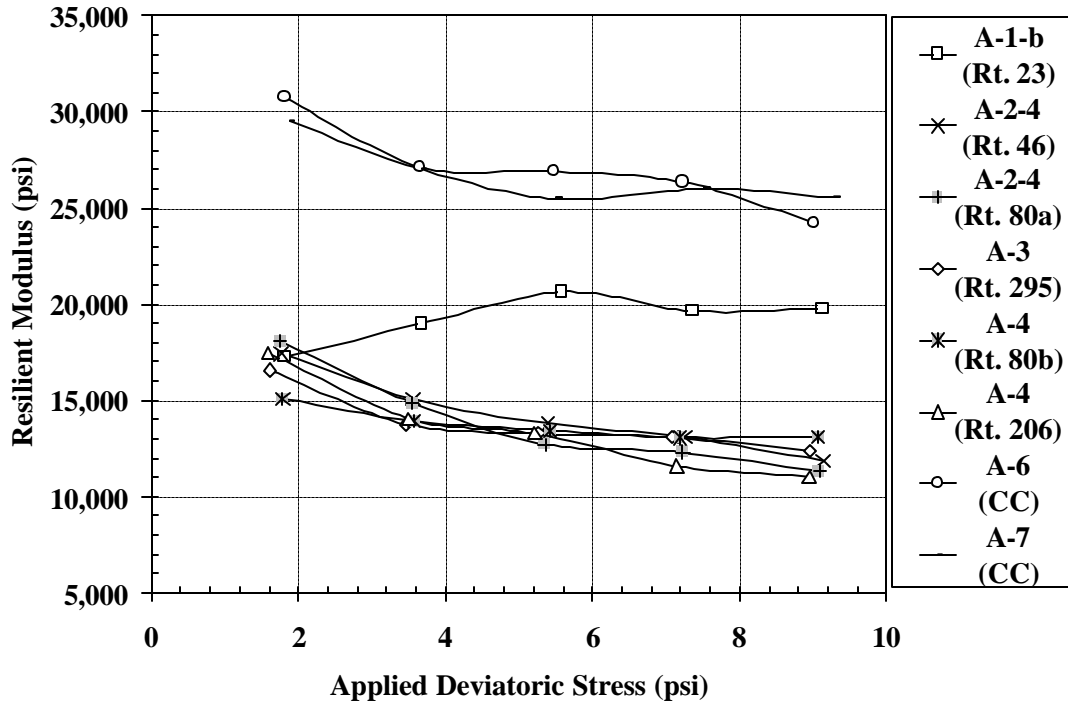


Figure 4.26 All Soil Types Compacted at Their Respective Optimum Moisture Contents and Tested at a Confining Pressure = 6 psi

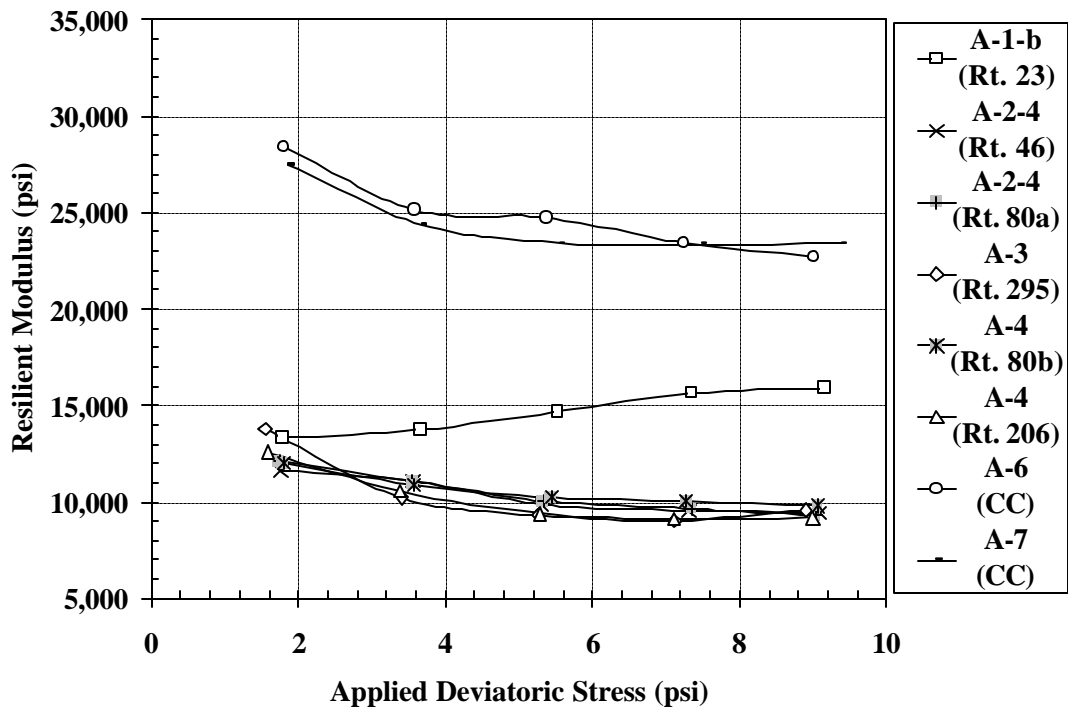


Figure 4.27 All Soil Types Compacted at Their Respective Optimum Moisture Contents and Tested at a Confining Pressure = 4 psi

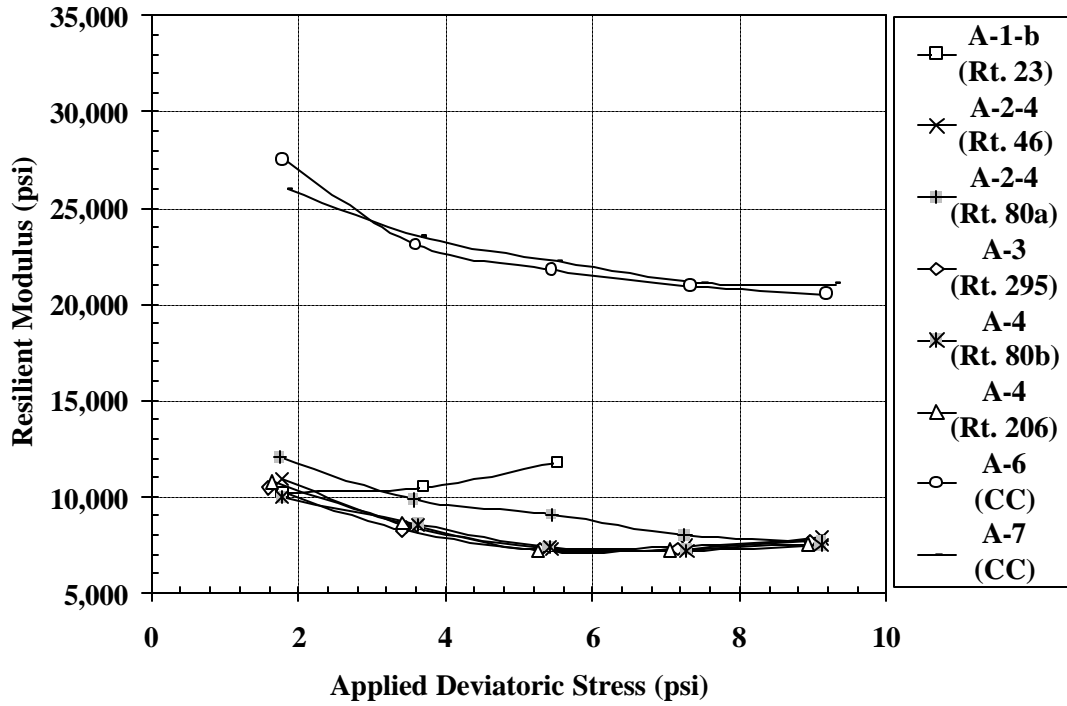


Figure 4.28 All Soil Types Compacted at Their Respective Optimum Moisture Contents and Tested at a Confining Pressure = 2 psi

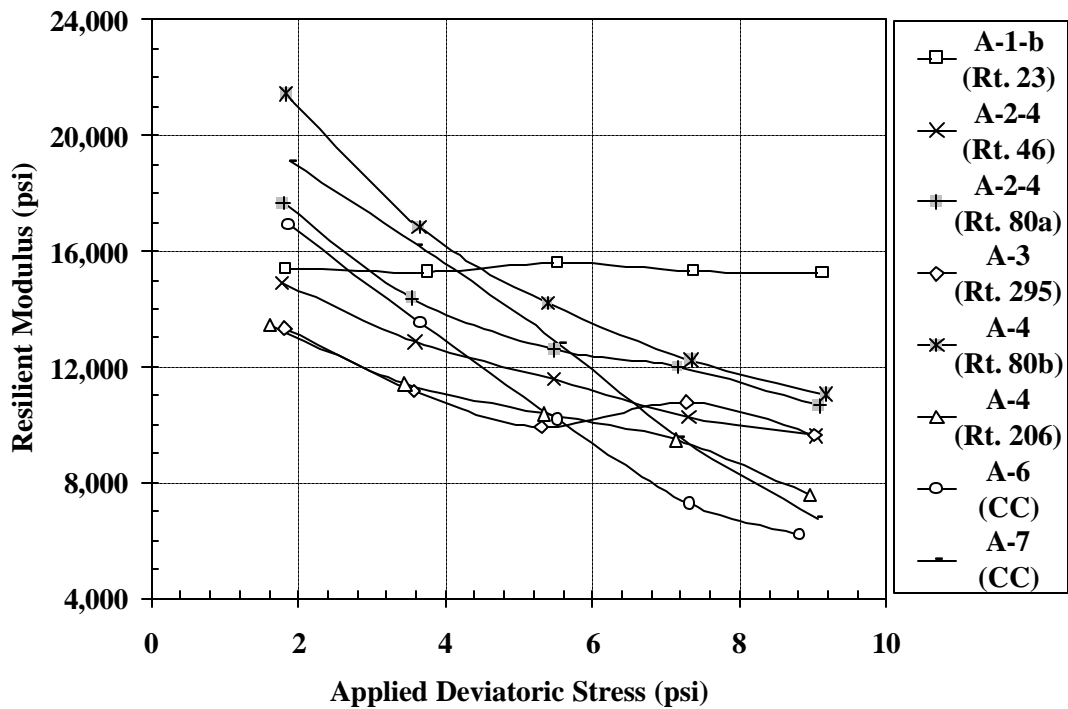


Figure 4.29 All Soil Types Compacted 2 % Wet of Their Respective Optimum Moisture Content and Tested at a Confining Pressure = 6psi

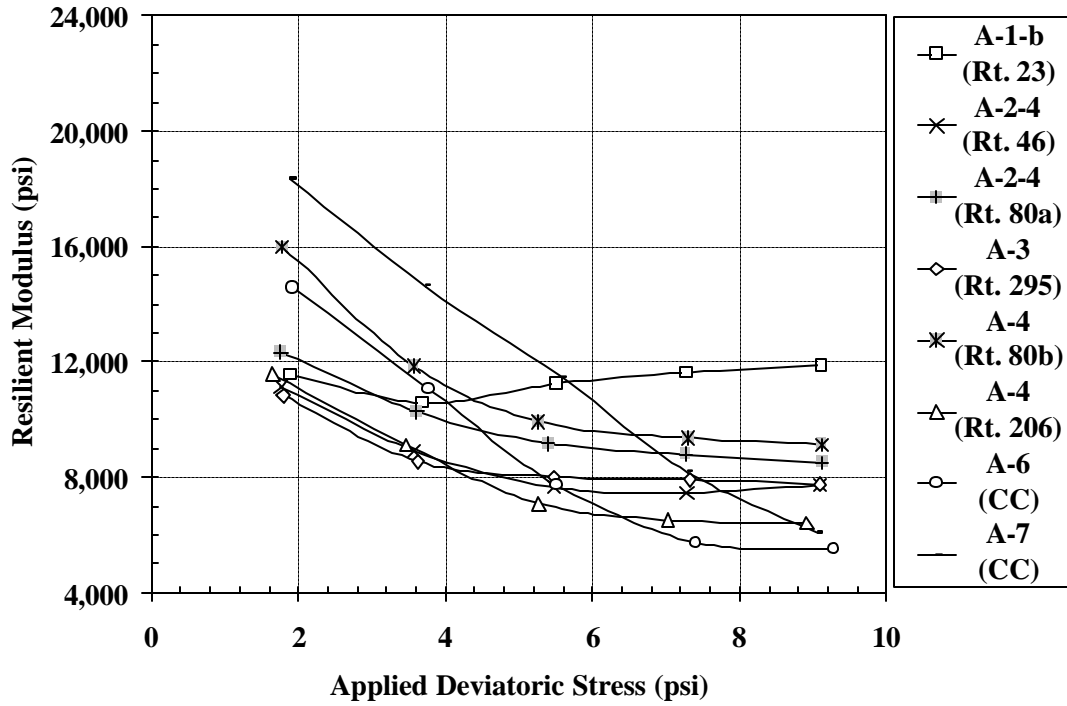


Figure 4.30 All Soil Types Compacted 2 % Wet of Their Respective Optimum Moisture Content and Tested at a Confining Pressure = 4 psi

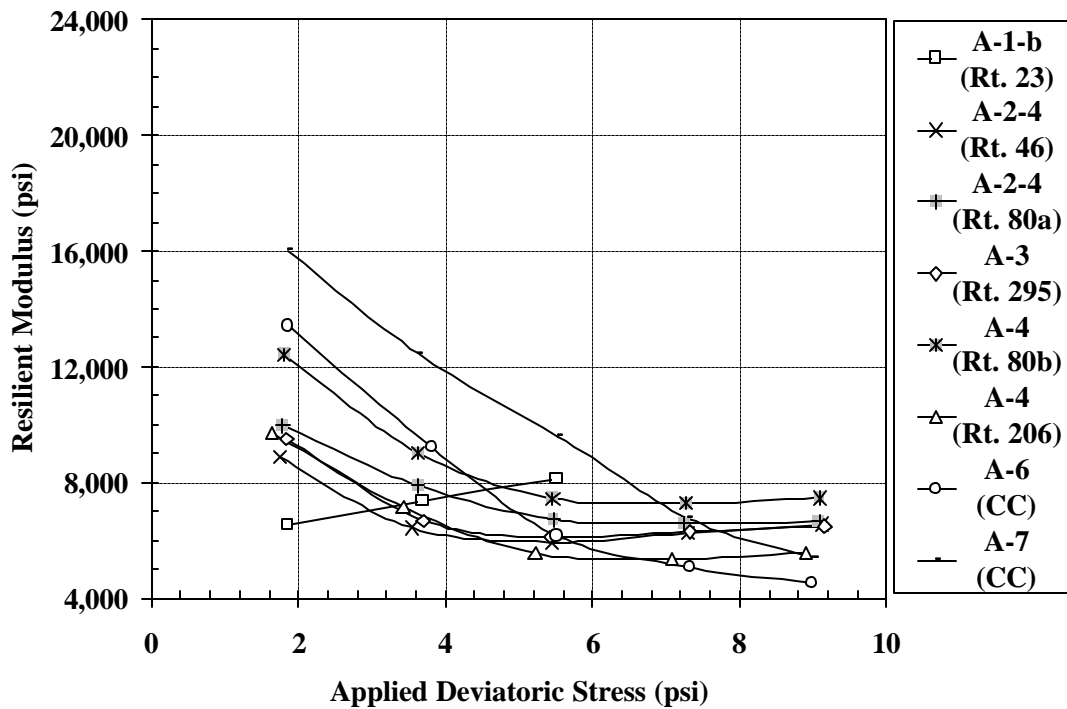


Figure 4.31 All Soil Types Compacted 2 % Wet of Their Respective Optimum Moisture Content and Tested at a Confining Pressure = 2 psi

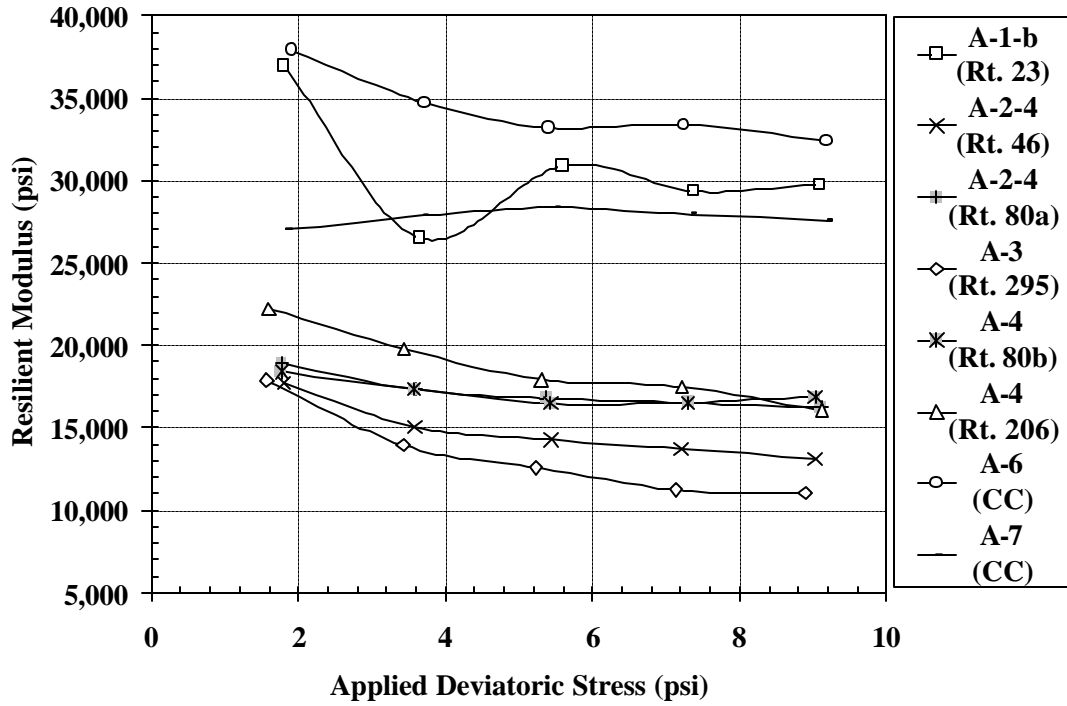


Figure 4.32 All Soil Types Compacted 2 % Dry of Their Respective Optimum Moisture Content and Tested at a Confining Pressure = 6 psi

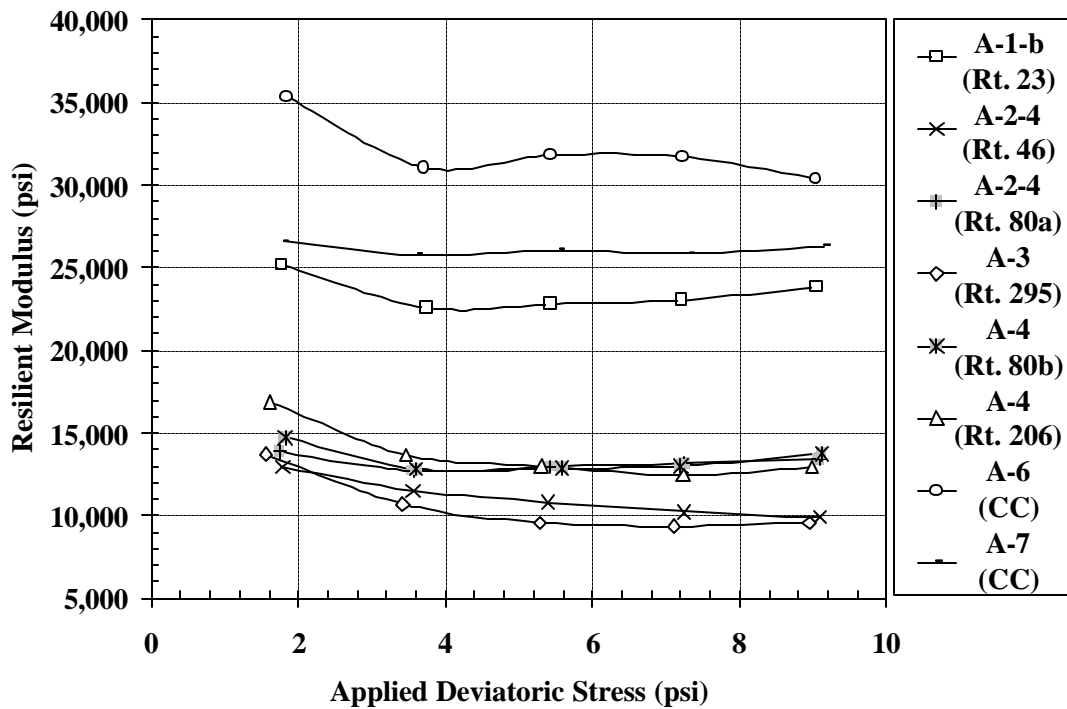


Figure 4.33 All Soil Types Compacted 2 % Dry of Their Respective Optimum Moisture Content and Tested at a Confining Pressure = 4 psi

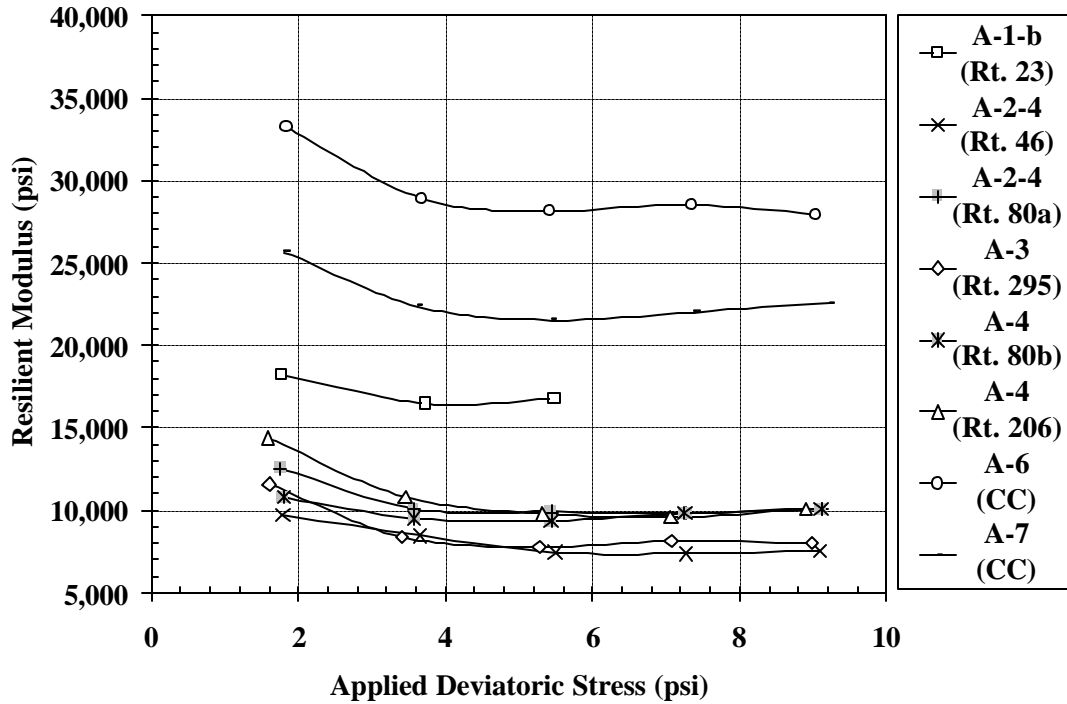


Figure 4.34 All Soil Types Compacted 2 % Dry of Their Respective Optimum Moisture Content and Tested at a Confining Pressure = 2 psi

4.3.1 Comparison of Type 2 Materials at Different Moisture Contents

As shown on figure 4.35 and 4.36, Type 2 Rt. 46 and 80a materials were not significantly influenced by moisture content. These materials were further classified as AASHTO A-2-4 type soils. The average resilient modulus of the Rt. 46 material at optimum and 2% dry of optimum is similar during the initial loading sequences with a slight increase of the 2% dry material at higher cyclic stress ratios. Rt. 80a had a 10% higher resilient modulus during the initial loading sequence and increased to 29% during the final loading sequences. At optimum and 2% wet of optimum, the resilient modulus was similar during the initial loading sequences with the 2% wet of optimum 10% lower than the material compacted at optimum for the final loading sequences.

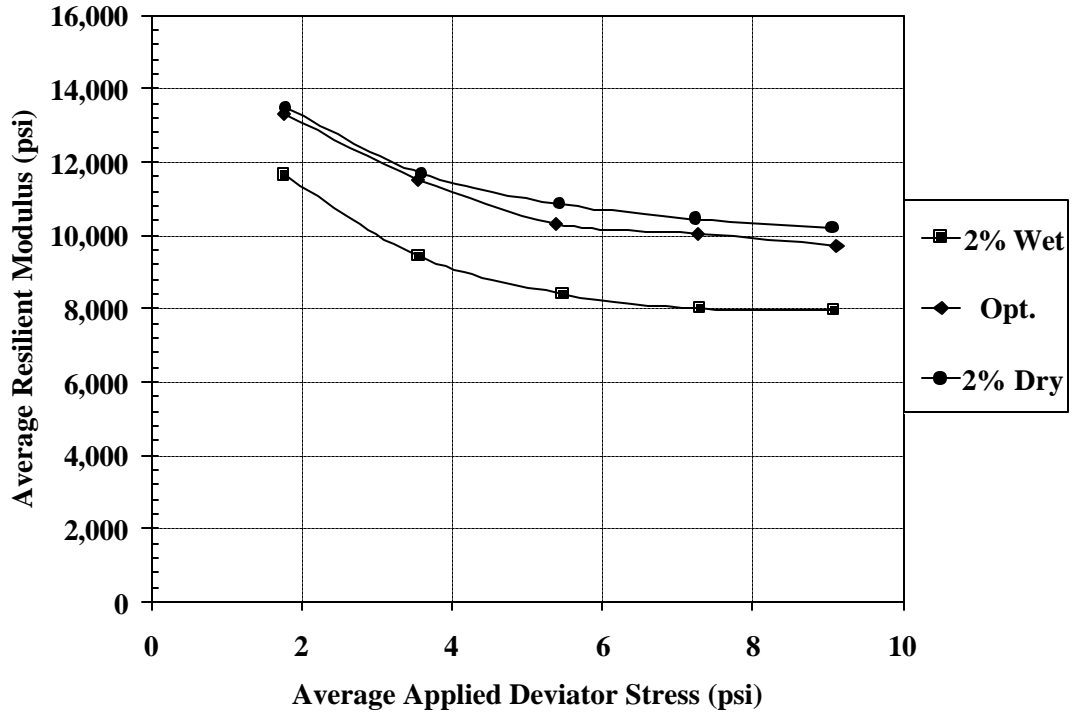


Figure 4.35 Comparison of AASHTO Type 2 (Rt 46) Resilient Modulus Test Results (A-2-4)

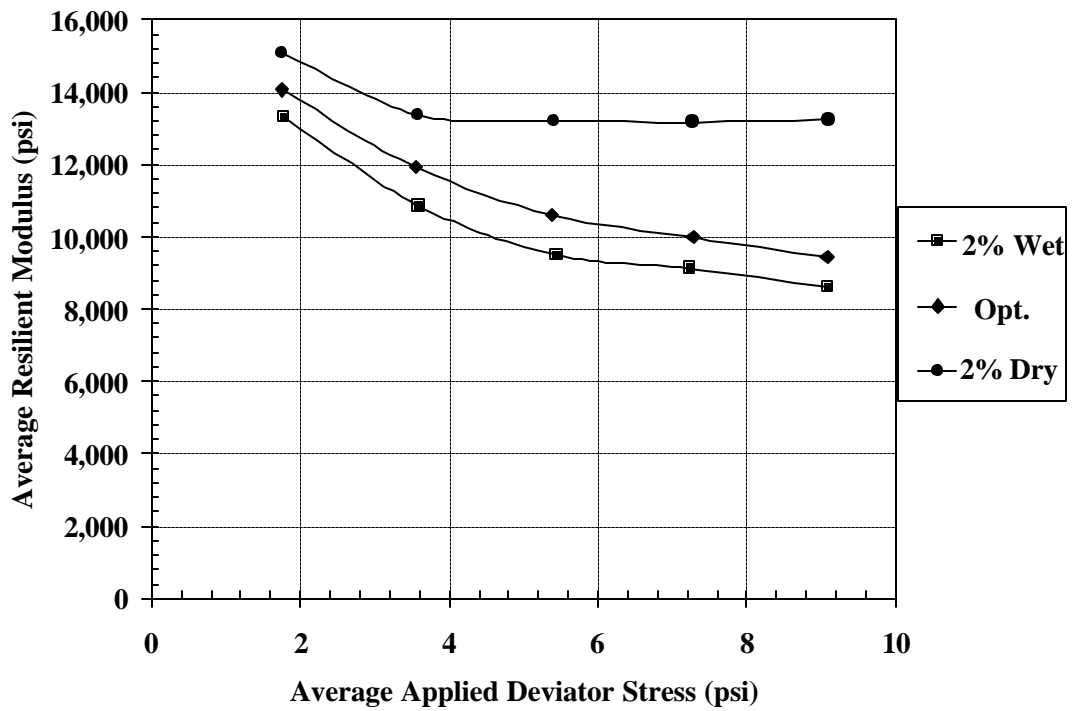


Figure 4.36 Comparison of AASHTO Type 2 (Rt 80a) Resilient Modulus Test Results (A-2-4)

Figures 4.37 and 4.38 show the resilient modulus of type 2 Rt 80b and 206, respectively. As illustrated in the figures, the A-4 soils are more affected by variations in moisture content than previously mentioned A-2-4 soil. The average resilient modulus for the Rt. 206 soil was 36% higher for the samples compacted 2% dry of optimum and 22 % lower for the wet samples as compared to the optimum sample. The variation of resilient modulus was influenced significantly by the variation in moisture content during the final sequences. The sample compacted 2% dry of optimum was 40% higher than the optimum sample with the wet sample 31% during the final loading sequences. The Rt. 80b samples undergo a similar response to the loading sequences, except for the 2% wet sample. The 2% wet sample actually has an average resilient modulus higher than the samples compacted at optimum or at 2% dry of optimum. However, due to the elevated moisture content, the sample suffers from extreme strain softening and is eventually less than the optimum sample at the final two applied deviator stresses (10 % less). However, when comparing the 2% dry sample to the optimum sample, the resilient modulus of the 2% dry sample is on average 25% higher than the optimum sample, with the difference increasing as the applied deviator stress increases. One thing to consider is that the performance of the Rt. 80b 2% wet sample does not seem to fall under the typical trend shown in the other soil samples tested. This may be due to poor contact at ends, which is eventually overcome at the higher applied contact stresses.

As shown figure 4.39 the resilient modulus for type 2 AASHTO A-3 soil is not as significantly affected by a variation in moisture content as compared to the four other Type 2 materials tested. The resilient modulus of the sample compacted 2% dry of optimum is slightly higher during the initial loading sequence and final loading sequences

as compared to the optimum sample. The sample compacted 2% wet of optimum is an average of 18% lower of the optimum sample for all loading sequences.

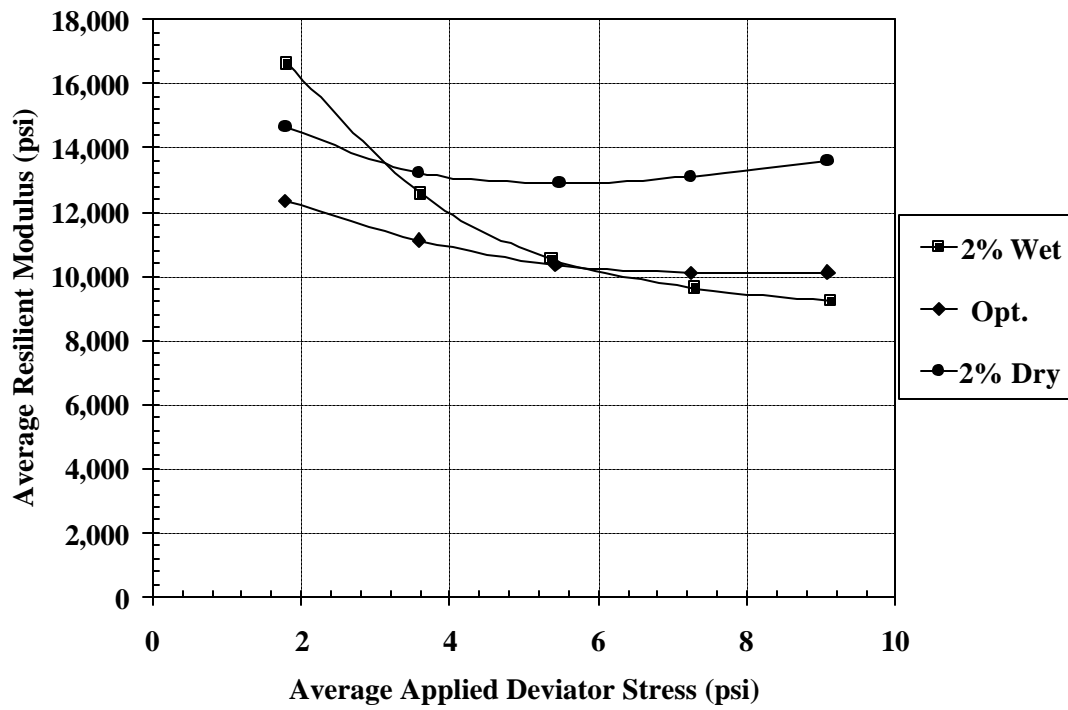


Figure 4.37 Comparison of AASHTO Type 2 (Rt 80b) Resilient Modulus Test Results (A-4)

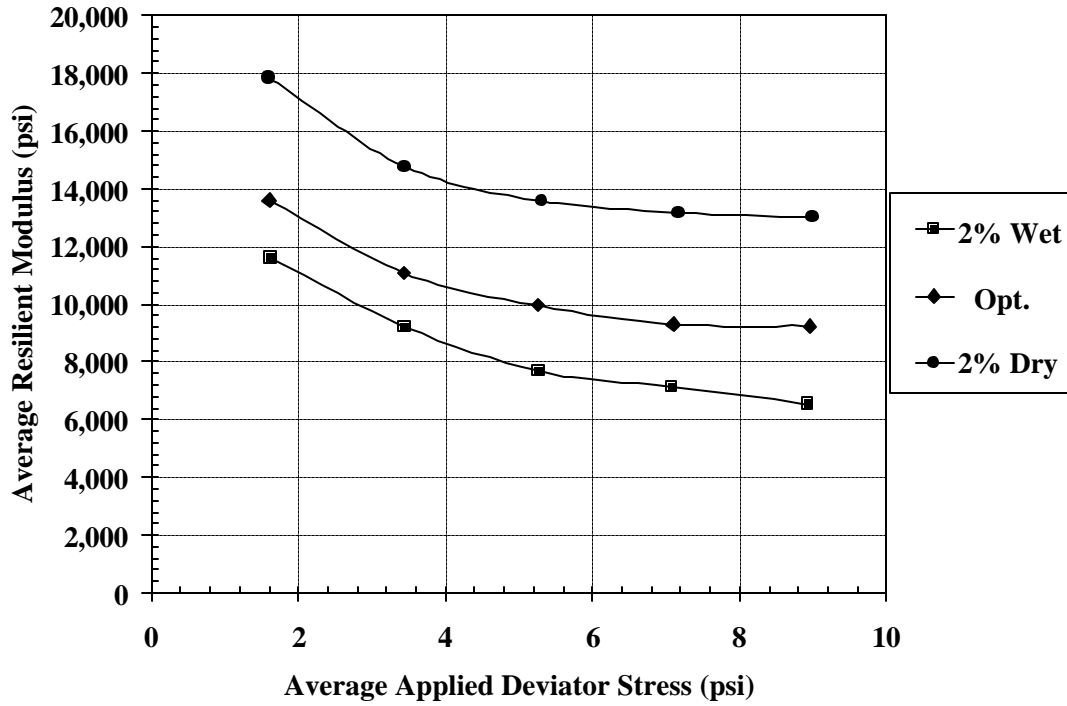


Figure 4.38 Comparison of AASHTO Type 2 (Rt 206) Resilient Modulus Test Results (A-4)

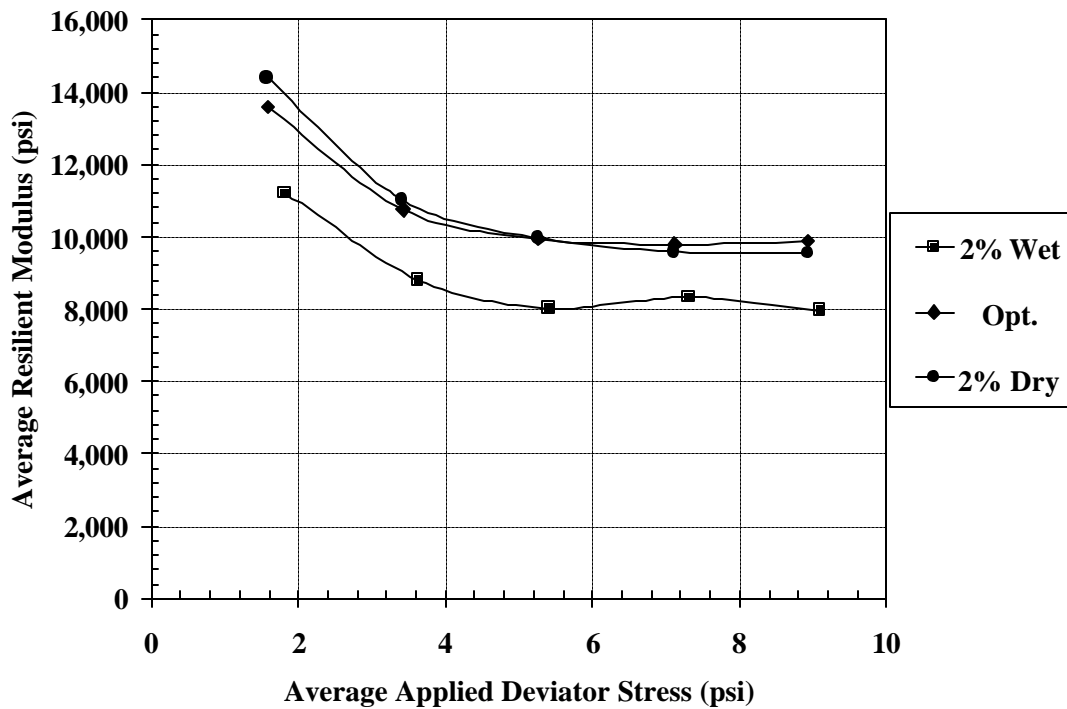


Figure 4.39 Comparison of AASHTO Type 2 (Rt 295) Resilient Modulus Test Results (A-3)

The average results of the two Cumberland county soils with their respective moisture content designation are shown as Figures 4.40 and 4.41. As shown in Figure 4.40, the A-6 soil is extremely affected by the existence of an elevated moisture content. The sample compacted 2% wet of optimum is an average of 70% lower of the optimum sample, with the difference increasing with increasing applied deviator stress. The sample compacted 2% dry of optimum has a uniform increased value for the resilient modulus at all applied deviator stresses, averaging approximately 30% higher than the optimum sample. Meanwhile, the A-7 sample appears to be even more affected when the moisture content exceeds the optimum. As shown in Figure 4.41, the 2% wet of optimum has a significant decrease in resilient modulus as the deviator stress increases. On an average, the 2% wet of optimum sample is 150% less than the resilient modulus value of the optimum sample, with a 50% difference at the lower deviator stresses and an approximately 225% difference at the higher deviator stresses. On the other hand, the 2% dry of optimum sample and the optimum sample are relatively equal throughout the entire range of deviator stresses applied. Both the optimum and the dry of optimum samples for the A-6 and the A-7 samples also demonstrate an elevated resilient modulus when compared to the other soils at the same moisture-compaction levels. This is mainly due to the fact that both the A-6 and the A-7 soils were compacted under the modified compaction method (T180-94), creating a very dense sample for these particular moisture contents.

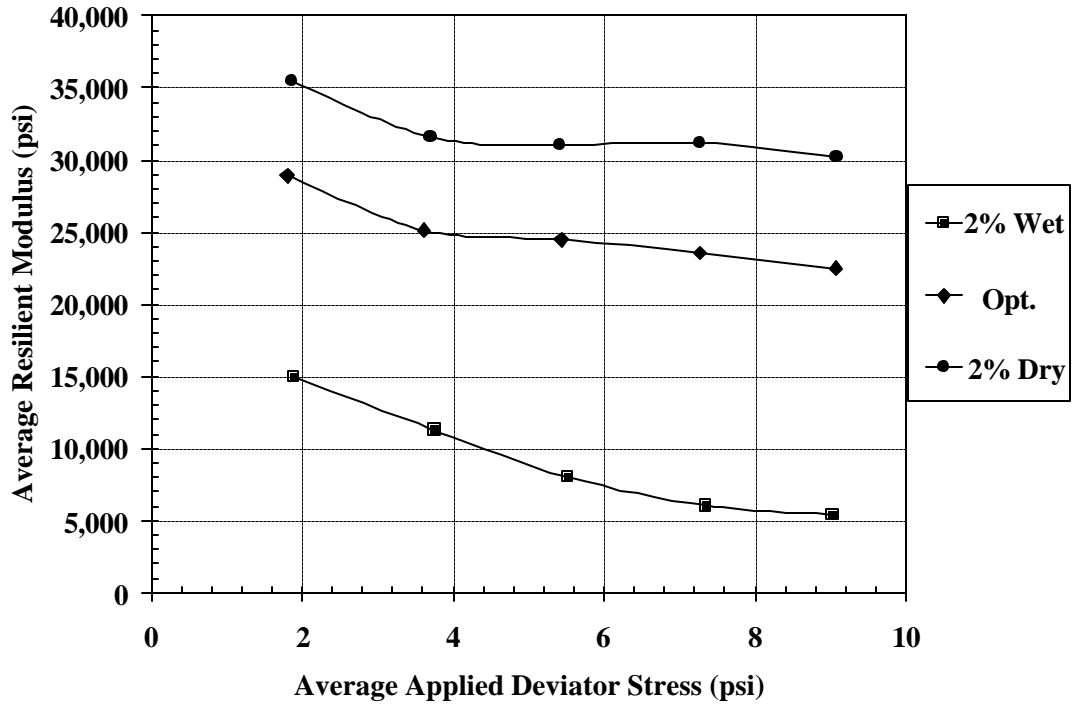


Figure 4.40 Comparison of AASHTO Type 2 (Cumberland County A-6) Resilient Modulus Test Results.

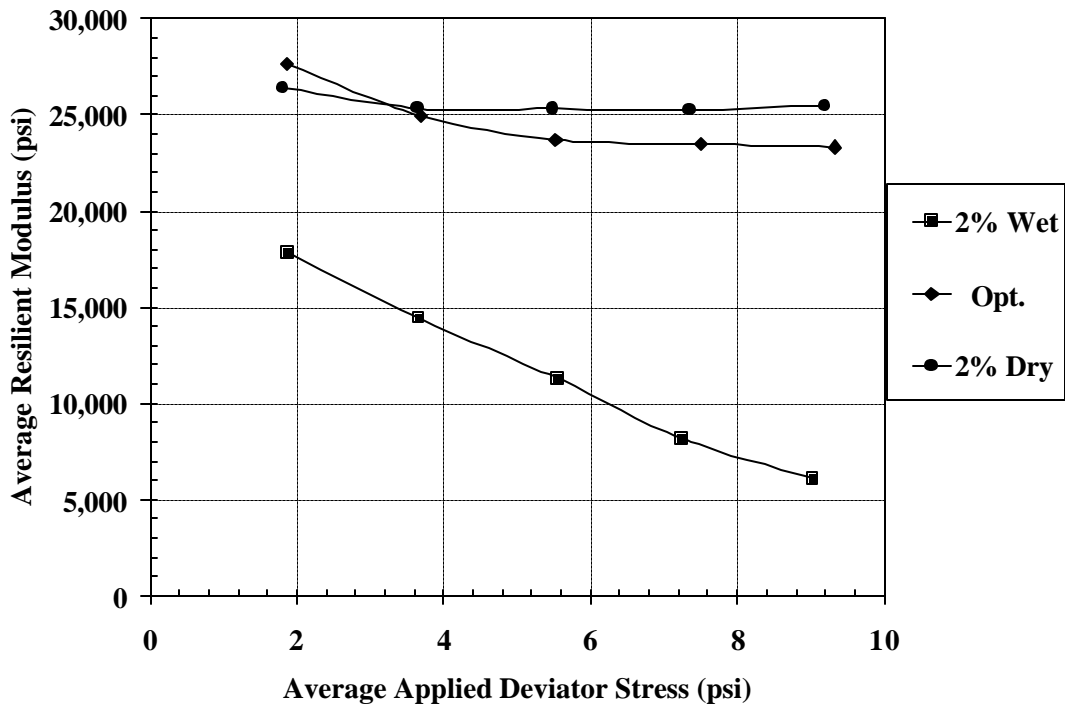


Figure 4.41 Comparison of AASHTO Type 2 (Cumberland County A-7) Resilient Modulus Test Results.

4.4 Test Results and Discussion

1. New Jersey AASHTO A-1-b granular soils undergo strain hardening during the resilient modulus test, thereby increasing the resilient modulus with increasing deviatoric stress, provided the deviatoric stress ratio does not exceed 1.35. Well-graded granular soils are very sensitive to change in moisture content from the very small pores, which are highly influenced by soil suction.
2. AASHTO Type 2, A-2-4 and A-4 fine-grained soils behaved similarly during the resilient modulus test. The resilient modulus decreased with increasing cyclic deviatoric stress, which can be explained by strain softening. The sensitivity of these materials to water content is less pronounced due to the structure and fabric as compared to Type 1 materials.
3. AASHTO A-3, fine beach sand did not exhibit the same characteristics as the previously mentioned soils. As with the A-4 and A-2-4 soils, the A-3 material exhibited a decrease in resilient modulus with increasing deviatoric cyclic stress ratios. However, it was not as sensitive to changes in water content.
4. AASHTO A-6 and A-7 seem to only be slightly affected when the sample is on the dry side of optimum. However, the sample is extremely affected on the wet side of optimum. Extreme strain softening occurs in the 2% wet of optimum

samples, with the most difference occurring at the higher applied deviator stresses where the calculated resilient modulus values are approximately 5,000 psi.

V. PORE PRESSURE GENERATION AND DISSIPATION

5.1 Introduction

It is widely known that pavement subgrades experience temporary seasonal changes in water content and undergo changes in their long-term average annual water content. Increases in subgrade water content are accompanied by decreases in subgrade resilient modulus and overall decrease in pavement performance. Conversely, a decrease in subgrade water content is accompanied by an increase in resilient modulus, stiffness and overall pavement performance. When the ground surface is sealed off with a pavement system and accompanied by good drainage, the uppermost part of the subgrade will not exhibit a large variation in water content provided the water table does not contribute to the overall moisture content. For subgrade depth near the phreatic surface (water table) soil suction and capillary effects contribute to water content in the subgrade. At depths above the phreatic surface, the water pressures are below atmospheric pressure, causing the water to migrate higher into the subgrade. Suction arises from the phenomena, which reduces the free energy of water. This leads to surface tension or capillary effects at the solid-water-gas interfaces. Some of the main influences of water infiltration are shown in figure 5.1. All these factors contribute to the increase of water content in the subgrade and in severe cases achieve conditions at or near saturation as shown on figure 5.2

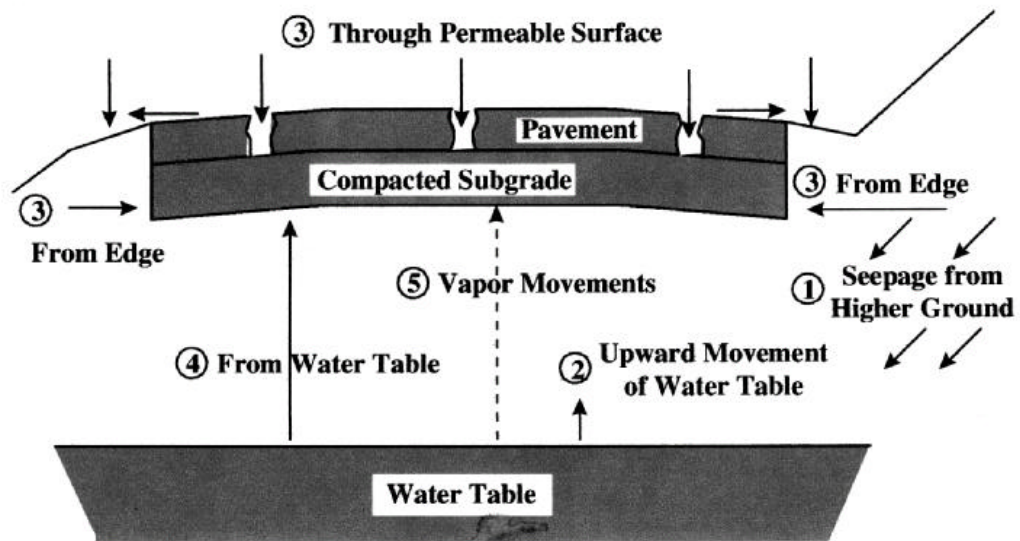


Figure 5.1 Schematic of Water Infiltration in Pavement System (Hall and Rao 1998)

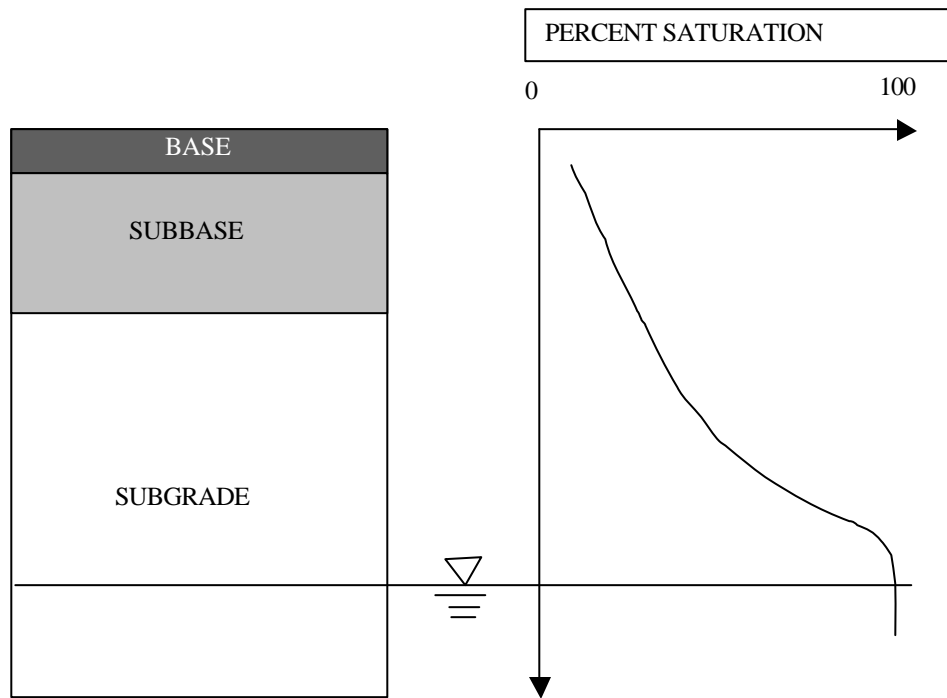


Figure 5.2 Schematic of Percent Saturation with Depth

The flexible pavement design procedures presented in AASHTO requires the use of mechanical properties for the asphaltic concrete, base course, and subgrade. The stiffness of the subgrade soil is represented by the resilient modulus. Using resilient modulus values for each subgrade material encountered on a pavement project will allow pavement engineers to design a higher performance pavement system using mechanistic design procedures. Typically, the resilient modulus is determined at or near optimum water content in the laboratory in accordance with AASHTO TP46-94.

Pavement subgrades, usually compacted close to (i.e. 2% above or below optimum) optimum water content and at maximum dry density during construction

experience seasonal variations in water content (Drumm et.al 1997). Most fine-grained soils exhibit a decrease in resilient modulus as the moisture content is increased, leading to an increase in deflection and permanent deformation. In general, an increased deflection in the subgrade leads to decrease in pavement design life (Thomson and Elliot 1985; Elliot and Thorton 1998). Elfino and Davidson (1989) conducted resilient modulus tests on specimens subjected to water content variations after compaction. The water contents were varied through the natural matric suction developed in the specimen, corresponding to a specified elevation above the water table. These tests indicated clayey sand and silty specimens exhibited both an increase in water content and a decrease in resilient modulus relative to the conditions at optimum water content. Poorly graded sand specimens exhibited a decrease in moisture content with increasing height above the water table and an increasing resilient modulus due to matric suction (Drumm et.al. 1997).

Raad et al. (1992) studied the behavior of typical granular materials with different gradations under saturated, undrained, repeated triaxial loading conditions set forth by AASHTO Designation T 274-82. Their research is the comparative behavior of open-graded and dense graded base courses, and the influence of fines on the dynamic response. Their results indicated that the dense graded aggregates exhibited the highest resilient modulus values, while open-graded aggregates had the lowest. However, their results indicated when the materials were saturated, they would develop excess pore water pressure, which would lead to a decrease in resilient modulus. Open-graded aggregates are more likely to resist the generation of pore pressure than that of dense graded aggregates under saturated conditions. As shown of figure 5.3, saturated

contractive soils (loose) are subject to liquefaction potential above the steady state line while dilative soils (dense) below the steady state line are not susceptible. Pavement systems (base, subbase, and subgrade) are generally well prepared and compacted to achieve a dense to very dense state. Therefore, any reduction of strength may be caused by cyclic mobility due to large strains. These large strains may be transferred to the base and subbase directly below the paved surface. Subgrades are considerably lower in the pavement system and are not subjected to large axial stresses, which would develop excessive strains. Additionally, the effective minor principle stresses increases with depth providing additional support for the subgrade.

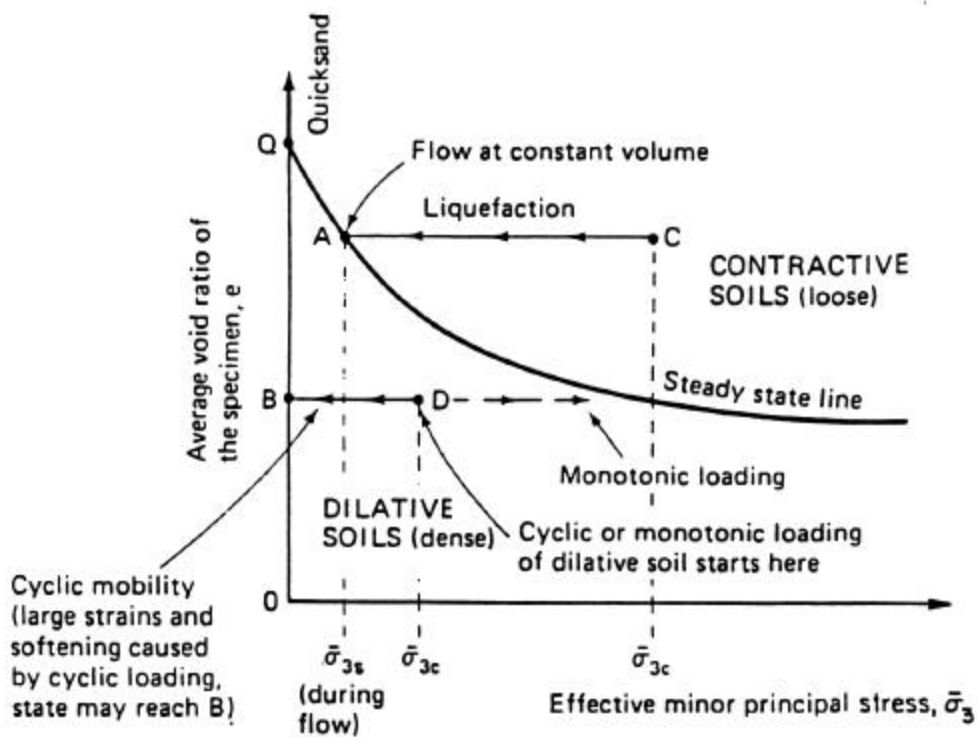
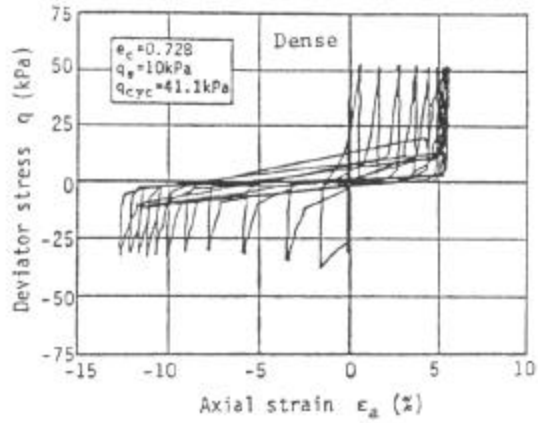
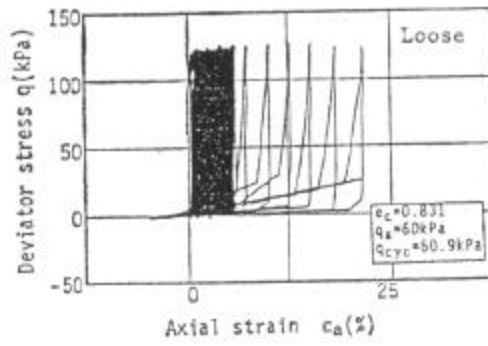
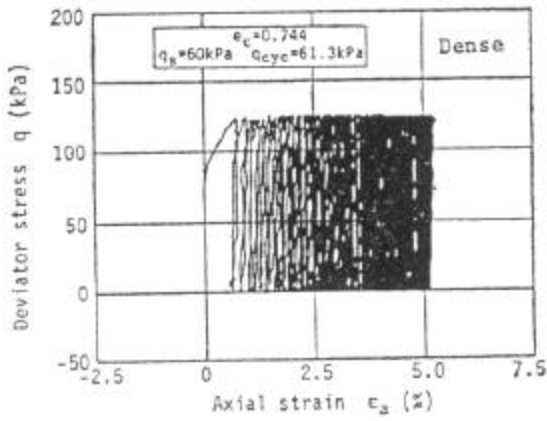


Figure 5.3 Steady State Diagram Showing Liquefaction Potential Based on Undrained Tests of Saturated Sands (Castro and Paulos, 1976)

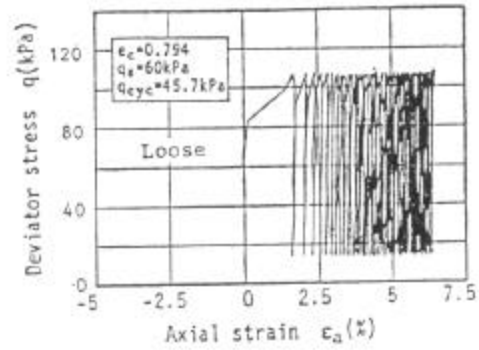
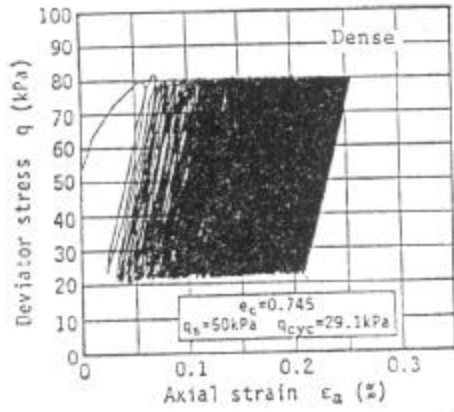
Additional studies by Hyodo et al. 1991 evaluated the undrained cyclic triaxial behavior of saturated sands. As shown in figure 5.4 cyclic tests were performed considering both reversal and no reversal of cyclic shear stresses. Figure 5.4 (a) represents reversal of the deviatoric stress, (b) represents intermediate reversal and (c) represents no reversal. In the case of no reversal (dense), the deviatoric stress ratio is 0.48, which corresponds to cyclic deviatoric stress ratios of 0.45 for sequences 2, 7, and 11 in the resilient modulus test for subgrade soils. Their tests indicate that in the case of no reversal, the stress path for the loose sand ($D_r = 50\%$) was similar to that of the dense one in the intermediate case, but the path of the dense never reached the failure envelope. All stress paths show that the maximum pore pressure reaches the value of the initial effective confining pressures in the samples with stress reversal. In the case of no reversal, only residual strains were observed, with the residual strain of the dense smaller than that of the loose ones, which was not enough to cause failure. The characteristics of failure correlated with the pattern of cyclic stress reversal are summarized in table 5.1. The failure was observed in all types except in the case of no reversal on the dense samples. The pattern of failure was classified by liquefaction or residual deformation.



(a)



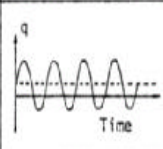
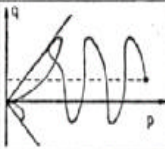
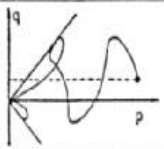
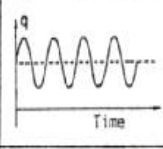
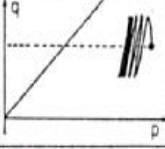
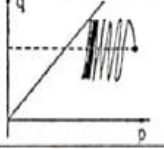
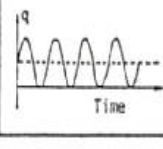
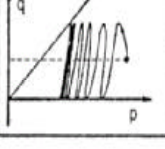
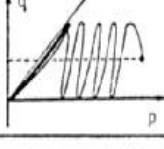
(b)



(c)

Figure 5.4 Relationship Between Deviator Stress and Axial Strain (Hyodo et. al. 1991)

Table 5.1 Classification of Failure Correlated with Pattern of Cyclic Stress Reversal (Hyodo et al.1991)

Pattern of cyclic stress		Effective stress path		Characteristic of failure	
Stress reversal	Wave form	$D_r=70\%$	$D_r=50\%$	$D_r=70\%$	$D_r=50\%$
Reversal $q_s < q_{cyc}$				Liquefaction	Liquefaction
No reversal $q_s > q_{cyc}$				No failure	Residual deformation
Intermediate $q_s \approx q_{cyc}$				Residual deformation	Liquefaction or Residual deformation

5.2 Effect of Pore Pressure/Saturation on Resilient Modulus of Fine Sand

Samples of type 2, A-3 (Rt. 295) soils were compacted at optimum moisture content using AASHTO designation TP46-94 type 2 compaction procedures as described in chapter 3. These samples were then placed in the triaxial chamber and back-saturated to achieve saturated or near saturated conditions. Upon completion of saturating the samples, resilient modulus tests were performed while measuring the pore pressure generated in the sample during the test. The tests were run following AASHTO TP46-94 testing sequence for subgrade soils as shown in Table 3.2. AASHTO suggests leaving the drainage valves open throughout the test, however, to determine if any pore pressures are generated during the test, the drains were kept closed. Two pore pressure transducers were used to measure the generation of pore pressure within the sample. One was connected to the top platen and one to the bottom platen. The pore pressures at the top and bottom of the sample were averaged if there were no significant differences, otherwise it was noted.

A typical graph of resilient modulus vs. percent strain is presented on figure 5.5. The figure shows the cyclic loading sequence for three different confining pressures, each with 5 increasing loading sequences. Each of the five loading sequences consists of 100 loading cycles with increasing applied deviatoric cyclic stresses from 1.8 psi to 9.0 psi. During the first loading sequence at a confining pressure of 6.0 psi, the accumulated strain was 0.24 percent. The second loading sequences at a confining pressure of 4.0 psi increased the permanent strain from 0.24 percent to 0.48 percent with a net increase of

0.24 percent strain. The final loading sequence at a confining pressure 2.0 kPa increased the permanent strain from 0.48 percent to 0.98 percent strain with a net increase of 0.5 percent strain.

Determining pore pressure generations during the entire resilient modulus test proved to be difficult due to the change of confining and deviatoric stresses throughout the test. As shown in figure 5.6, the pore pressure increased 0.48 psi during the first 500 cycles. The increase in pore pressure within the sample decreases the effective confining stress. As specified by AASHTO TP46-94 the effective confining stress for the first 5 sequences or 500 cycles should be 6.0 psi. However, with a pore pressure increase of 0.48psi, the net effective confining stress is lowered, thereby decreasing the resilient modulus and increasing the permanent deformation on the sample. During the next five loading sequences or 500 loading cycles, the pore pressure only increased by 0.03 psi. Typically the accumulated permanent strain for the first five loading sequences would be less than the second five because of the decrease in confining pressure for the second. However, the increase in pore pressure during the first five loading sequences decreased the effective confining pressure, decreasing the resilient modulus and increasing the permanent strain. This may explain why the accumulated permanent strain for the first and second 5 loading sequences are similar. During the final 5 loading sequences, the pore pressure decreased to -0.4 psi, which suggests the densely packed soil particles rolling over each other increasing the volume of the sample, thus decreasing the internal pore pressure.

As discussed earlier, the resilient modulus of granular materials is sensitive to confining pressure. As the effective confining stress decreases, the permanent deformation increases. The resilient modulus is measured assuming the sample has accumulated all the permanent deformation in the loading cycle and the additional deformations are assumed to be completely recoverable. This assumption may be true for the first two loading sequences at each of the three different confining stresses. For the remaining three loading sequences for each the three confining stresses, the measured resilient modulus over the last five loading cycles in each sequence is not completely elastic as shown on figure 5.5

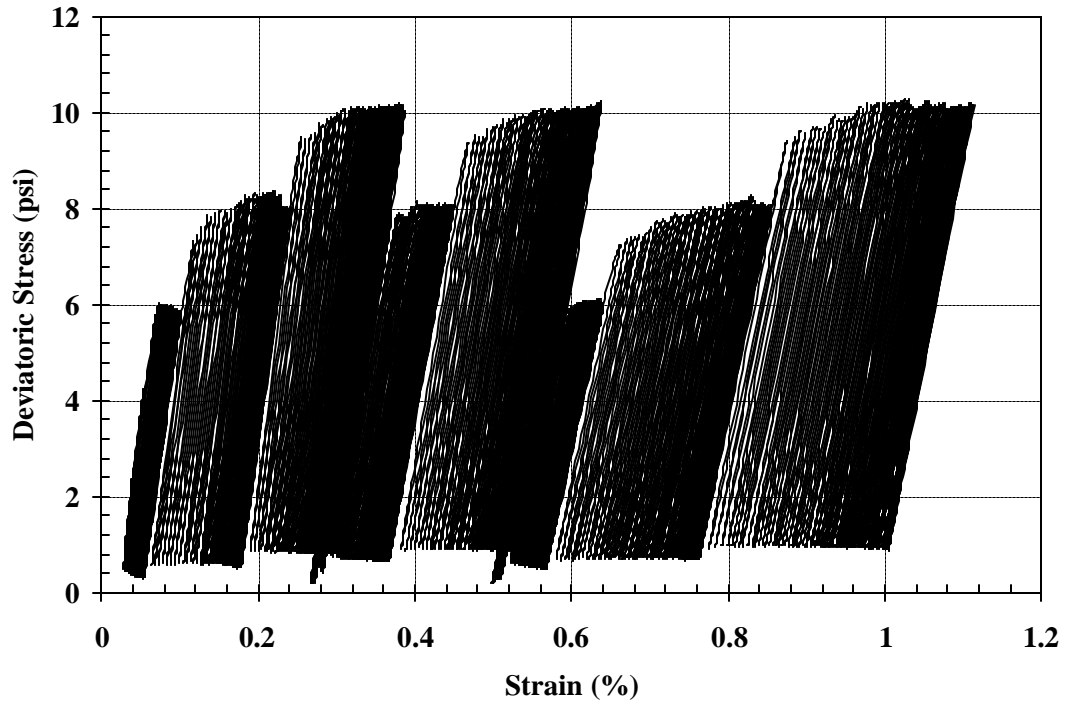


Figure 5.5 Deviatoric Stress vs. Percent Strain

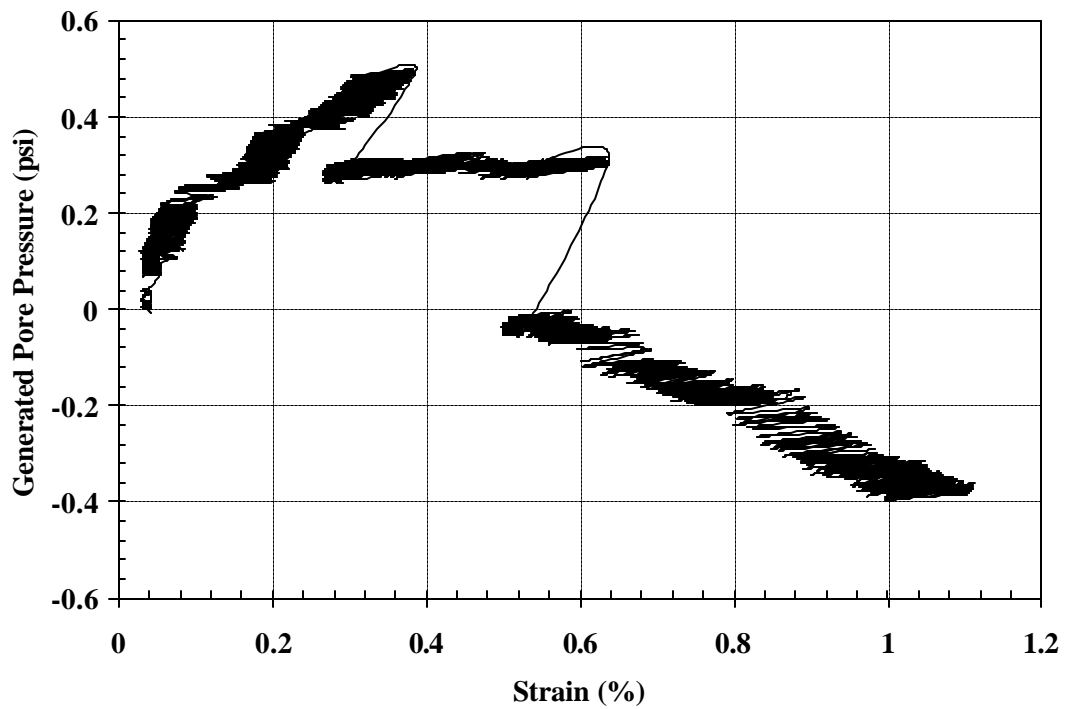


Figure 5.6 Pore Pressure Generation During a Resilient Modulus Test

VI. NUMERICAL MODEL FOR RESILIENT MODULUS

6.1 Introduction

Resilient modulus (M_r) has been used to describe the nonlinear stress-strain behavior of granular base and subbase soils. After repeated loading and unloading sequences, each layer accumulates only a small amount of permanent deformation, with recoverable or resilient deformation. Researchers have used the concept of resilient modulus to explain the behavior of pavement systems. (Santha, 1994).

Under repeated load tests, it is observed that as the number of loading cycles increases, the energy dissipated during a given loading cycle decreases. This is evident by a decrease in stress-strain hysteresis, and is accompanied by an increase in the secant modulus. After a number of loading cycles, the modulus becomes nearly constant, and the response can be assumed to be approximately elastic. This steady value of modulus is defined as the resilient modulus, M_r , and is assumed to occur after 100 loading cycles for a given stress ratio.

The resilient modulus is obtained by subjecting a specimen to repeated loading at a particular stress level and measuring the recoverable strain. Ideally, the specimen is exhibiting only elastic strains at the time the resilient modulus is measured. Typically the resilient modulus is measured while the specimen is still exhibiting plastic deformation. However, most specimens accumulate 50% of the permanent deformation after the first 10 load cycles (Muhanna et al. 1998). In some soils the resilient modulus is measured while the specimen is still exhibiting permanent deformation. The resilient modulus can

therefore be thought of as the secant Young's modulus of the material, which is typically different than the initial tangent value of Young's modulus shown in figure 6.1 (Houston et al., 1993); where σ_1 = total vertical stress, σ_3 = confining pressure, and $(\sigma_1 - \sigma_3) = \sigma_d =$ deviatoric stress due to the applied load.

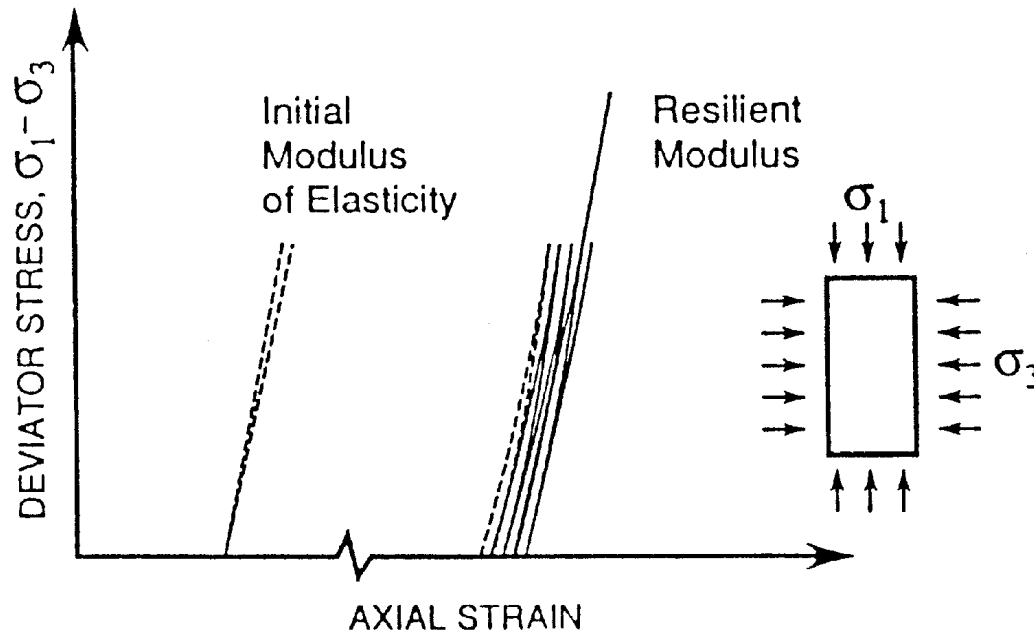


Figure 6.1 Initial Modulus of Elasticity Compared to Resilient Modulus

It is a known fact that when stresses on a soil specimen are increased to a level higher than ever applied previously, plastic strains will develop (Seed et al. 1962). When a specimen is overstressed by a spherical stress, plastic deformation occurs when the bonds between the particles are broken and tend to form in a more dense state. When the deviatoric stress is increased, plastic deformation occurs when the bonds between the particles are broken and don't form into a more dense state, but rather in a weaker state, which decreases the ability to resist shear stress (Houston et al. 1993).

The measured modulus is sensitive to an increase in either normal or shear stress to levels higher than ever applied before because plastic strains are induced. However, when significant plastic strains occur, the resilient modulus cannot be measured in a straightforward manner because elastic and plastic strains must first be separated. Thus, the resilient modulus is most readily quantified when the following conditions are met:

The stresses applied (both shear and spherical) are less than or equal to the maximum level of stress previously applied. The stress has been applied for a sufficient number of times so the strains become essentially completely recoverable (Houston et al. 1993).

Resilient modulus has been used to describe the nonlinear characteristics of base and subbase soils. Granular materials and cohesive soils are nonlinear and stress dependant under cyclic loading. Stress path and magnitude significantly affect elastic and resilient modulus of the soil. In the past, many models have been used to describe the stress-strain behavior of base and subbase soil under cyclic loading. To justify the resilient modulus predictions from the models, large databases of resilient modulus values have to be recorded using a variety of base and subbase materials.

6.2 Estimation of Resilient Modulus

Some early attempt have been made to correlate the resilient modulus of the soil by using California bearing ratio (CBR) and R-value determined by a stabilometer. Since

the resilient modulus is determined through a cyclic or dynamic test and the CBR and R-values are determined by static tests, they do not accurately predict the resilient modulus. The correlation between the CBR and resilient modulus is shown by equation 6.1, where the coefficient may vary from 750 to 3000, resulting in a large deviation from the actual resilient modulus. The correlation of R-value to an equivalent resilient modulus is shown by equation 6.2. Typically, CBR values over 25 and R-values over 60 overestimate the actual resilient modulus.

$$M_r = 1500 (\text{CBR}) \quad (6.1)$$

$$M_r = 1155 + 555 (R) \quad (6.2)$$

6.3 Statistical Models for Resilient Modulus Prediction

Linear and nonlinear regression techniques have been used to obtain the different parameters for the following models. Elhannani's model (1991) can be used for predicting the response to cyclic deviatoric stress with cyclic cell pressure data. Using the K- θ , Pappin and Brown models (1980), approximate predictions can be made of axial stiffness under the cycling of both stresses using parameters obtained from more-simple cyclic deviatoric stress data (Karasahin et al. 1993). The bulk stress and universal models are used for predicting resilient modulus from the results obtained from the AASHTO resilient modulus test. Comparison of AASHTO/SHRP granular model and the UTEP model (Feliberti et al. 1992) were compared where the AASHTO/SHRP model was based

on the relationship between M_r and deviatoric stress, and the UTEP model was based on bulk stress and strain level.

Granular material is nonlinear and stress dependent, therefore, nonlinear stress-strain relationship should be used to model the real base and subbase behavior. The first five models, which will be discussed will be expressed in terms of mean pressure (p) which is one third the first stress invariant (J_1) and q which is the deviatoric stress (Houston et al. 1993).

6.3.1 K-q Model

This model is typically used by pavement engineers to introduce a stress dependent M_r because it is easily implemented in finite element and back calculations programs. The model is expressed in equation 6.3.

$$M_r = A(3p_{\max})^B \quad (6.3)$$

Some of the shortcomings of this model is the Poisson's ratio is assumed to be constant under a variety of stress conditions, and the effect of deviatoric stress is not recognized in this model. This model has been developed from a simple triaxial test where the initial deviatoric stress is zero, and the model is good for only relatively small deviatoric stress. This is clearly not the case in the field where the deviatoric stress could be higher than in the laboratory.

6.3.2 Pappin and Brown Model

When considering resilient modulus testing is useful to separate the behavior into shear and volumetric strain components along with deviatoric and radial stress components. It is known that volumetric strain decreases with the increase of confining pressure. Volumetric strain is directly affected by the amount of fines present in the specimen. A specimen with increasing fines would result in an increasing volumetric strain. Shear strains follow the same trends, indicating an increase in stiffness of the specimen from the finer to coarser gradation (Kamal et al. 1993).

The Pappin and Brown Model was developed in this manner. It was designed to model general stress path excursions regardless of the p, q stress state. The model could be expressed in equation 6.5 and 6.6.

$$\varepsilon_v = (p/A)^B(1 - C(q^2/p^2)) \quad (6.5)$$

$$\varepsilon_s = (p/D)^{E*}(q/p) \quad (6.6)$$

where $\varepsilon_v, \varepsilon_s$ are the volumetric and shear strain, respectively, and having material constants A and D have units of stress. The stress paths are assumed to be from zero, indicated by p and q. The bulk and shear moduli can be written in equation 6.7 and 6.8.

$$K = p/\varepsilon_v \quad (6.7)$$

$$G = q/3\varepsilon_s \quad (6.8)$$

6.3.3 Boyce Model

Boyce also developed a model using similar principles along with applying the theorem of reciprocity. The model is nonlinear elastic and isotropic. The model may be expressed in equation 6.9 and 6.10 (Boyce, 1980).

$$\varepsilon_v = p^B [(1/A) - ((1-B)/6C) * (q^2/p^2)] \quad (6.9)$$

$$\varepsilon_s = (p^B/3C) * (q/p) \quad (6.10)$$

In these equations, constants A and C have dimensions controlled by constant B. Mayhew found that the influence of the mean normal stress on the bulk modulus differs from that on the shear modulus (G), even when the ratio q/p is constant (Mayhew, 1983).

6.3.4 Elhannani Model

Elhannani introduced anisotropy into the original Boyce model that can be expressed in equation 6.11 and 6.12 (M. Elhannani. 1991), where p_a is atmospheric pressure (100 kPa) and A, C, and D have units of stress. The atmospheric pressure was used as a normalizing factor to make the stress components non-dimensional.

$$\varepsilon_v = p_a^{(1-B)} p^B [(1/A) - ((1-B)/6C) * (q/p)^2 - (B/D)(q/p)] \quad (6.11)$$

$$\varepsilon_s = p_a^{(1-B)} p^B [(1/3C) * (q/p) - 1/D] \quad (6.12)$$

6.3.5 Bulk Stress Model

The bulk stress model is used for modeling the resilient modulus using the concept of bulk stress. The model may be shown in equation 6.13. The bulk stress (θ) is the first stress invariant, P_a is atmospheric pressure expressed in the same units as M_r and θ , and k_1, k_2 are material and physical constants.

$$M_r = k_1 P_a (\theta/P_a)^{k_2} \quad (6.13)$$

The shortcoming of this model is that it does not adequately model the effect of the deviatoric stress, which is the key factor when measuring resilient modulus. (Santha, 1994)

6.3.6 Uzan Model

This model is a modified version of the K- θ Model with the introduction to the effect of deviatoric stress. The model is expressed in equation 6.14. σ_r is the radial stress. Yet the problem of a constant Poisson's ratio and zero initial deviator stress due to the constant coefficients still remains.

$$M_r = A (3p_{\max})^B q^C \quad q > 0.1\sigma_r \quad (6.14)$$

6.3.7 AASHTO / SHRP Model

AASHTO / SHRP both propose a relationship between M_r and the bulk stress (θ) which can be shown in equation 6.15.

$$M_r = 10^{k_1} \theta^{k_2} \quad (6.15)$$

AASHTO / SHRP both propose a relationship between M_r and the deviatoric stress (σ_d) which can be shown in equation 6.16.

$$M_r = 10^{k_1} \sigma_d^{k_2} \quad (6.16)$$

The constants k_1 , k_2 correspond to the material and physical characteristics of the soil.

6.3.8 UTEP Model

Hardin and Drenvich (1972) found two parameters, void ratio and average confining stress, significantly influence the modulus of soils. Bulk stress and confining stress are the two parameters that define the state of stress and strain level (Felberti et al. 1992). The level of strain is considered as direct parameter in both models. Equation 6.17 represents resilient modulus as a function of bulk stress, while equation 6.18 represents resilient modulus as a function of confining stress.

$$M_r = 10^{k_1} \theta^{k_2} \varepsilon^{k_3} \quad (6.17)$$

$$M_r = 10^{k_1} \sigma_c^{k_2} \varepsilon^{k_3} \quad (6.18)$$

6.3.9 Hyperbolic Model

Boateng-Poku and Drumm (1989) have determined there is a stress dependant nonlinear relationship for resilient modulus that is often characterized by exponential or bilinear relationships. A hyperbolic model for the stress softening response of fine-grained subgrades will be presented. A nonlinear relationship between resilient modulus and deviator stress can be conveniently represented by a hyperbolic function in equation 6.19, where a and b are material parameters.

$$M_r = (a + b \cdot \sigma_d) / \sigma_d \quad \text{for } \sigma_d > 0 \quad (6.19)$$

6.3.10 AASHTO Model

AASHTO specifications suggest the use of a power model on a log of M_r vs. log of deviatoric stress using least square regression. The Model can be expressed in equation 6.20, where k_1 and k_2 are material parameters.

$$M_r = k_1 \sigma_d^{k_2} \quad (6.20)$$

6.3.11 Universal Model (Modified Uzan)

Uzan (1985) demonstrated that the bulk stress model could not precisely describe nonlinear soil characteristics; therefore it was modified to more precisely model the nonlinearity of granular soils. The Universal model may also be used to predict the nonlinearity of fine grained and cohesive soils. Fine grained and cohesive soils are slightly influenced by confining stresses and greatly influenced by deviatoric stresses. Therefore since the Universal model integrates both of these factors, it is well suited for these soils as shown in equation 6.21, where k_1, k_2, k_3 are material and physical parameters, P_a is the atmospheric pressure, θ is the bulk stress ($\sigma_d + 3\sigma_3$), and σ_d is the deviatoric stress.

$$M_r = k_1 P_a (\theta/P_a)^{k_2} * (\sigma_d/P_a)^{k_3} \quad (6.21)$$

6.4 Comparison of Predicted and Experimental Results

In order accurately predict the nonlinearity of the soils during the resilient modulus test, the use of deviatoric and bulk stress in the Universal model was chosen. The Universal model was transformed to linear form in order to carry out linear regressions. The linear form of this equation is shown in equation 6.22.

$$\text{Log} (M_r) = \text{Log} (k_1 P_a) + k_2 \text{Log} (\theta/P_a) + k_3 \text{Log} (\sigma_d/P_a) \quad (6.22)$$

Linear regressions were performed for each soil at various moisture contents, where k_1 , k_2 , and k_3 soil parameters were determined. These soil parameters were then used to predict the resilient modulus for each stress condition of each sample tested. The stresses and resilient modulus properties were normalized with respect to atmospheric pressure in order to keep the constants non-dimensionalized. The atmospheric pressure used in this analysis was 14.7 psi. Figures 6.2 - 6.9 shows the predicted resilient modulus versus the actual resilient modulus.

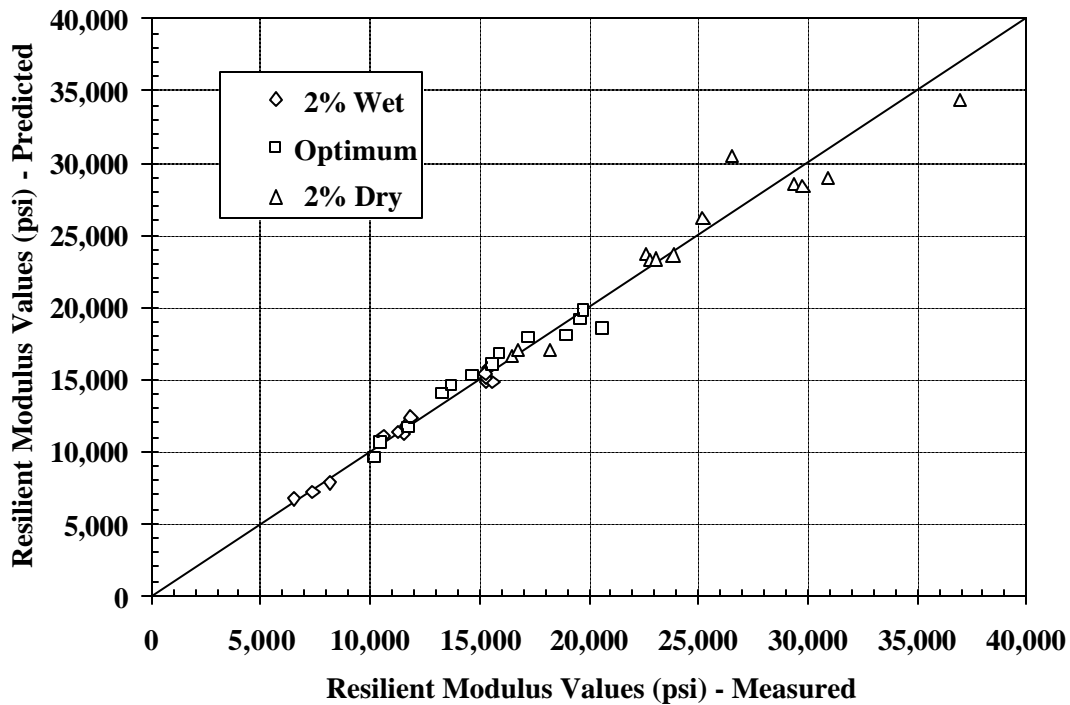


Figure 6.2 Plot of Predicted Resilient Modulus versus Measured Resilient Modulus for A-1-b (Rt. 23) Type Soils

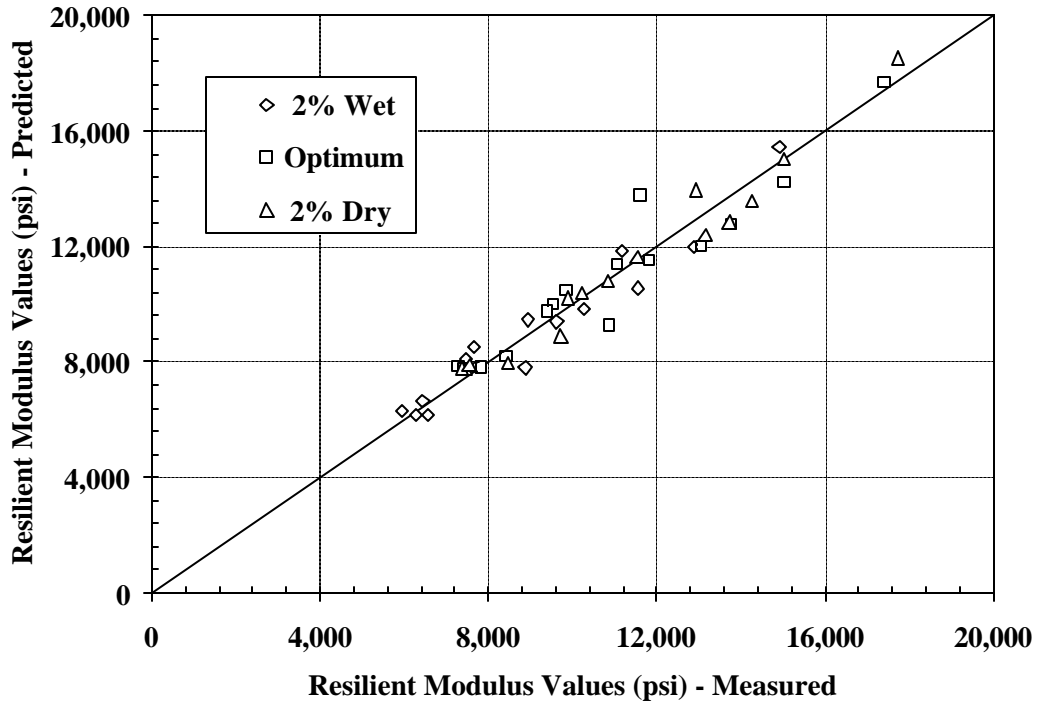


Figure 6.3 Plot of Predicted Resilient Modulus versus Measured Resilient Modulus for A-2-4 (Rt. 46) Type Soils

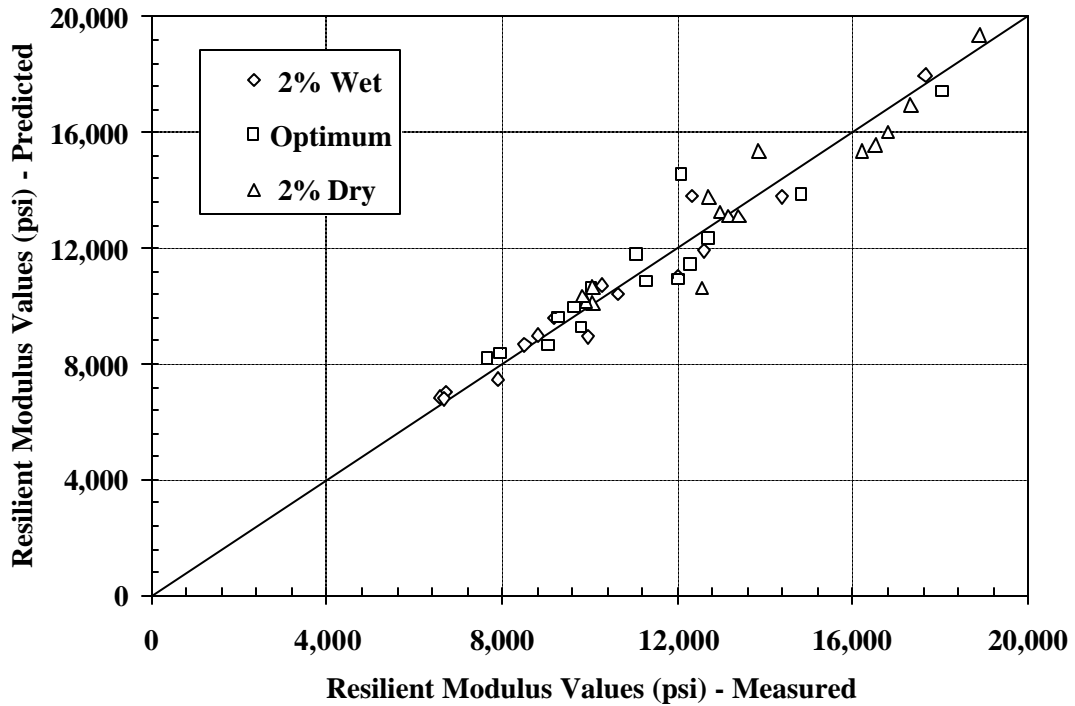


Figure 6.4 Plot of Predicted Resilient Modulus versus Measured Resilient Modulus for A-2-4 (Rt. 80a) Type Soils

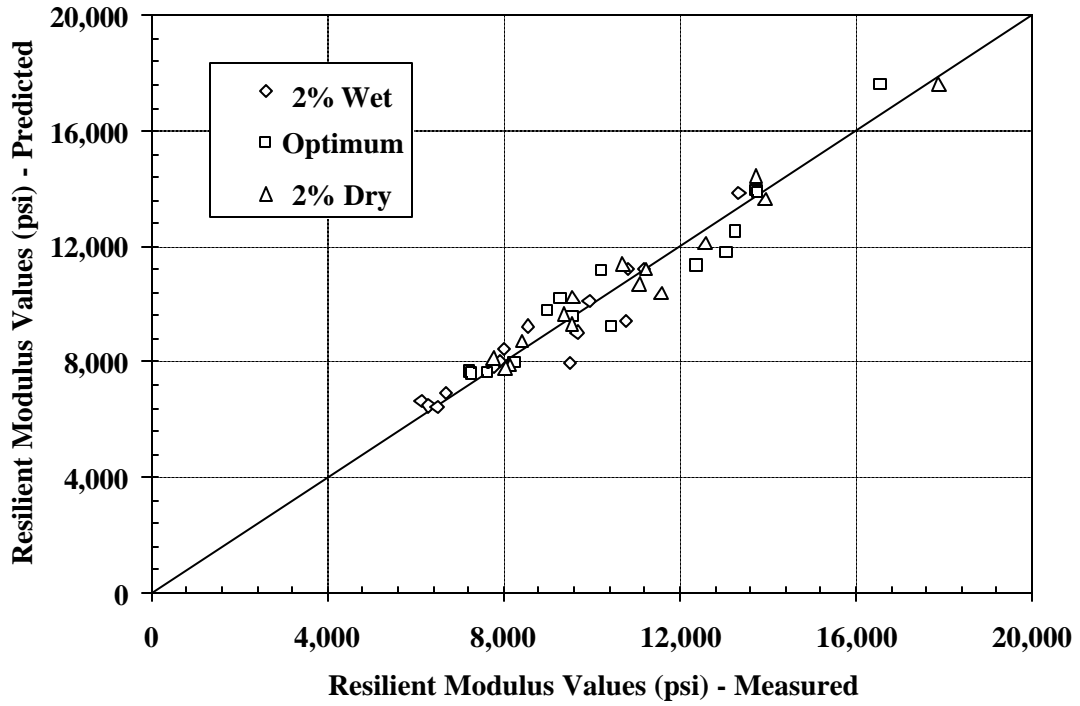


Figure 6.5 Plot of Predicted Resilient Modulus versus Measured Resilient Modulus for A-3 (Rt. 295) Type Soils

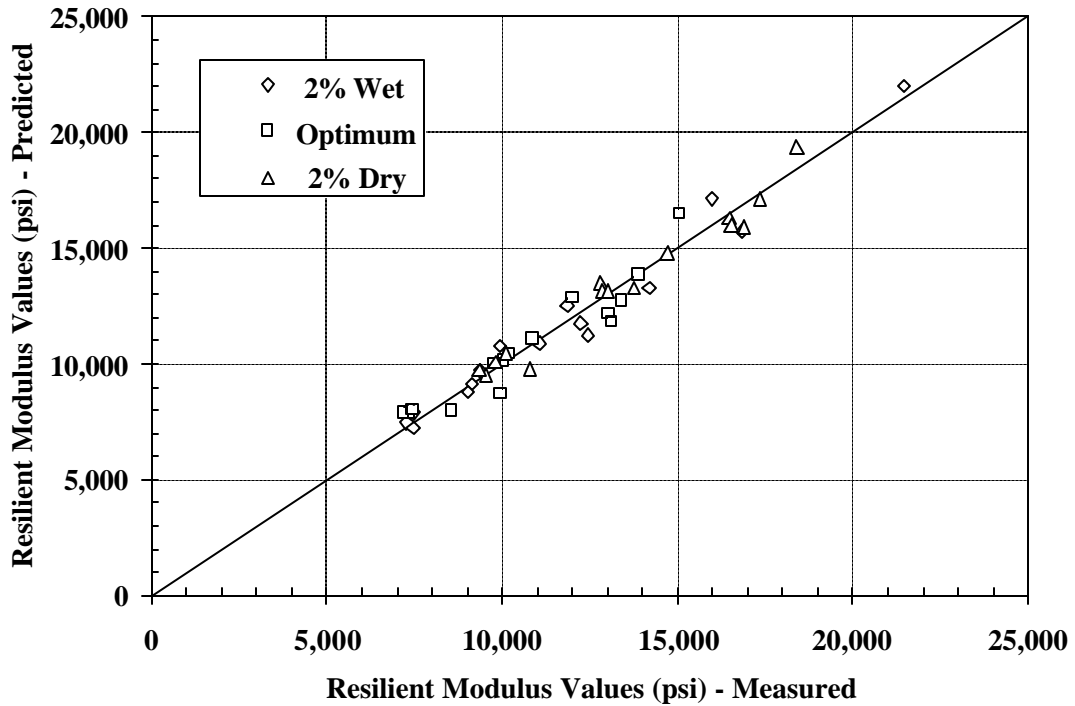


Figure 6.6 Plot of Predicted Resilient Modulus versus Measured Resilient Modulus for A-4 (Rt. 80b) Type Soils

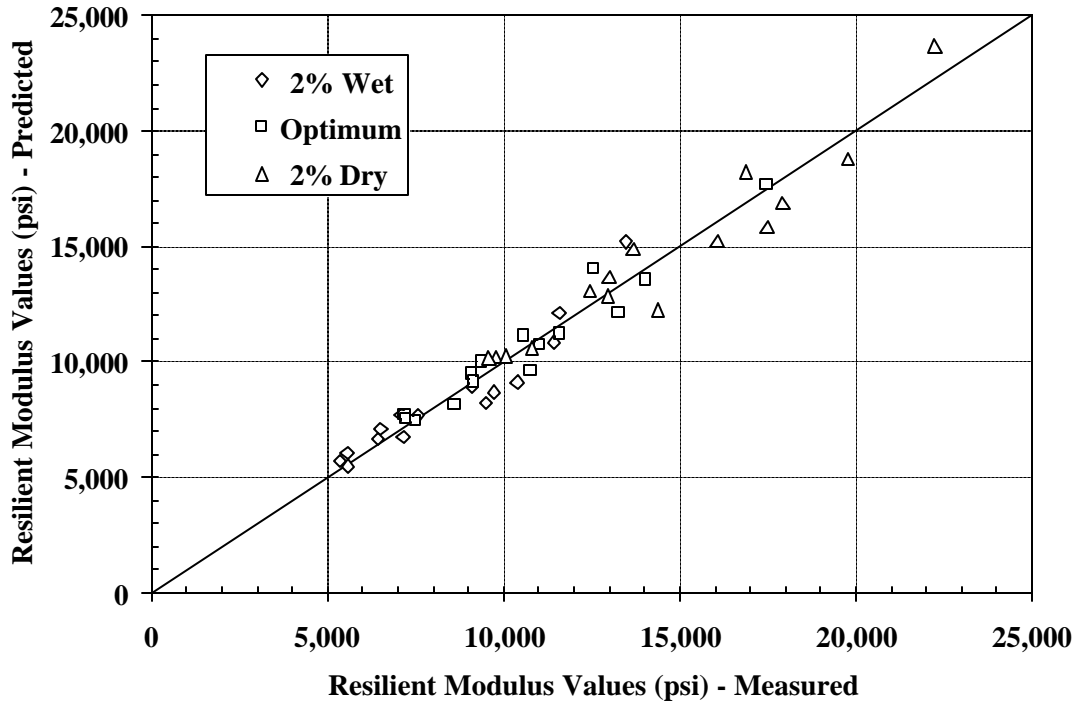


Figure 6.7 Plot of Predicted Resilient Modulus versus Measured Resilient Modulus for A-4 (Rt. 206) Type Soils

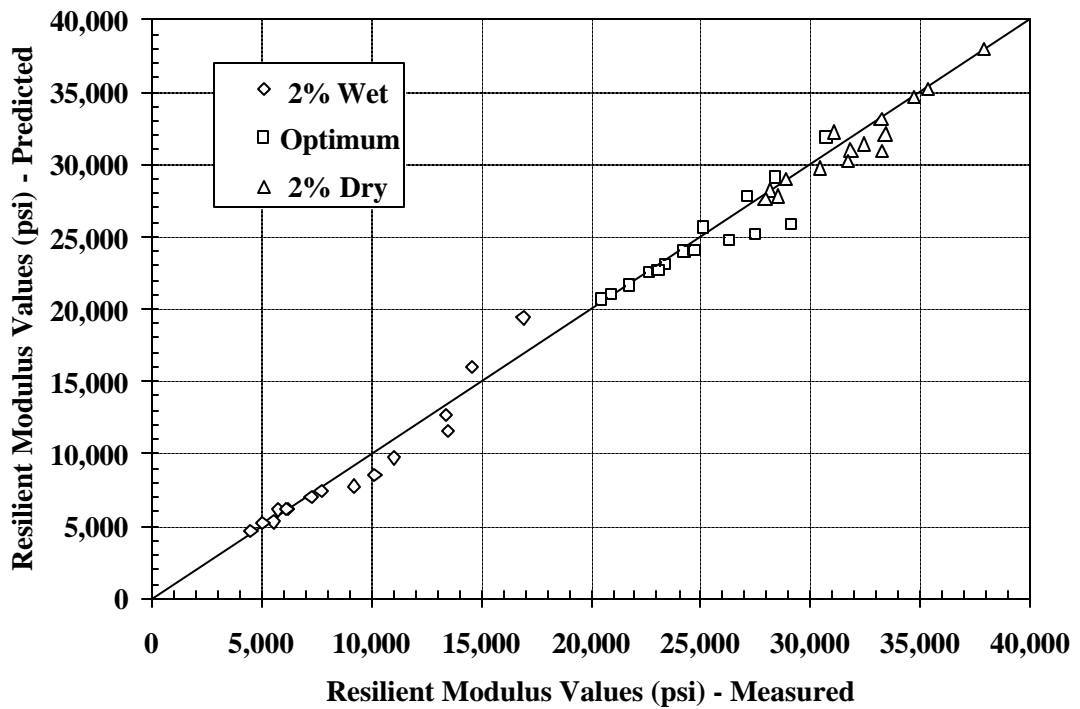


Figure 6.8 Plot of Predicted Resilient Modulus versus Measured Resilient Modulus for A-6 (Cumberland County) Type Soils

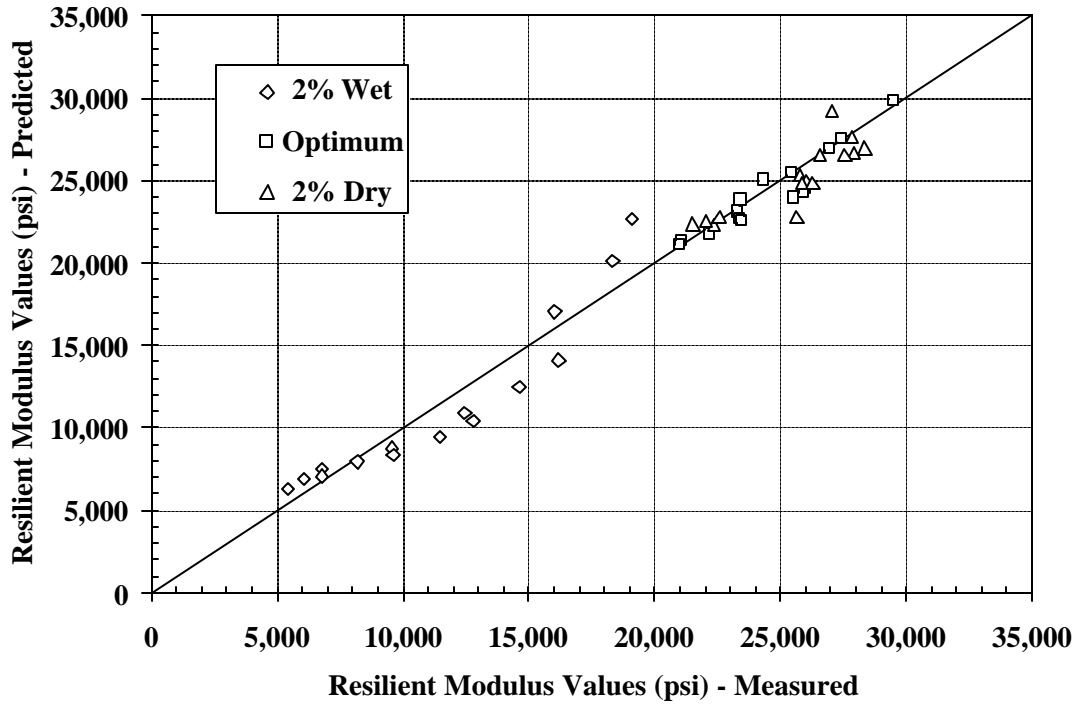


Figure 6.9 Plot of Predicted Resilient Modulus versus Measured Resilient Modulus for A-7 (Cumberland County) Type Soils

6.4 Discussion of the Results

The Universal model underestimated the actual resilient modulus by a maximum of 18 % and overestimated the actual resilient modulus by a maximum of 22 %. The Universal model may be used to estimate the resilient modulus with any combination of confining stress, deviatoric stress, and water content with the use of the material constants provided in table 6.1

Table 6.1 Soil Parameters for the Universal Model

Soil Location	AASHTO Classification	Moisture Content Type	Soil Parameter (k_1)	Soil Parameter (k_2)	Soil Parameter (k_3)	Coefficient of Determination (r^2)
Rt. 23	A-1-b	2% Wet	521.62	0.93	-0.2068	0.99
		OMC	834.48	0.6803	-0.0792	0.95
		2% Dry	1032.07	0.7713	-0.2774	0.94
Rt. 46	A-2-4	2% Wet	314.54	0.7532	-0.4614	0.94
		OMC	410.71	0.7026	-0.4046	0.91
		2% Dry	410.56	0.8072	-0.4166	0.96
Rt. 80a	A-2-4	2% Wet	340.97	0.7675	-0.4948	0.96
		OMC	440.57	0.5085	-0.3913	0.89
		2% Dry	599.39	0.6571	-0.2769	0.91
Rt. 295	A-3	2% Wet	344.81	0.6029	-0.3921	0.91
		OMC	399.77	0.7107	-0.3973	0.93
		2% Dry	413.94	0.5674	-0.3986	0.96
Rt. 80b	A-4	2% Wet	346.48	0.7448	-0.5927	0.97
		OMC	433.4	0.6982	-0.3497	0.91
		2% Dry	585.62	0.7453	-0.275	0.97
Rt. 206	A-4	2% Wet	273.71	0.6025	-0.5177	0.92
		OMC	389.67	0.6515	-0.4161	0.94
		2% Dry	539.87	0.7211	-0.3934	0.93
Cumberland County	A-6	2% Wet	202.6	0.4735	-0.8388	0.95
		OMC	1278.9	0.2636	-0.2343	0.94
		2% Dry	1699.32	0.231	-0.1707	0.92
Cumberland County	A-7	2% Wet	284.32	0.3307	-0.7753	0.89
		OMC	1290.4	0.2262	-0.1864	0.89
		2% Dry	1430.67	0.2748	-0.1173	0.88

VII. SENSISTIVITY ANALYSIS OF RESILIENT MODULUS VALUES IN PAVEMENT SECTIONS

7.1 Introduction

When a design engineer determines a resilient modulus value to use for pavement design, there are some degrees of inherent error involved. The design engineer should not expect to find a resilient modulus value that represents the year round value of the soil or even the “true” resilient modulus value for that particular loading and confining scheme. However, after determining a resilient modulus value for design, the design engineer should have confidence that even with some degree of error, the pavement section would not prematurely fail.

To evaluate the effect of the variability of the resilient modulus value in the subgrade layer of a pavement system, a sensitivity analysis was conducted. The sensitivity analysis looked at two different systems; a full-depth asphalt pavement and a conventional pavement system, figures 7.1 and 7.2 respectively. The sensitivity analysis utilized the elastic layer program EVERSTRESS 5.0. The program was developed by the Washington State Department of Transportation to determine stresses, strains, and deflections in a layered elastic system (semi-infinite) under circular surface loads. The program can handle up to 5 layers, 20 loads, and 50 evaluation points. The program can even take into account stress dependent stiffness characteristics.

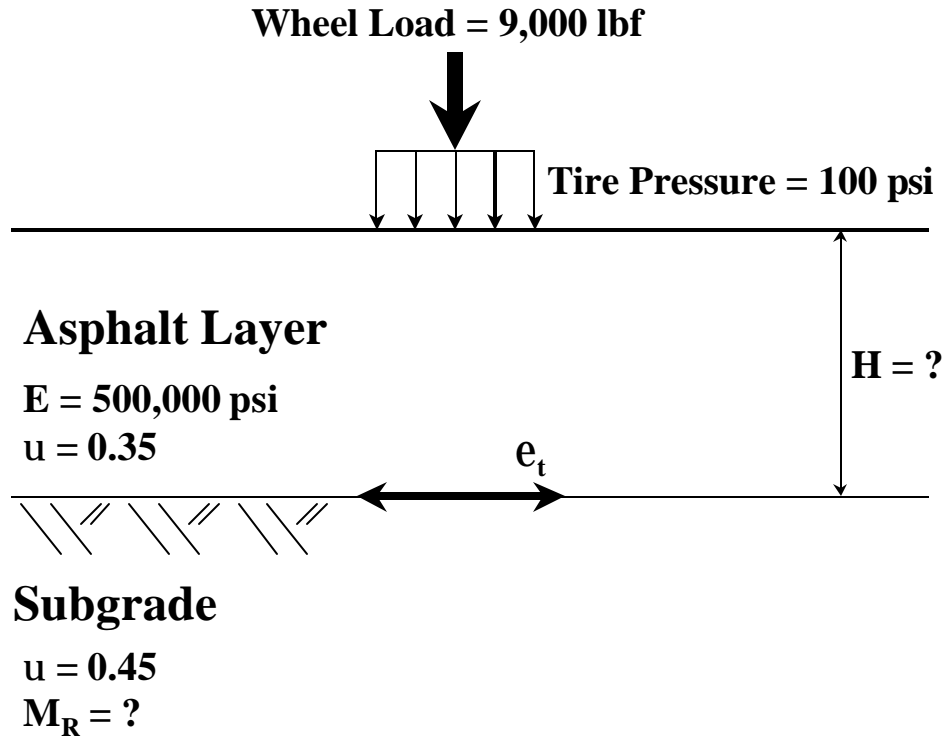


Figure 7.1 – Full-Depth Pavement Section in Sensitivity Analysis

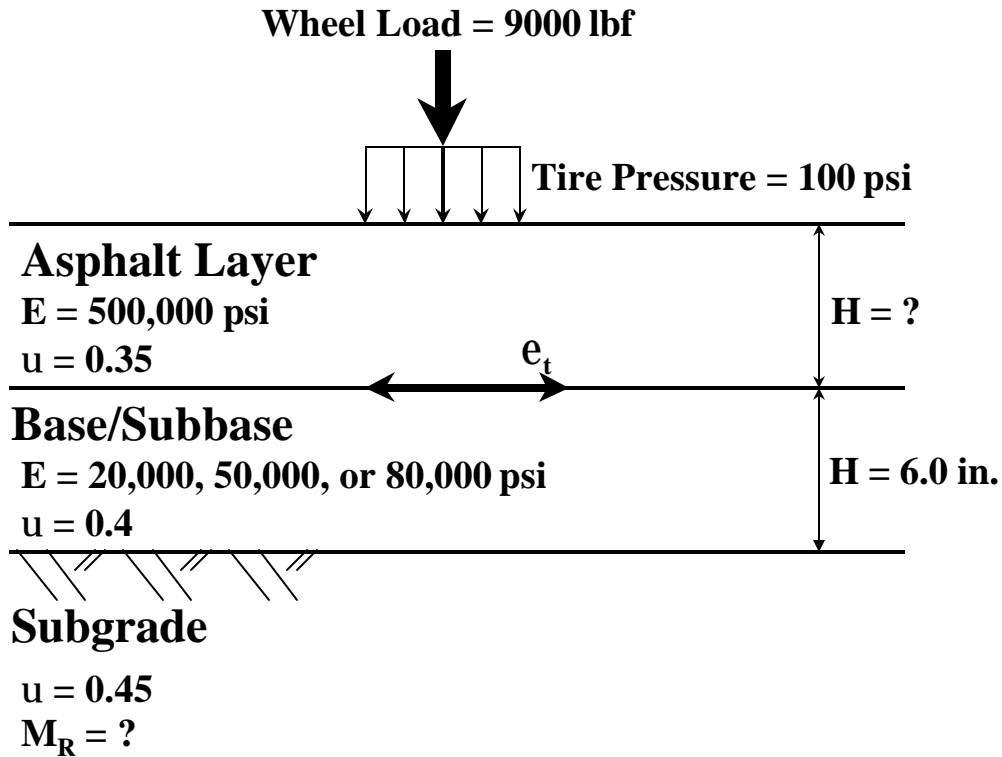


Figure 7.2 – Conventional Pavement Section in Sensitivity Analysis

7.2 Sensitivity Analysis Set-up and Results

The full-depth pavement consisted of asphalt layer of varying thickness, with a modulus of 500,000 psi and a poisson's ratio (ν) of 0.35. The subgrade modulus for the full-depth pavement system varied from 2.5 ksi to 30 ksi, with a poisson's ratio of 0.45. Results from the analysis are shown in figure 7.3. The number of loading repetitions until fatigue failure was determined from the Asphalt Institutes equation for fatigue failure (equation 7.1). In the equation, N_f is the allowable number of load repetitions to control fatigue cracking, ϵ_t is the tensile strain at the bottom of the asphalt layer (which is determined from EVERSTRESS 5.0), and E^* is the modulus of the asphalt layer.

$$N_f = 0.0796 (\epsilon_t)^{-3.291} |E^*|^{-0.854} \quad (7.1)$$

However, it should be noted that this equation was developed assuming an air void volume of 5 % and an asphalt binder volume of 11 %. Although these are not true characteristics of New Jersey asphalt layers, the sensitivity analysis was developed to look at the relative changes in the needed asphalt layer thickness due to changes in the resilient modulus value of the subgrade layer.

As shown in figure 7.3, the change in the resilient modulus value for the subgrade soil has a large impact in the design thickness of the asphalt layer, especially at low subgrade resilient modulus values. As an example, if a design engineer uses a resilient modulus value of 10,000 psi for the subgrade, the full-depth thickness of the asphalt layer

for two million 18 kip axle load repetitions would be approximately 8.25 inches. However, if for some instance the actual resilient modulus were 5,000 psi (whether it is due to poor quality control during compaction or due to weather conditions), the full depth requirement to achieve two million 18 kip axle load repetitions before fatigue failure would be 9.0 inches. In fact, if this were an actual case, fatigue failure in the full-depth pavement layer would occur after approximately 1,250,000 load repetitions, essentially decreasing the life of the pavement by 37.5 %. A decrease from a resilient modulus value 20,000 psi to 15,000 psi results in a difference in pavement thickness of approximately 0.5 inches, less than the previous 0.75 inch difference. However, the life of the asphalt pavement section is still reduced by approximately 28 %. This indicates that in stiffer subgrades, the same change in resilient modulus value will have less of an effect on the pavement section life in full-depth asphalt sections.

The same basic analysis was conducted for a conventional pavement section, shown earlier as figure 7.2. However, for this analysis, not only was the resilient modulus of the subgrade varied, but so was the base/subbase section. The base/subbase section's resilient modulus was set at three different values; 20,000 psi, 50,000 psi, and 80,000 psi. For each one base/subbase modulus used, the subgrade resilient modulus was varied from 2,500 psi to 30,000 psi. Results of the analysis are shown as figures 7.4 – 7.6. However, the thickness of the base/subbase layer was held constant at 6.0 inches. The same essential trend from the full-depth analysis can be seen for the conventional pavement section. The same situational examples from the full-depth pavement are utilized in the conventional pavement and the example results are shown in table 7.1.

The last line in the table is shown as not applicable (NA) since both of the number of loading repetitions until fatigue failure for 5 inches of asphalt is above two million.

Table 7.1 – Example Results from Sensitivity Analysis

Base/Subbase Modulus (psi)	Design Subgrade Modulus (psi)	Actual Subgrade Modulus (psi)	Change in Asphalt Layer Thickness (inches)	% Decrease in Pavement Life (%)
20,000	10,000	5,000	0.55	29%
	20,000	15,000	0.2	13%
50,000	10,000	5,000	0.55	25%
	20,000	15,000	0.2	13%
80,000	10,000	5,000	0.55	23%
	20,000	15,000	NA	NA

7.3 Discussion of the Results

A sensitivity analysis was conducted two different pavement section schemes; a full-depth asphalt pavement and a also a conventional pavement section. The analysis was conducted to determine if the resilient modulus of the subgrade had a dramatic effect on the asphalt layer thickness so the pavement could reach 2 million loading repetitions from an 18 kip axle vehicle before fatigue cracking would begin. From the figures 7.3 – 7.6 and also table 1, the subgrade has a more pronounced effect on the asphalt layer thickness when the subgrade resilient modulus is lower. The stiffer the subgrade layer, the more support is provided for the asphalt layer, enabling to lessen the required asphalt thickness for the same design ESAL’s. Therefore, it can be concluded from the sensitivity analysis that the design engineer should take extra caution when designing pavement sections that have a subgrade resilient modulus less than 10,000 psi.

VIII. DESIGN PROCEDURE FOR DETERMINING SUBGRADE RESILIENT MODULUS FOR PAVEMENT DESIGN

8.1 Introduction

The following section is a design procedure for determining the design resilient modulus value. The section is modified from the FHWA publication, Publication No. FHWA-RD-97-083.

Obviously, before the design procedure can take place, a subsurface investigation is needed to determine the soil type(s) below the future pavement structure. Once the soil layer(s) are determined, subdivide the subsurface into sections of similar conditions. From the sections, take sufficient and appropriate auger, split tube, and/or undisturbed samples for laboratory testing (soil classification). If the soil layer is to be left with the proposed pavement section built over top of it, conduct the resilient modulus test on the undisturbed sample or at the wet density representative of the field condition. However, if the soil layer is to be excavated and then placed back under a particular degree of compaction, determine the moisture-density curve for the soil. AASHTO T-99 should be used for coarse-grained soils, while AASHTO T-180 should be used for medium to high plasticity fine-grained soils (FHWA Publication No. FHWA-RD-97-083). All reconstituted samples prepared in the laboratory should be conducted under the procedures outlined in AASHTO TP46-94.

8.2 Design Procedure

To further illustrate the design procedure, the remainder of the chapter will be illustrated in the form of an example problem. For this example problem, the soil and pavement structure has the following properties and is shown as Figure 8.1

Asphalt Section: Unit weight (γ_{ac}) of 148 pcf and a thickness (z_{ac}) of 6 inches

Base Material: Crushed aggregate material with a unit weight (γ_{base}) of 132 pcf and a thickness (z_{base}) of 10 inches

Subgrade Soil: Classified as cohesive clay with a unit weight (γ_{sub}) of 105 pcf and a thickness (z_{sub}) of 3 feet

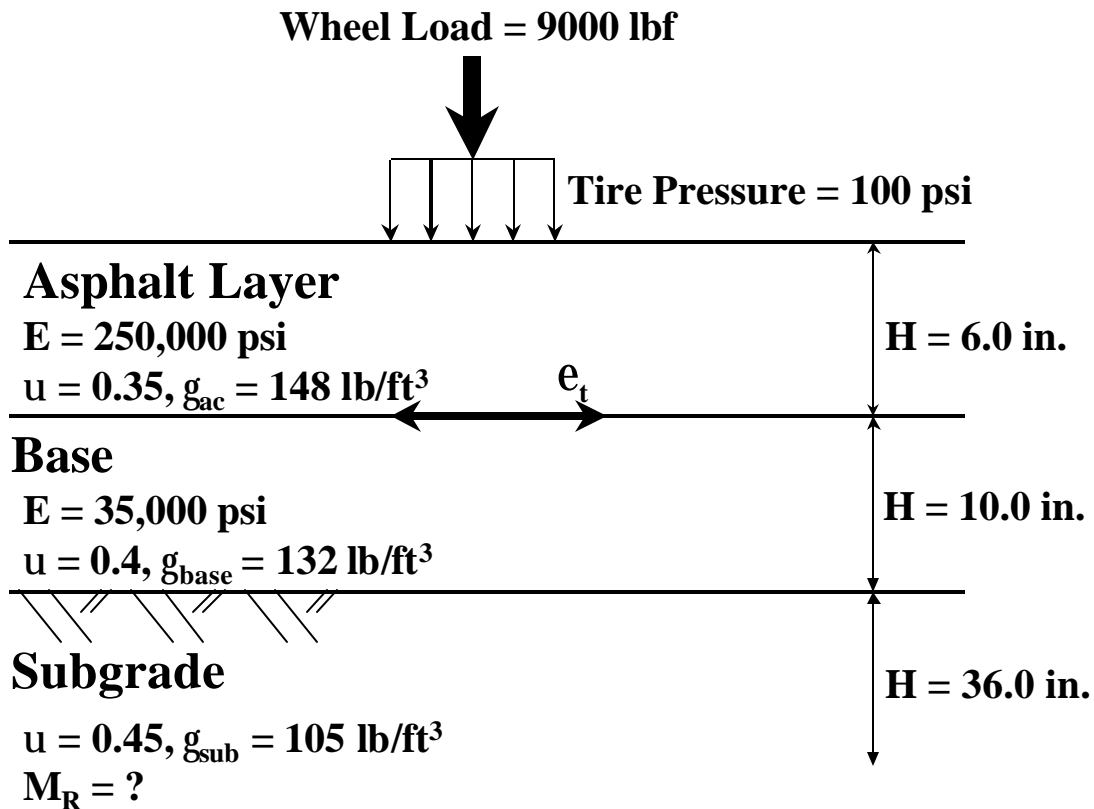


Figure 8.1 – Example Problem Layer Properties and Dimensions

Resilient modulus testing was also conducted on a number of subgrade soil samples with the average non-linear elastic constants for the Universal Model shown below:

$$k_1 = 329$$

$$k_2 = 0.16$$

$$k_3 = -0.38$$

After the resilient modulus value test is conducted at the appropriate sample density, the design engineer must calculate the at-rest earth pressure coefficient (k_o) for the soil layer of interest. A conservative method to calculating k_o is through equation 8.1

$$k_o = \frac{u}{(1-u)} \quad (8.1)$$

The term (u) is known as the poisson ratio. Table 8.1 shows typical poisson ratios for different materials (Huang, 1993).

Table 8.1 – Poisson Ratios for Different Materials

Material	Range of Values	Typical Value
Hot Mix Asphalt	0.30 - 0.40	0.35
Portland Cement Concrete	0.15 - 0.20	0.15
Untreated Granular Materials	0.30 - 0.40	0.35
Cement-Treated Granular Materials	0.10 - 0.20	0.15
Cement-Treated Fine-Grained Soils	0.15 - 0.35	0.25
Lime-Stabilized Materials	0.10 - 0.25	0.20
Lime-Fly Ash Mixtures	0.10 - 0.15	0.15
Loose Sand or Silty Sand	0.20 - 0.40	0.30
Dense Sand	0.30 - 0.45	0.35
Fine-Grained Soils	0.30 - 0.50	0.40
Saturated Soft Clays	0.40 - 0.50	0.45

Therefore, for the example problem, the at-rest earth pressure coefficient is:

$$k_o = \frac{u}{(1-u)} \quad (8.1)$$

From table 8.1, a poisson ratio value for the soil is 0.45.

$$k_0 = \frac{0.45}{(1 - 0.45)} = 0.818$$

* If the soil consists of a coarse grained soil (i.e. mostly a sand or gravelly soil), the following equation (equation 8.2) can also be used, where (ϕ) is the undrained friction angle from the static triaxial test:

$$k_0 = 1 - \sin \phi \quad (8.2)$$

After the at-rest earth pressure coefficient (k_0) is determined, the at-rest lateral stress (p_0) must be computed. This is conducted using a weighted-average approach (equation 8.3) and then calculating the lateral pressure (equation 8.4) just entering the subgrade layer. The depth of 0.25 ft into the subgrade layer was chosen since the sample size for the subgrade resilient modulus test is approximately 0.5 ft and the greatest amount of loading will be “felt” in the upper region of the subgrade layer.

$$y_p = \frac{\mathbf{g}_{ac}(z_{ac}) + \mathbf{g}_{base}(z_{base})}{z_{ac} + z_{base}} \quad (8.3)$$

$$\mathbf{g}_p = \frac{148 \text{ pcf} \left(\frac{6}{12} \text{ ft} \right) + 132 \text{ pcf} \left(\frac{10}{12} \text{ ft} \right)}{\left(\frac{6}{12} \text{ ft} \right) + \left(\frac{10}{12} \text{ ft} \right)}$$

$$\mathbf{g}_p = 138 \text{ pcf}$$

$$p_o = k_o \left[\mathbf{g}_p (z_{ac} + z_{base}) + \mathbf{g}_{sub} \left(\frac{z_{sub}}{2} \right) \right] \quad (8.4)$$

$$p_o = 0.818 \left[138 \text{ pcf} \left(\frac{16}{12} \text{ ft} \right) + 105 \text{ pcf} \left(\frac{0.25}{2} \text{ ft} \right) \right]$$

$$p_o = 161.25 \text{ psf} = 1.12 \text{ psi}$$

* Note: It is important to know what units are needed. As shown in the above derivation, the “inches” needed to be changed to “feet” by dividing by 12.

Now that the weighted-average unit weight of the pavement layers is determined, the increase in lateral stress due to the applied wheel load needs to be determined. The minimum lateral stress (σ'_3) due to the applied traffic load is computed with elastic layered theory for an 18-kip (80 kN) single axle load at a depth of 3 inches (0.25 ft) into the subgrade. The calculation was conducted using EVERSTRESS 5.0 assuming the conditions shown in figure 8.1, as well as the subgrade having a modulus of 10,000 psi. The increase in lateral pressure ($\sigma'_3 =$ confining pressure) due to the traffic load is:

$$s'_3 = 0.25 \text{ psi}$$

Thus, the in-situ lateral stress is (equation 8.5):

$$s_3 = s'_3 + p_o \quad (8.5)$$

$$s_3 = 0.25 \text{ psi} + 1.94 \text{ psi}$$

$$s_3 = 2.19 \text{ psi}$$

Once the lateral stress value has been determined, the in-situ deviator stress (σ'_d) for the assumed pavement structure must now be determined. Again, the deviator stress is computed with elastic layered theory under the same conditions as the increase in

confining pressure (lateral stress). From the EVERSTRESS 5.0 program, the increase in deviatoric pressure due to the applied traffic load is:

$$s'_d = 4.75 \text{ psi}$$

Thus, the in-situ deviator stress can now be determined by using equation 8.6.

$$s_d = s'_d + p_o \left(\frac{1}{k_o} - 1 \right) \quad (8.6)$$

$$s_d = 4.75 + 1.12 \left(\frac{1}{0.818} - 1 \right)$$

$$s_d = 5.0 \text{ psi}$$

Two of the three needed components have been determined, the in-situ confining stress (σ_3) and the in-situ deviator stress (σ_d). The final value needed is the in-situ bulk stress (θ). This can be achieved by using equation 8.7.

$$q = s'_x + s'_y + s'_z + (1 + 2k_o)(z_{sub}g_{sub} + z_p g_p) \quad (8.7)$$

where,

$\sigma'_x, \sigma'_y, \sigma'_z$ – normal stresses computed with elastic layer theory in the horizontal (transverse and longitudinal) and vertical direction, respectively, from a wheel load applied at the pavement's surface

z_p – total depth of asphalt and base/subbase layers

γ_p – weighted average unit weight of the asphalt and base/subbase layers

$$q = 0.25 \text{ psi} + 0.25 \text{ psi} + 4.75 \text{ psi} + (1 + 2(0.818)) \left[\left(\frac{\left(\frac{3}{12} \right)^{105}}{144} \right) + \left(\frac{\left(\frac{16}{12} \right)^{138}}{144} \right) \right] \text{ psi}$$

$$q = 9.1 \text{ psi}$$

Now, the in-situ resilient modulus can be determined. Using the Universal Model discussed in Chapter 6, in form of equation 8.8, the non-linear elastic constants determined from the resilient modulus testing on the subgrade soil are inputted into equation 8.8.

$$M_R = k_1 (\text{AtmPa}) \left[\frac{q}{\text{AtmPa}} \right]^{k_2} \left[\frac{s_d}{\text{AtmPa}} \right]^{k_3} \quad (8.8)$$

where,

AtmPa – reference atmospheric pressure = 14.7 psi

$$M_R = 329 (14.7) \left[\frac{9.1}{14.7} \right]^{0.16} \left[\frac{5.0}{14.7} \right]^{-0.38}$$

$$M_R = 6,747 \text{ psi} (44.1 \text{ MPa})$$

Although the calculated resilient modulus value is 6,747 psi, this is determined based on “best case” scenario. Unfortunately, the resilient modulus varies throughout the year due to seasonal variations in moisture content. To illustrate the seasonal variation of the subgrade resilient modulus, it is assumed that the variation is conditional based on the season itself. For example, the spring season induces thawing of the frozen ground, as well as normally rainy conditions in New Jersey. Therefore, it can be assumed for 1.5

months of the year, the ground is wet and the in-situ resilient modulus is 60 % of its normal value and for 1.5 months following, the subgrade is beginning to “dry out” and is 80 % of the normal value. As a result, the resilient modulus during the year is:

9 months – 6,747 psi (46.5 MPa)
 1.5 months – 4,048 psi (27.9 MPa)
 1.5 months – 5,398 psi (37.2 MPa)

Once the seasonal variation has been determined, the effective roadside resilient modulus (M'_R) is calculated. This is shown as equations 8.9 and 8.10 and is known as the AASHTO serviceability criterion.

$$U_f = 1.18 \times 10^8 (M_R)^{-2.32} \quad (8.9)$$

$U_f (M_R = 6,747 \text{ psi}) = 0.1543$
 $U_f (M_R = 4,048 \text{ psi}) = 0.5048$
 $U_f (M_R = 5,398 \text{ psi}) = 0.2589$

$$U_f = \frac{\sum U_f}{n} \quad (8.10)$$

$$U_f = \frac{\sum U_f}{n} = \frac{9(0.1543) + 1.5(0.5048) + 1.5(0.2589)}{12}$$

$$U_f = 0.2112$$

Equation 8.9 is once again used to determine the effective roadside resilient modulus (M'_R), however, it is used in the form of equation 8.11.

$$M'_R = \sqrt[2.32]{\frac{U_f}{1.18 \times 10^8}} = \left(\frac{U_f}{1.18 \times 10^8} \right)^{\left(\frac{1}{2.32} \right)} \quad (8.11)$$

$$M'_R = \sqrt[2.32]{\frac{0.2112}{1.18 \times 10^8}} = \left(\frac{0.2112}{1.18 \times 10^8} \right)^{\left(\frac{1}{2.32} \right)}$$

$$M'_R = 5,893 \text{ psi}$$

The next step in the design procedure is to determine the potential for permanent deformations due to excessive traffic loading. Using the effective roadside resilient modulus based on the serviceability criteria, the allowable number of load applications for a specific axle weight and configuration and tire pressure (N) is determined from equation 8.12.

$$\text{Log}(N) = 0.955(\text{Log}(M_R)) - 4.082(\text{Log}(\epsilon_v)) - 10.90 \quad (8.12)$$

where,

N = number of allowable load applications

M_R = effective roadside resilient modulus

ϵ_v = vertical compressive strain at the top of the subgrade layer

The vertical compressive strain (ϵ_v) is once again calculated using elastic layered theory, and, once again, the program EVERSTRESS 5.0 was utilized. The same assumptions from earlier in the example problem were used, however, instead of assuming an average resilient modulus value of 10,000 psi, the subgrade resilient modulus value used is the effective roadside resilient modulus equaling to 5,893 psi. From the calculation, the vertical compressive strain (ϵ_v) at the top of the subgrade soil is:

$$\epsilon_v = 7.04 \times 10^{-4} \text{ in./in.}$$

Once ϵ_v is calculated, the number of allowable load repetitions can be determined as follows:

$$\text{Log}(N) = 0.955(\text{Log}(M_R)) - 4.082(\text{Log}(\epsilon_v)) - 10.90$$

$$\text{Log}(N) = 0.955(\text{Log}(5,893)) - 4.082(\text{Log}(7.04 \times 10^{-4})) - 10.90$$

$$\text{Log}(N) = 5.569$$

$$N = 10^{5.569}$$

$$N = 370,680$$

If the design number of 18-kip (80-kN) equivalent axle loads (ESAL's) is less than the above value, then there is sufficient cover to prevent extensive permanent deformations in the subgrade. If the design number of 18-kip (80-kN) ESAL's are greater than the above value, then the pavement structural thickness as defined by AASHTO will need to be increased.

IX. CONCLUSIONS AND RECOMMENDATIONS

9.1 Conclusions

Resilient properties of a combination transported/residual subgrade soils of New Jersey were determined with respect to changes in parameters which most influence stiffness characteristics of the soils, i.e., confining pressure, deviatoric stress, and initial or compacted water content.

1. The changes in resilient values were more pronounced for Type 1 soils (coarse, granular material) under varying confining pressures as compared to the seven Type 2 (fine material) soils tested. Changes in confining pressure are more influential on the intergranular stress distribution of coarse cohesionless materials than fine materials
2. Type 1 soils assume a very rigid structure at the dry side of the optimum with a resulting increase in resilient properties as compared to Type 2. As a result, Type 1 soils are more sensitive to initial moisture content during compaction. Compaction and placement specifications should note such behavior. However, the A-6 and A-7 soils tested in this study were very susceptible to strain softening when compacted on the wet side of optimum.
3. The stiffness of Type 2 material does not change significantly at 2% above the optimum moisture content. The structure and fabric of finer materials as type 2 does not exhibit significant rigidity, or lack thereof, within the 2% variation of molding water content. Therefore, changes in resilient properties were less

pronounced for Type 2 soils compared to Type 1, when compared to samples tested on the dry side of optimum. However, some of the fine-grained samples tested on the wet side of optimum showed a significant decrease in rigidity when tested.

4. Pore pressure generation and dissipation significantly changes the strength characteristics of subgrade soils. The problem is more acute when low permeability in soil slows down the dissipation of excess pore pressure. As a result, testing of fine sand under the resilient modulus testing loading regime shows that pore pressure generation accompanied by initial contraction of the soil results in a reduction in resilient values. The reduction in resilient modulus continues with reversing of specimen contraction and start of sample dilation. The phenomenon is similar to that observed for dynamic properties of fine sands under cyclic loads. Unfortunately, the AASHTO standards for resilient modulus testing call for a drained test, where the drainage values remain open. Thus, without modification of the testing standards, the measurement of pore pressure during the testing cannot be properly monitored.
5. A comprehensive statistical, predictive model was identified for estimation of resilient modulus values of the tested soils. The calibrated model accurately predicted the resilient properties of a specific material type at any given depth (confining pressure) in a pavement system.
6. A sensitivity analysis conducted using an elastic layer theory computer program, EVERSTRESS 5.0, illustrated the effect the subgrade modulus has on the

thickness of the asphalt layer for design against fatigue cracking. The analysis showed that for a full-depth pavement, as the stiffness of the subgrade layer decreases, the thickness of the asphalt layer must increase to provide adequate support to resist fatigue cracking. Similar results were concluded for a conventional, three layered pavement system.

7. A design procedure, based on the AASHTO publication, FHWA-RD-97-083, provided a guideline for pavement designers on how to determine the design, effective roadside resilient modulus for subgrade soils. However, the downfall of the procedure is the need for an elastic layered solution/computer program to determine both the increase in deviatoric and confining stress due to traffic loading, as well as the tensile strain induced at the top of the subgrade layer due to traffic load.

9.2 Recommendations

1. Work needs to continue to better understand the phenomena of resilient properties accompanied by permanent deformation under the given AASHTO loading regime. In some soils, higher resilient modulus may be obtained after accumulating high permanent deformations. However, some soils may experience very little permanent deformation and have a low resilient modulus.
2. A modification to the resilient modulus test specification should be considered to evaluate the effect of pore pressure on the resilient modulus properties of soils. Currently, the testing standards calls for a drained test, which may or may not

hold true for site conditions. The use of a cyclic triaxial test, without varying the bulk stresses, although with the drainage valves closed to provide an undrained condition, may provide some insight into the potential for pore pressure generation. The test conditions could easily simulate the confining pressures and deviatoric stresses that the subgrade soil would experience by conducting the same initial analysis conducted in chapter 8.

3. Work needs to be initiated into correlation of resilient properties of the soils to nondestructive field evaluation of subgrade stiffness using seismic pavement analyzer (SPA) (Nazarian et al. 1993 or falling weight deflectometer (FWD). Any potential correlation, albeit indirect, will lead to a more realistic determination of subgrade properties under vehicular loads.
4. To aid in the design procedure, design charts need to be developed for the determination of the elastic layer solutions of the increase in deviatoric and confining stress, as well as in induced tensile strains at the top of the subgrade layer due to traffic loading. The charts would need to be comprehensive enough that the pavement design does not need to rely on computer programs like EVERSTRESS 5.0.

REFERENCES

- Barksdale, R.D. The Aggregate Handbook, National Stone Association, Washington D.C. 1993.
- Bergen, A.T. and Monismith, C.L. "Characteristics of Subgrade Soils in Cold Regions for Pavement Design Purposes," Highway Research Record 431, Highway Research Board, National Research Council, Washington D.C. 1973, pp. 25-37
- Boateng-Poku, Y. and Drumm, E.C. "Hyperbolic Model for the Resilient Modulus Response of Fine-Grained Subgrade Soil," Resilient Moduli of Soils ASCE Geotechnical Special Publication No. 24 , 1989 pp. 1-14
- Boyce, J.R. "A Nonlinear Model for the Elastic Behavior of Granular Materials Under Repeated Loading," Proceedings, International Symposium on Soils Under Cyclic and Transient Loading, Swansea, England, 1980, pp. 521-542
- Castro, G. "Liquefaction of Cyclic Mobility of Saturated Sands," Journal of Geotechnical Engineering Division, ASCE 101 (GT6), pp. 552-569
- Chamberlain, E.J., Cole, D.M. and Durell, G.F. Resilient Modulus Determination for Frost Conditions. State of the Art Pavement Response Monitoring Systems for Roads and Air Fields. Special Report 89-23, U.S. Army Cold Regions Research and Engineering Laboratory (CRREL), Hanover, H, 1989, pp.320-333.
- Cole, D.M., Irwin, L.H. and Johnson, T.C. "Effect of Freezing and Thawing on Resilient Modulus," Presented at the 60th Annual Meeting, Transportation Research Board, National Research Council, Washington D.C., January 1981.
- Dehlen, G. L. (1969). "The Effect of Non-Linear Material in the Behavior of Pavements Subjected to Traffic Loads," Ph.D. Thesis, University of California, Berkley.
- Drumm, E. C., Reeves, J.S., Madgett, M.R., and Trolinger W.D. "Subgrade Resilient Modulus Correction for Saturation Effects," Journal of Geotechnical and Geoenvironmental Engineering, Vol. 123, July, 1997.
- Elfino, M. K., and Davidson, J.L. "Modeling Field Moisture in Resilient Moduli Testing." Resilient moduli of soils: laboratory Conditions, ASCE, New York, N/Y., No. 24, 31-51 1989.
- Elhannani, M. "Modelisation et Simulation Numerique des Chaussees Souples," Ph.D. Thesis. University of Nantes, France, 1991.
- Elliot, R.P. and Thornton, S.I. "Resilient Modulus and AASHTO Pavement Design." Transportation Research Record. 1192, 116-124 1988

- Feliberti, M., Nazarian, S., and Srinivasan, T. "Critical Evaluation of Parameters Affecting Resilient Modulus Tests On Subgrades," Texas Department of Transportation Research Report 1177-2, Vol. 1, 1992.
- FHWA-RD-97-083, 1997, *Design Pamphlet for the Determination of Design Subgrade in Support of the 1993 AASHTO Guide for the Design of Pavement Structures*, Federal Highway Administration, 27 pp.
- Finn, F.N., Nair, K., and Monismith, C.L. (1972). "Application of Theory in the Design of Asphalt Pavements," Proceedings of the 3rd International Conference of the Structural Design of Asphalt Pavements, University of Michigan, Ann Arbor, Michigan, 392-409.
- Fredlund, D.G., Bergan, A.T., and Sauer, E.K. (1975). "Deformation Characterization of Subgrade Soils for Highways and Runways in Northern Environments," Canadian Geotechnical Journal Vol. 12, 213-223.
- Fredlund, D.G., Bergan, A.T., and Wong, P.K. (1977). "Relation Between Resilient Modulus and Stress Conditions for Cohesive Subgrade Soils," Transportation Research Record Vol. 642, 73-81.
- Hall, K.D. and Rao S. (1998). "Developing Methods for Predicting Subgrade Moisture Levels Using In-Situ Moisture Content Data" Transportation Research Record, TRB paper # 980281, National Research Council, Washington D.C., 1998
- Hardcastle, J.H. "Subgrade Resilient Modulus for Idaho Pavements" Idaho Transportation Department, FHWA Report No. RP110-d, 1992
- Hardin, B.O. and Drnevich, V.P. "Shear Modulus and Damping in Soils: Measurement and Parameters Effects," Journal of the Soil Mechanics and Foundation Division, ASCE, Vol. 98, SM7, 1972, pp. 603-624.
- Houston, W., Houston, S., and Anderson, T. "Stress State Considerations for Resilient Modulus Testing of Pavement Subgrade," Transportation Research Record 1406, TRB, National Research Council, Washington D.C., 1993, pp. 124-132.
- Huang, Y.H. *Pavement Analysis and Design*, Englewood cliffs, New Jersey, Prentice Hall 1993
- Hyodo, M., Murata, H. Yasufuku, N., and Fujii, T. "Undrained Cyclic Shear Strength and Residual Shear Strain of Saturated Sand by Cyclic Triaxial Tests," Soils and Foundations, Japanese Society of Soil Mechanics and Foundation Engineering, Vol. 31, No. 3, Sept 1991, pp. 60-76.
- Kamal, M.A., Dawson, A.R., Farouki, O. T., Hughes, D.A.B., and Sha'at, A. A. "Field and Laboratory Evaluation of the Mechanical Behavior of Unbound Granular Materials

in Pavements," Transportation Research Record 1406, TRB, National Research Council, Washington D.C., 1993, pp. 88-97

Karasahin, M., Dawson A.R., and Holden J.T. "Applicability of Resilient Constitutive Models of Granular Material for Unbound Base Layers," Transportation Research Record 1406, TRB, National Research Council, Washington D.C., 1993, pp. 89-107.

Maher, M.H., Papp Jr., W. J., Gucunski, N. "Measurement of Soil Resilient Properties Using Non-contacting Proximity Sensors," Transportation Research Record 1548, TRB, National Research Council, Washington D.C. 1996, pp. 16-23.

Mayhew, H., "Resilient Properties of Unbound Road Base Under Repeated Triaxial Loading," TRRL Laboratory Report 1088. TRRL, Crowthorne, Berkshire, England, 1983.

Muhanna, A.S., Rahman, M.S., Lambe, P.C. "A Model for Resilient Modulus and Permanent Strain of Subgrade Soils" TRB, 1998

Nazarian, S., and Feliberti, M. "Methodology for Resilient Modulus Testing of Cohesionless Subgrades," Transportation Research Record 1406, TRB, National Research Council, Washington D.C., 1993, pp. 108-115

Nazarian, S., Pezo, R., Melarkode, S., and Picornell, M. "Testing Methodology for Resilient Modulus of Base Materials," Transportation Research Record 1547, TRB, National Research Council, Washington D.C., 1996, pp. 46-52

Pappin, J.W. and Brown, S.F. "Resilient Stress Strain Behavior of a Crushed Rock" Proceedings, International Symposium on Soils Under Cyclic and Transient Loading, Swansea, Great Britain, Vol. 1, 1980, pp. 169-177

Pezo, R.F., G. Claros, and W.R. Hudson. "An Efficient Resilient Modulus Test for Subgrades and Nongranular Subbase Material," Presented at 71st Annual Meeting of the Transportation Research Board, Washington, D. C., 1992.

Pezo, R., and Hudson, W. R. (1994). "Prediction Models of Resilient Modulus for Non-granular Materials." Geotechnical Testing Journal., 17(3), 349-355

Pezo, R.F., Kim, D.S., Stokoe II, K.H., and Hudson, W.R. "A Reliable Resilient Modulus Testing System" Transportation Research Record 1307, TRB, National Research Council, Washington D.C., 1991, pp. 90 - 98.

Raad, L., Minassian, G.H., and Gartin, S., "Characterization of Saturated Granular Bases Under Repeated Loads." Transportation Research Record 1369 TRB, National Research Council, Washington D.C., 1992, pp. 73 - 82.

- Raad, L. and Zeid, B.A. "Repeated Load Model for Subgrade Soils: Model Development" Transportation Research Record 1278, TRB, National Research Council, Washington D.C., 19, pp. 72 - 82.
- Rada, G. and Witczak, M.W. "Comprehensive Evaluation of Laboratory Resilient Moduli Results for Granular Material," Transportation Research Record 810, National Research Council, Washington, D.C. 1981 pp. 23-33.
- Santha, B.L. "A Study on Resilient Modulus of Subgrade Soil: Comparison of Two Constitutive Equations and Predictability of k Parameters using Material and Physical Properties of Soil," Paper 940270 Georgia Department of Transportation, 1994.
- Seed, H., Chan, C., and Lee, C. "Resilience Characteristics of Subgrade Soils and Their Relation to Fatigue in Asphalt Pavements," Proceedings, International Conference on the Structural Design of Asphalt Pavements, University of Michigan, 1962, pp. 611-636.
- Seed, H.B., Chan, C.K., and Lee, C.E. (1962). "Resilient Characteristics of Subgrade Soils and Their Relation to Fatigue Failures in Asphalt Pavements," Proceedings International Conference on the Structural Design of Asphalt Pavements, University of Michigan, Ann Arbor, Michigan, 611-636
- Smith, N., Eaton, R. and Stubstad, J. "Repetitive Loading Tests on Membraned-Enveloped Road Sections During Freeze-Thaw Cycles," Journal of the Geotechnical Engineering Division, ASCE, Vol. 104, No. GT10, Oct., 1978, pp. 1277-1288.
- Thompson, M.R. and Elliot, R.P. "ILLI-PAVE-Based Response Algorithms for Design of Conventional Flexible Pavements." Transportation Research Record. 1043, 50-57 1985.
- Thompson, M.R. and Robnett, Q.L. (1976). "Final Report, Resilient Properties of Subgrade Soils." Illinois Cooperative Highway and Transportation Serial No. 160, University of Illinois, Urbana-Champaign, Illinois.
- Uzan, J. "Characterization of Granular Material," Transportation Research Record 1022, TRB, National Research Council, Washington D.C. 1985, pp. 52-59
- Vinson, T.S. "Parameters Effects on Dynamic Properties of Frozen Soil," Journal of the Geotechnical Engineering Division, ASCE, Vol. 104, No. GT10, Oct., 1978, pp. 1289-1306.
- Wu, S. "Capillary Effects on Dynamic Modulus of Fine-Grained Cohesionless Soils," Ph.D. Thesis University of Michigan, 1983